UNIVERSITY OF OKLAHOMA

GRADUATE COLLEGE

OLFACTORY BULB CODING AND ODOR DISCRIMINATION

A Dissertation

SUBMITTED TO THE GRADUATE FACULTY

In partial fulfillment of the requirements for the

degree of

Doctor of Philosophy

By

MAX L. FLETCHER II
Norman, Oklahoma
2005

UMI Number: 3174274

UMI®

OLFACTORY BULB CODING AND ODOR DISCRIMINATION

A Disertation APPROVED FOR THE
DEPARTMENT OF ZOOLOGY

BY

_____
Donald Wilson

_____
Regina Sullivan

_____
Joseph Bastian

_____
Robert Rennaker

_____
Ari Berkowitz

ACKNOWLEDGMENTS

TABLE OF CONTENTS

Chapter 1

Functional Organization of the Olfactory System

The olfactory system must be able to identify and discriminate thousands of odorants within an animal's environment. These odorants are important in all aspects of survival including communication, mate recognition, reproduction, navigation, detection of predators, and localization of food sources. It is essential that an animal not only be able to learn and remember significant odors, but also be able to learn new odors as new situations arise.

Olfactory Epithelium

In general, odorants are small, volatile, lipophilic molecules weighing less than 300 daltons (Turin and Yoshii, 2003). Perception of olfactory stimuli begins with the binding of odorant molecules to olfactory receptor (OR) proteins located on olfactory sensory neuron (OSN) dendrites within the nasal epithelium. The olfactory epithelium is coated with mucus that is believed to facilitate recognition of odorant molecules by receptor neurons. For example, odorant-binding proteins within the mucus and are thought to participate in odorant-receptor binding and, potentially, odorant removal (Buck, 1996).

Olfactory sensory neurons each project a single apical dendrite to the epithelial surface where it extends several non-motile cilia (Getchell, 1986). Located on the surface of each cilium are 7-transmembrane G protein-coupled receptor molecules (Pace et al., 1985). Each OSN expresses only one of a large multi-gene family of receptors throughout their cilia (Buck and Axel, 1991; Treloar et al., 1996; Malnic et al., 1999; Touhara et al., 1999; Serizawa et al., 2000; Bozza et al., 2002), although see (Mombaerts, 2004; Goldman et al., 2005).

Interestingly, the OR gene family comprises the largest gene family with over 1,000 of the total 30,000 genes in mammals (Mombaerts, 1999).

Olfactory signal transduction begins when odorant molecules bind to the G-protein-coupled receptors on the cilia (Pace et al., 1985; Malnic et al., 1999). The binding of odorant molecules to olfactory receptors initiates several chemical cascades within the receptor neurons that generate excitatory responses (Getchell and Shepherd, 1978b; Firestein and Werblin, 1989), although odor-induced inhibitory potentials have also been reported (Dionne, 1992). In general, odorant-receptor binding is thought to increase intracellular cAMP levels, which in turn, causes opening of cyclic nucleotide-gated channels that result in cell depolarization (Getchell and Shepherd, 1978a; Pace et al., 1985; Brunet et al., 1996). Other odorant-evoked pathways have also been discovered including increased production of IP_3 (Breer and Boekhoff, 1991; Schandar et al., 1998) and cGMP (Nakamura and Gold, 1987), although it is unclear how these pathways contribute to receptor responses.

There appears to be a distinct topographical pattern of OR gene expression within the olfactory epithelium. In situ hybridization studies in rodents have revealed that OSNs expressing the same OR gene are all located within one distinct zone (Ressler et al., 1993; Vassar et al., 1993; Sullivan et al., 1995). However, within each of the four zones, the pattern of OR gene expression is seemingly random. This zonal patterning is apparent as soon as OR gene expression can be detected during embryogenesis and does not require the olfactory bulb (Sullivan et al., 1995).

Olfactory receptor neurons respond to overlapping sets of odorants with individual odorants capable of activating more than one receptor type (Sicard and Holley, 1984; Sato et al., 1994; Araneda et al., 2000; Kajiya et al., 2001; Bozza et al., 2002; Duchamp-Viret et al., 2003). Thus, different odors are encoded at the receptor sheet level by different groups of receptor neurons (Malnic et al., 1999; Bozza et al., 2002; Duchamp-Viret et al., 2003). Olfactory receptor neurons then transmit this code to the olfactory bulb where their axons synapse with bulbar output neurons in spherical regions known as glomeruli.

Olfactory Bulb

The zonal compartmentalization seen in the epithelium is then projected onto the olfactory bulb glomerular layer as OSNs in each zone project their axons to corresponding zones in the olfactory bulb (Fujita et al., 1985; Mori et al., 1985; Vassar et al., 1994). Sensory neurons expressing homologous OR genes project their axons to a small subset of specific glomeruli in the olfactory bulb (Ressler et al., 1994; Vassar et al., 1994; Mombaerts et al., 1996; Bozza and Kauer, 1998; Tsuboi, 1999; Treloar et al., 2002), although there is some evidence that glomeruli receive inputs from receptor neurons expressing different receptor types (Treloar et al., 1996). Glomeruli with similar RFs are clustered in the same region of the bulb (Uchida et al., 2000; Inaki et al., 2002) with OSNs expressing the same OR gene projecting to two glomeruli, one on the medial side and one on the lateral side of each bulb (Nagao et al., 2000). Thus, each glomerulus serves as an independent functional unit conveying the receptive field (molecular receptive range) of the receptor neurons that innervate it. Based on this,

exposure to a specific odorant would stimulate a specific subset of receptor neurons, which in turn, would activate a group of glomeruli forming a specific spatial pattern of glomerular activity in the olfactory bulb for that odor based upon the odorant's molecular features (Sharp et al., 1975; Stewart et al., 1979; Guthrie et al., 1993; Friedrich and Korsching, 1997; Rubin and Katz, 1999; Uchida et al., 2000; Xu et al., 2000; Meister and Bonhoeffer, 2001; Spors and Grinvald, 2002; Leon and Johnson, 2003; Bozza et al., 2004).

The glomeruli themselves are made up of an array of OSN axon terminals, output neuron dendrites, and dendrites from various interneurons encased in an astrocyte shell. Anatomical studies have shown a highly compartmental organization within each glomerulus. Based upon OSN axon input, two regions can be identified, one region containing many OSN axon terminals, and another with relatively few OSN axons (Kosaka et al., 1997; Kasowski et al., 1999). The glomeruli of the olfactory bulb appear morphologically similar to glomeruli found in other brain regions such as the thalamus (Pinching and Powell, 1971a).

Several types of interneurons are found among the glomeruli, most notably are periglomerular cells (PG), external tufted cells (ET), and short axon cells (SA). Periglomerular cells are small cells that extend dendrites into single glomeruli (Pinching and Powell, 1971a, b; Shepherd et al., 2004). Different PG subtypes have been identified based on dendritic compartmentalization within glomeruli. For example, a majority of PG cells extend their dendrites into glomerular compartments lacking OSN axon terminals, suggesting that they do not receive input directly from OSNs and mostly likely are associated with output

neurons (Toida et al., 1998; Hayar et al., 2004a). PG cells can also be distinguished based on neurotransmitter production, with both dopaminergic (Halasz et al., 1977; Davis and Macrides, 1982; McLean and Shipley, 1988) and GABAergic (Ribak et al., 1977) cells identified. $GABA_B$ receptors are found only in the glomerular layer of the olfactory bulb (Bowery et al., 1987) and $GABA_B$ agonists have been shown to inhibit mitral cell responses to OSN stimulation (Nickell et al., 1994; Aroniadou-Anderjaska et al., 2000). D_2 receptors are expressed in the glomerular layer, presumably on OSN axons (Nickell et al., 1991; Koster et al., 1999). D_2 agonists block olfactory nerve excitation of mitral cells, while D_2 antagonists increase mitral cell responsiveness (Ennis et al., 2001). Thus, two distinct populations of PG cells appear to serve different roles in glomerular inhibition, one providing presynaptic inhibition of incoming OSN activity via the D_2 system the other providing inhibition at the mitral cell level via $GABA_B$ receptor activation.

Another cell type found in the glomerular layer is the external tufted cell. These cells are located within or immediately deep to the glomerular layer and project their primary dendrites into the glomeruli (Pinching and Powell, 1971a, b, c). ET cells extend a primary dendrite that diverges exclusively in single glomeruli (Aungst et al., 2003; Hayar et al., 2004a). Within each glomeruls, ET cell dendrites receive excitatory monosynaptic input from OSN axons (Hayar et al., 2004a; Hayar et al., 2004b) as well as form reciprocal synapses with PG dendrites similar to those seen between mitral and granule cells (Pinching and Powell, 1971b). Unlike deeper tufted cells, ET cells lack secondary dendrites and

restrict their primary axon to only part of the glomerulus (Pinching and Powell, 1971b). ET cell axons extend throughout the periglomerular region, giving off collaterals that extend onto neighboring PG and SA cells (Pinching and Powell, 1971a, b, c; Aungst et al., 2003; Hayar et al., 2004a).

The last major cell type found in the glomerular layer is the short axon cell. In contrast to PG cells, SA cells form excitatory interglomerular connections and are thought to be glutamatergic (Aungst et al., 2003). SA cells extend dendrites into neighboring glomeruli, while projecting axons to glomeruli up to 1 mm (15-18 glomeruli) away (Pinching and Powell, 1971a, b, c; Aungst et al., 2003). Together, the short axon cells, external tufted cells, and periglomerular cells form a circuit of lateral inhibition within the glomerular layer (Aungst et al., 2003; Hayar et al., 2004a). When excited by presynaptic input into their corresponding glomeruli, the ET cells would then excite the SA and PG cells associated with neighboring glomeruli, thus forming an on-center, off-surround network (Aungst et al., 2003; Hayar et al., 2004a). Based on this, the glomeruli receiving the strongest OSN input would inhibit the output of neighboring glomeruli; thus forming the first stage of processing of odorant information within the olfactory bulb.

This pattern of afferent input is then transferred to the main output cells of the olfactory bulb, the mitral cells. Mitral cells have a primary dendrite that extends apically and arborizes inside specific glomeruli where it synapses with receptor neuron axons (Price and Powell, 1970b; Pinching and Powell, 1971a). In mammals, mature mitral cells send a primary dendrite into a single glomerulus

(Lin et al., 2000; Matsutani and Yamamoto, 2000). Secondary dendrites of the mitral cells extend laterally through the layer deep to the glomeruli, the external plexiform layer (EPL), forming dendrodendritic reciprocal synapses with smaller axonless interneurons known as granule cells (Price and Powell, 1970e; Mori et al., 1983; Orona et al., 1984; Shepherd et al., 2004). Mitral cell lateral dendrites can extend as far as 1mm across the bulb (Mori et al., 1983; Orona et al., 1984). Mitral cells extend their axons deep into the olfactory bulb where they come together to form the lateral olfactory tract (LOT), which terminates in the olfactory cortex (Shepherd et al., 2004). In addition to forming the LOT, mitral cell axons also give rise to thin collaterals that terminate in the granule cell layer as well as the layer immediately deep to the mitral cell layer, the internal plexiform layer (IPL) (Kishi et al., 1984; Orona et al., 1984). Mitral cells are glutamatergic; they release glutamate from their axon terminals in the olfactory cortex as well as from their lateral dendrites (Wellis and Kauer, 1993; Isaacson and Strowbridge, 1998; Wada et al., 1998).

Tufted cells similar to those found in the glomerular layer can also be found in the external plexiform layer. These cells are generally divided into two types: internal tufted and middle tufted cells (Shepherd et al., 2004). These cells extend a single apical dendrite into their associated glomerulus as well as having lateral dendrites that extend across the EPL. Internal tufted cells are located at the EPL-mitral cell layer border and are morphologically similar to mitral cells. Most tufted cells are located in the middle of the EPL and are considered middle tufted cells. Middle tufted cell axons extend through the IPL and join the LOT

where they travel to the anterior olfactory cortex, anterior piriform cortex, and the olfactory tubercle (Haberly and Price, 1977; Schoenfeld et al., 1985).

A population of tufted cells also forms an associational system within the bulb where it links lateral and medial glomerular columns on opposite sides of the bulb that receive input from OSNs expressing the same odorant receptor (Schoenfeld et al., 1985; Liu and Shipley, 1994; Belluscio et al., 2002). The tufted cells associated with one glomerulus project axons that terminate on the dendrites of granule cells associated with the opposite glomerulus (Liu and Shipley, 1994; Belluscio et al., 2002).

Besides differences in location, physiological differences between tufted and mitral cells have been observed. For example, tufted cells show lower excitation thresholds to olfactory nerve stimulation (Schneider and Scott, 1983) as well as less lateral inhibition (Christie et al., 2001; Nagayama et al., 2004). Middle tufted cells and mitral cells also receive inhibitory input from distinct subsets of interneurons (Mori et al., 1983; Orona et al., 1983; Macrides et al., 1985; Greer, 1987). In addition, tufted cells respond to odorants with higher firing rates than mitral cells (Nagayama et al., 2004). These anatomical and physiological differences suggests that mitral and tufted cells may serve different functions and possibly contribute to different aspects of the olfactory code (Macrides et al., 1985; Nagayama et al., 2004; Shepherd et al., 2004).

Immediately deep to the mitral cell layer is the thin internal plexiform layer (IPL), which is relatively low in cell density. This layer is made up of mitral/tufted cell axons and granule cell dendrites. Axons from neuromodulatory regions such

as the raphe nucleus (serotonin) (McLean and Shipley, 1987), the locus coeruleus (norepinephrine) (Shipley et al., 1985), and HDB (acetylcholine) (Zaborszky et al., 1986) also terminate in the IPL.

Below the IPL is a layer of GABAergic neurons known as the granule cell layer (GCL) (Shepherd et al., 2004). Granule cells (GCs) are relatively small, axonless interneurons that are grouped together in small horizontal clusters. The primary dendrites of the GCs extend into the EPL where they branch out and form reciprocal synapses with the secondary dendrites of mitral and tufted cells (Price and Powell, 1970e). Neighboring GCs are thought to be electrically coupled through gap junctions that could serve to synchronize GC activity (Reyher et al., 1991). GCs respond to antidromic activation of mitral cells, stimulation of the ONL, as well as odor stimulation (Mori and Kishi, 1982; Wellis and Scott, 1990).

Different classes of GCs can be distinguished based on soma location and dendritic synapses. Superficial GC dendrites extend into the superficial EPL and synapses mainly with tufted cell dendrites (Mori et al., 1983; Orona et al., 1983; Greer, 1987). Deep GC dendrites only extend into the deeper parts of the EPL and synapse with mitral cell dendrites (Mori and Kishi, 1982; Orona et al., 1983). Another population, the intermediate GCs, have dendrites that ramify into all parts of the EPL (Shepherd et al., 2004).

Centrifugal inputs from olfactory cortical areas also terminate in the granule cell layer. Different subsets of fibers from the AOC project to the superficial and deep parts of the GCL (De Olmos et al., 1978; Haberly and Price,

1978b; Davis and Macrides, 1981; Luskin and Price, 1983a; Shipley and Adamek, 1984). Taken together, the segregation of tufted and mitral cell targets, centrifugal specificity, and the laminar distribution of GCs suggests mitral and tufted cells interact with different GC populations, which further supports the idea that the olfactory bulb uses two, possibly independent, parallel odor coding pathways (Orona et al., 1983; Nagayama et al., 2004).

Projections from the PC also terminate in the GCL, with more posterior parts of PC projecting to progressively to deeper regions of the GCL (Rall and Shepherd, 1968; Price and Powell, 1970a; Mori and Takagi, 1978; Jahr and Nicoll, 1982). These projections are thought to be excitatory (Nakashima et al., 1978; Davis and Macrides, 1981; Luskin and Price, 1983b) and could elicit granule cells to inhibit mitral cell activity. This centrifugal feedback allows for an inhibitory mechanism from cortical regions in addition to the feedforward inhibition and lateral inhibition of mitral cell activity present in the bulb. It is hypothesized that these local interactions aid in the bulb's ability to spatially and possibly temporally encode odors.

Mitral-Granule Cell Interactions

In the EPL, more than 80% of all synapses are involved in reciprocal connections (Shepherd et al., 2004). A majority of these synapses are between the lateral dendrites of mitral/tufted cells and the spines (gemmules) on granule cell dendrites (Rall et al., 1966; Rall and Shepherd, 1968). Interestingly, this synapse was the first dendrodendritic synapse identified in the nervous system.

Early microscopy and electrophysiological experiments revealed that mitral/tufted (M/T) cell dendrites form type 1 (excitatory) synapses onto granule cell dendrites, while granule cell dendrites form type 2 (inhibitory) synapses onto M/T cell dendrites (Rall et al., 1966; Price and Powell, 1970d; Jahr and Nicoll, 1982; Schneider and Scott, 1983). In this circuit, the output from the OSN is conveyed by action potentials to the M/T cell soma and then back-propagated into the apical as well as lateral dendrites (Bischofberger and Jonas, 1997; Chen et al., 1997; Margrie et al., 2001; Chen et al., 2002; Christie and Westbrook, 2003). This activity is sufficient to stimulate glutamate release from the lateral dendrites onto granule cell spines (Jahr and Nicoll, 1982; Isaacson and Strowbridge, 1998; Schoppa et al., 1998). Glutamate would then stimulate GCs to release GABA back onto M/T cells, causing inhibition (Rall et al., 1966; Jahr and Nicoll, 1980; Nowycky et al., 1981; Isaacson and Strowbridge, 1998). The extent of this inhibition is dependent upon distance from the M/T cell soma. For example, proximal GABA release inhibits AP firing by blocking somatic currents, while distal GABA release can block AP back-propagation through the lateral dendrites (Lowe, 2002; Xiong and Chen, 2002).

The M/T-GC synaptic interactions give rise to several different mechanisms of altering mitral cell output. First, granule cells can mediate mitral/tufted cell feedback inhibition. In this situation, a single M/T cell activates GC spines associated with its own dendrites leading to GABA release from the GC back onto the same M/T cell (Nowycky et al., 1981; Jahr and Nicoll, 1982; Isaacson and Strowbridge, 1998). This self-inhibition can be blocked with NMDA

receptor antagonists suggesting that M/T self-inhibition is mediated through NMDA receptors in GC spines (Isaacson and Strowbridge, 1998; Schoppa et al., 1998; Chen et al., 2000; Halabisky et al., 2000). However, evidence of non-NMDA receptor-mediated feedback inhibition of M/T cells (Wellis and Kauer, 1993; Isaacson and Strowbridge, 1998; Isaacson, 2001) suggests multiple pathways for GC cell feedback inhibition of M/T cells.

Second, GCs could induce M/T cell local lateral inhibition. In this case, M/T cells could strongly activate GC spines leading to a spread of depolarization to neighboring GC spines associated with other nearby mitral cells. (Jahr and Nicoll, 1982; Woolf et al., 1991; Isaacson and Strowbridge, 1998; Egger et al., 2003). Additionally, these reciprocal synapses could mediate a more global form lateral inhibition. In this case, strongly activated GCs could fire action potentials that could propagate throughout their dendritic trees, thus releasing GABA onto all the associated M/T cells (Chen et al., 2000; Egger et al., 2003). Based on mitral and granule cell dendritic lengths, it is possible that each granule cell could synapse with several mitral cells from many glomeruli covering a wide region of the bulb. Thus, this lateral and global inhibition could be important in reducing signal to noise ratios and sharpening M/T cell tuning specificity, which would serve to enhance the ability of the olfactory bulb to process and discriminate odors (Rall et al., 1966; Mori et al., 1999).

Another consequence of M/T-GC reciprocal synaptic interactions is the generation of oscillatory activity. Both odor-induced and intrinsic oscillations are seen in the olfactory bulb (Adrian, 1950; Freeman, 1972; Neville and Haberly,

2003; Lagier et al., 2004; Fletcher et al., 2005) and these oscillations have been proposed to be important in olfactory bulb odor coding (Laurent et al., 2001). Theoretical models and experimental studies suggest that gamma (35-100 HZ) band oscillations are generated by the negative feedback loop between M/T cells and GCs (Rall and Shepherd, 1968; Eeckman and Freeman, 1990; Kashiwadani et al., 1999; Neville and Haberly, 2003; Lagier et al., 2004). Further support for this idea comes from recent studies showing that $GABA_A$ receptor antagonists in the EPL effectively block LFP gamma oscillatory activity (Lagier et al., 2004).

Although current source density analysis has suggested that gamma frequency oscillations are generated mainly by granule cell synaptic currents (Buonviso et al., 2003; Neville and Haberly, 2003), other cellular events could potentially contribute. For example, M/T cells can exhibit 20-40 Hz subthreshold oscillations that persists even in the presence of GABA antagonists (Chen and Shepherd, 1997; Heyward et al., 2001). M/T cell action potentials, when in phase with the LFP, tend to occur in the descending phase of the oscillation and GC action potentials show no phase relationship to the LFP suggesting they do not contribute to the LFP as much as synaptic potentials and subthreshold membrane oscillations (Freeman, 1968; Kashiwadani et al., 1999; Laurent et al., 2001; Lagier et al., 2004).

Processing of Molecular Information in the Olfactory Bulb

A central goal in the study of olfaction is to determine how a molecule or group of molecules leads to an odor percept. Thus, the olfactory system must transform odorant information into a spatiotemporal pattern of neural activity that

can be transferred throughout. The OSNs in the epithelium along with the olfactory bulb are thought to act as a feature detection system. In this way, odorants would be encoded at the receptor sheet as a collection of features represented by different patterns of OSN activity.

Since OSNs expressing the same receptor proteins all converge onto one, or a small group of specific glomeruli in the olfactory bulb, the pattern of odor-induced presynaptic activity seen in the glomerular layer would represent the subset of receptor neurons activated by the odorant. This pattern of activity is not simply reiterated onto the cortex by the mitral/tufted cells, but rather, recent data suggest a two-stage system by which afferent information is further enhanced through mechanisms such as feedback and lateral inhibition at both the glomerular and mitral cell level. For example, as discussed above, center-surround lateral inhibition can occur among glomeruli in the olfactory bulb through the short axon cell-periglomerular cell circuit (Aroniadou-Anderjaska et al., 1997; Wachowiak and Cohen, 1999; Aroniadou-Anderjaska et al., 2000; Aungst et al., 2003). This level of processing provides both presynaptic and postsynaptic inhibition within glomeruli (Wellis et al., 1989; Imamura et al., 1992; Katoh et al., 1993). Based on this, patterns of afferent activity could be shaped by inhibitory interactions to help reduce overlap between similar odor-evoked patterns of glomerular activity.

The next stage of processing involves granule cell inhibition of mitral/tufted cell activity. Mitral/tufted cells appear to have overlapping but individually distinct odorant receptive fields (molecular receptive ranges) with individual mitral cells

15

responding to different odor classes or features. Lateral inhibition of neighbor mitral cell activity via dendrodendritic reciprocal synapses could aid in fine-tuning individual olfactory bulb responses to specific odors. Since mitral cells that are excited by a group of similar molecular features might all be activated to varying degrees, lateral inhibition ensures that only the mitral cells encoding the specific features of the odor are sending on the information and not mitral cells excited by receptor neurons with similar molecular specificity. Recent evidence supports this idea with the discovery of center-surround-like inhibition of mitral cell activity (Luo and Katz, 2001). In this case, activation of a mitral cell's principal glomerulus leads to that mitral cell's activation, while activation of surrounding glomeruli leads to inhibition.

Thus, this two-stage processing and the resulting lateral inhibition could potentially transform the odor map seen at the glomerular level into a new map of odor identity at the mitral cell level. This refined map would be conveyed on to the higher olfactory centers. In this way, at each stage of odor processing from epithelium to cortex, the spatiotemporal map for a given odorant could be fined tuned to reduce representational overlap and contribute to the ability of the olfactory system to identify and discriminate odors.

In addition to spatial patterns, temporal activity patterns could also play a role in the processing of molecular information. In pulmonates, afferent input is not static, but oscillates with respiratory cycle. Thus, respiratory rhythm oscillations, odor-evoked high-frequency oscillations, and intrinsic oscillations ,together with specific spatially activated glomerular patterns could serve to

create temporally as well as spatially dynamic map of activity in the olfactory bulb. For example, high temporal resolution voltage-sensitive dye imaging of odor-evoked glomerular activity has shown olfactory bulb activity phase locking to the nasal respiration cycle as well as sequential activation of glomerular units during odor stimulation (Spors & Grinvald, 2002). Additionally, both single-unit and intracellular recordings from mitral cells have shown complex temporal odor-evoked responses (Chaput and Holley, 1985; Wellis et al., 1989; Wellis and Scott, 1990; Philpot et al., 1997). Taken together, these results suggest a dynamic olfactory bulb odor coding mechanism in which changing patterns of spatially active glomeruli would serve as the basis of the early olfactory code.

Olfactory Bulb Oscillations

Both odor-induced and spontaneous LFP oscillations have been reported in a variety of vertebrates, yet their exact relationship to olfactory odor coding is yet to be fully understood (Adrian, 1938; Adrian, 1942; Adrian, 1950; Bressler and Freeman, 1980; Satou, 1990; Neville and Haberly, 2003; Fletcher et al., 2005). Three main olfactory system oscillatory frequencies have been identified: theta (3-12 Hz), beta (15-40 Hz), and gamma (35-100 Hz). Theta frequency oscillations are highly coupled to respiration and have been found in the olfactory bulb and hippocampus during sniffing, suggesting they may play a role synchronizing associated brain areas during odor investigation and learning (Ravel and Pager, 1990; Kay and Laurent, 1999; Spors and Grinvald, 2002).

High frequency oscillations are thought to reflect synchronous activation of olfactory bulb cells. Based on this, it has been suggested that odor coding would

17

be dependent on the precise synchronization of dynamic assemblies of coincident mitral cell firing as reflected by increased odor-evoked gamma oscillations (Laurent, 2002). Interestingly, this spike timing-dependent theory of odor coding is based mostly on work done in the insect olfactory system, which is anatomically and physiologically distinct from the mammalian olfactory system (Laurent, 2002). Evidence for this theory comes from experiments in which altered olfactory oscillations affected odor discrimination (Laurent and Davidowitz, 1994; Stopfer et al., 1997; Friedrich and Laurent, 2001). For example, in honeybees, desynchronization of projection neuron ensembles by the application of the GABA antagonist picrotoxin leads to impaired discrimination of molecularly similar odorants, but not dissimilar odorants (Stopfer et al., 1997).

Despite the insect models, evidence for this mechanism in vertebrates, especially mammals, is quite sparse. For example, a recent study using $GABA_A$ receptor $\beta3$ subunit deficient mice suggested that gamma frequency oscillations are critical for odor discrimination in that disruption of the normal network oscillations lead to altered behavioral acuity (Nusser et al., 2001). These mice lack functional $GABA_A$ receptors on granule cells, and as a result, display increased local field potential oscillatory power. These results however, are somewhat difficult to interpret as the $\beta3$ subunit deficient mice displayed increased oscillatory activity with inconsistent discriminatory ability as compared to the wildtype controls.

However, studies in awake mammals have shown olfactory bulb gamma response patterns are modulated more by behavioral context of the odorant than the odorant itself (Freeman and Schneider, 1982; Gray and Skinner, 1988; Ravel et al., 2003). For animals highly trained in odor discrimination tasks, gamma oscillatory activity increases prior to odor sampling, suggesting potential top-down influences on attention and thus gamma band activity (Ravel et al., 2003).

Beta band activity however, seems to be modulated in a more odor-specific way (Kay and Laurent, 1999; Ravel et al., 2003). Odor learning is associated with an increase in the amplitude and duration of the odor-induced beta band oscillations (Ravel et al., 2003). Considering that LFP oscillatory activity reflects activation of olfactory bulb output cells, increased oscillatory power could be due to either tighter, more precise synchronization of mitral cell firing or to an increased number of recruited neurons. Although data from the locust olfactory system suggests increased synchrony (Laurent, 2002), recent evidence focusing on experienced induced changes of mitral cell odor responses suggest that experience (learning) causes a shift in mitral cell responses toward the experienced odor (Fletcher and Wilson, 2003). These data suggests that the increased beta band activity seen after learning could be due to a learning-induced shift in mitral cell receptive fields such that many cells show increased responsiveness to the experienced odor, thereby causing an increase in the number of cells activated by that odor and thus, increased LFP oscillations.

Olfactory Cortex

19

Olfactory cortex has been defined as those areas receiving direct synaptic input from the olfactory bulb (Price, 1973). These areas include the anterior olfactory cortex, medial olfactory cortex, olfactory tubercle, piriform cortex, portions of the amygdala, and the entorhinal cortex (Haberly, 2001). In addition to the olfactory cortex many other brain areas are involved in odor processing and memory. Physiological and behavioral studies have offered insight into several secondary olfactory structures critically involved in olfactory related tasks. Theses areas include, but are not limited to, orbitfrontal cortex, amygdala, hypothalamus, mediodorsal nucleus of the thalamus, and prefrontal cortices.

Several features make the olfactory cortex distinct from other sensory cortical areas. First, the olfactory cortex has a much simpler laminar organization. In general, it contains only three layers as opposed to the six layers seen in neocortex. Another striking feature of the olfactory cortex is that there is no thalamic relay between receptor input and the cortex. In other sensory systems, thalamocortical relays can refine sensory input prior to its arrival in the cortex (Sherman, 1993). Despite these differences, the olfactory cortex remains similar to other sensory cortical areas in cell type, synaptic physiology, and local circuitry. For example, as in other thalamocortical systems there is a heavy feedback projection from olfactory cortex onto the olfactory bulb (Price and Powell, 1970c; Luskin and Price, 1983a; Neville and Haberly, 2004).

Anterior Olfactory Cortex

Immediately caudal to the main olfactory bulb is the first structure of the olfactory cortex, the anterior olfactory nucleus (AON). The AON was originally

considered a nucleus, but it is actually a laminated cortical structure made up of pyramidal cells (Herrick, 1924; Haberly and Price, 1978a). Based on this, Haberly has suggested that the AON be renamed the anterior olfactory cortex (AOC) (Haberly, 2001; Neville and Haberly, 2004). The AOC receives direct input from both mitral and tufted cells of the OB (Haberly and Price, 1977; Schoenfeld and Macrides, 1984; Scott et al., 1985) as well as input from other olfactory related areas such as piriform cortex, entorhinal cortex, amygdala, and hippocampus (Luskin and Price, 1983a, b; Van Groen and Wyss, 1990). In addition, the AOC receives modulatory input from the raphe nuclei, the locus coeruleus, and the nucleus of the diagonal band (De Carlos et al., 1989; McLean and Shipley, 1991; Shipley and Ennis, 1996). The output of the AOC projects mainly to the ipsilateral and contralateral olfactory bulbs, but projections to other olfactory areas such as the piriform cortex have been identified (De Olmos et al., 1978; Davis and Macrides, 1981; Luskin and Price, 1983a).

The AOC consists of four major subdivisions based upon their terminal fields within the olfactory bulb. The lateral, posterior, ventral, and dorsal subdivisions of the AOC project bilaterally to the deep glomerular layer as well as the superficial portion of the granule cell layer (Davis and Macrides, 1981; Luskin and Price, 1983a). These lateral and dorsal subdivisions also project to the contralateral bulb where they terminate within the granule cell layer only (Davis and Macrides, 1981). The medial subdivision projects to the granule cell layer of the ipsilateral bulb, while the external subdivision projects mainly to the contralateral bulb (Davis and Macrides, 1981; Shipley and Adamek, 1984).

The different subdivisions of the AOC may serve different roles in olfactory coding. For example, the external subdivision, the pars externa (AOCpE), is thought to be an integral part of an intrabulbar association system similar to the subpopulation of tufted cells that project directly to the contralateral bulb. In this case, the axons from the external subdivision cross the midline and project to the contralateral bulb via the anterior commissure (Davis and Macrides, 1981; Schoenfeld and Macrides, 1984). The centrifugal fibers terminate within the olfactory bulb with some degree of rostro-caudal topographical organization (Schoenfeld and Macrides, 1984), suggesting that the external subdivision of the AOC may link glomerular columns of similar specificity between the two bulbs. In this way, the AOCpE may ensure the pattern of odor-evoked activity is similar between the two bulbs.

The ipsilateral projections from the other AOC subdivisions also show some topographical organization. In this case however, the organization is more radially oriented (Luskin and Price, 1983a). Fibers from the pars medialis of the AOC project to the deep half of the GCL, while fibers from the rest of the AOC project to the superficial GCL (De Olmos et al., 1978; Haberly and Price, 1978b; Davis and Macrides, 1981; Luskin and Price, 1983a; Shipley and Adamek, 1984). This anatomical evidence suggests that there are potentially two, parallel pathways for odor coding within the olfactory system. One pathway (mitral cells) may be more concerned with odor feature discrimination, while the other pathway (tufted cells) could focus on odor intensity/detection. In support of this, recordings from mitral cells suggest they are better at discriminating odorants

than AOC cells (Boulet et al., 1978). In addition, middle tufted cells, which project to primarily to the AOC, tend to show less inhibition to related odorants and lower thresholds for spike responses (Scott et al., 1980; Schneider and Scott, 1983; Scott et al., 1985; Nagayama et al., 2004).

In addition to centrifugal input to the bulb, AOC axons also project to anterior piriform cortex. As with input to the bulb, there seems to be some loose topographical organization (Luskin and Price, 1983a). In this case, the more ventromedial parts of the AOC project to the ventromedial portion of anterior piriform cortex, while the more dorsolateral parts of the AOC project more dorsolaterally (Haberly and Price, 1978a; Luskin and Price, 1983a).

Piriform Cortex

As the AOC extends caudally and laterally, it transitions into piriform cortex (PC). Piriform cortex extends ventrolaterally along the entire length of the LOT. The piriform cortex consists of three cellular layers and is less complex than the six-layered neocortex (Haberly and Price, 1978b). The PC is divided into two regions: the anterior piriform cortex (APC) and the posterior piriform cortex (PPC). APC and PPC can be distinguished by the termination of the LOT, with PPC extending caudally beyond the myelinated fibers (Neville and Haberly, 2004).

The most superficial plexiform layer, layer I, consists mainly of dendrites and axons, with a few neurons. It is divided into two subdivisions, Ia and Ib. Layer Ia consists of M/T cell axons that branch off from the LOT into many smaller collaterals that spread tangentially across the layer (Price, 1973; Haberly

23

and Price, 1977). While layer Ia receives afferents from the LOT, layer Ib receives input mainly from association fibers from the PC as well as other areas of olfactory cortex (Price, 1973).

Layer II is a tightly packed, narrow cell layer that also can be divided into two sub-layers. IIa is more superficial and contains semilunar cells, while the deeper IIb is composed of pyramidal cell soma whose dendrites extend into layer I (Haberly and Price, 1978b). Layer III is a thicker layer that contains pyramidal cells, deeper mutlipolar cells, and associational axons (Neville and Haberly, 2004). Layer III is graded in structure, with cell density decreasing with decreasing depth (Haberly, 1983). Deep to layer III is the endopiriform nucleus. This nucleus, sometimes termed layer IV, is made up of spiny multipolar neurons (Tseng and Haberly, 1989).

The principle neuron of the piriform cortex is the pyramidal cell. These cells are morphologically similar to pyramidal cells in areas of cerebral cortex in that they possess a primary apical dendritic tree that extends toward the cortical surface and arborizes in layer Ia and Ib as well as numerous basal dendrites that can extend several hundred microns deep to the cell body (Haberly, 1983; Neville and Haberly, 2004). The primary axon extends deep into the cortex where it terminates on other pyramidal cells and interneurons. The myelinated primary axon gives rise to many unmyelinated collaterals that spread out into layers Ib and III and synapse with neighboring cells (Haberly and Presto, 1986). It appears that pyramidal cells make excitatory synapses on different subsets of pyramidal cells, synapsing on the basal dendrites of nearby pyramidal cells and

24

on the apical dendrites of cells farther away (Haberly, 1985). This associational fiber system exhibits topographical specificity. For example, the semilunar cells of layer IIa project to all parts of the piriform cortex, whereas association fibers from pyramidal cells project primarily caudally (Haberly and Price, 1978a, b). These association fibers terminate primarily in layer Ib (Haberly and Price, 1978a, b). As stated above, pyramidal cells also project axons to the olfactory bulb where they synapse onto granule cells (Rall and Shepherd, 1968; Price and Powell, 1970a; Mori and Takagi, 1978; Jahr and Nicoll, 1982). In addition to the associational and centrifugal connections, the PC also projects to several other olfactory and non-olfactory brain regions. These areas include entorhinal cortex, perirhinal cortex, orbital cortex, insular cortex, amygdala, hypothalamus, and thalamus (Luskin and Price, 1983b; Price et al., 1991; Johnson et al., 2000; Neville and Haberly, 2004).

Several different types of interneurons are located within the cortex as well. Subsets of these cells are GABAergic and are thought to be the main source inhibition within the cortex. For example, layers II and III contain a large number of mutlipolar neurons extending axons that arborize around pyramidal cell bodies. These neurons are thought to provide strong inhibition to the pyramidal cell population (Haberly, 1983; Satou et al., 1983; Tseng and Haberly, 1988; Ekstrand et al., 2001; Neville and Haberly, 2004). Another group of inhibitory neurons is located in layer Ia and have dendrites running parallel to the LOT. These horizontal cells, the largest neurons in the cortex, receive input from the LOT as well as from pyramidal cells and possess dendrites that synapse onto

the apical dendrites of the pyramidal cells (Haberly et al., 1987). Together, these interneurons can span large regions of piriform cortex and can participate in both feedforward and feedback inhibition within the cortex.

Based on this anatomy, pyramidal cells that are excited by afferent fibers would excite other pyramidal cells via their apical dendrites and excite non-pyramidal cells involved in both inhibitory feedback and feedforward loops (Haberly, 1985; Haberly and Bower, 1989; Neville and Haberly, 2004). Each pyramidal cell receives input from a large number of other pyramidal cells via both afferent and association fibers while also providing input to many cells. This organization is consistent with physiological and imaging data suggesting an ensemble code for odor identity where odors are represented by a spatially distributed array in a large number of different neurons (Sharp et al., 1977; Haberly, 2001; Wilson, 2001b; Illig and Haberly, 2003; Sugai et al., 2005). Genetic tracing of specific receptor types mapping to patchy, overlapping areas of olfactory cortex has further lent evidence to this idea (Zou et al., 2001).

Olfactory Cortex Oscillations

Similar to the OB, the PC also displays temporal patterns of both intrinsic and odor-evoked activity. For example, 3 to 8 Hz respiratory-coupled oscillations have been described in the PC (Freeman, 1959). These oscillations presumably reflect M/T cell activity during inhalation. High frequency oscillatory activity has also been reported within the PC. For example, spontaneous as well as odor-evoked beta-band (12 to 35 Hz) oscillations have been reported (Freeman, 1959; Bressler, 1984; Vanderwolf and Zibrowski, 2001). Beta-band oscillations are

thought to be generated in the PC and/or the entorhinal cortex and propagate to the OB via centrifugal innervation (Bressler, 1984; Kay and Freeman, 1998; Neville and Haberly, 2003). The functional significance of beta-band oscillations within the PC remains unclear. However, animals highly trained in olfactory discrimination tasks show increased odor-evoked beta-band activity in the olfactory bulb (Ravel et al., 2003). Since OB beta oscillations are generated in the PC, the increased OB oscillations may reflect learning-induced changes within the PC that are fedback into the bulb.

Gamma frequency oscillations also occur in the PC and have been shown to be highly coherent with the OB oscillations (Freeman, 1978; Bressler, 1984; Kay and Freeman, 1998). The source of PC gamma oscillations appears to be in the OB as they are abolished by transecting the LOT (Neville and Haberly, 2003). Gamma oscillations observed in the PC are thought to primarily reflect afferent input patterns to the PC as gamma oscillations are abolished by olfactory bulb removal (Becker and Freeman, 1968).

Encoding of Olfactory Information

In the epithelium, an odorant can bind to several different odorant receptors, each one recognizing different parts of its molecular structure. In this way the receptor sheet, together with the olfactory bulb, can act as an odorant feature detection system in which an individual odorant would be encoded by a subset of temporally synchronous, yet spatially diverse pattern of cell activity. This map, however, is not simply reiterated within the cortex. Maps of odor-evoked activity appear highly spatially distributed and overlap broadly for

different odors (Illig and Haberly, 2003; Sugai et al., 2005). Anatomical tracing experiments also show extensive overlap of pyramidal cells receiving input from different olfactory receptor neurons (Buonviso et al., 1991; Zou et al., 2001). Together, these studies suggest that pyramidal cells in the PC receive input from highly overlapping sets of M/T cell populations. In addition, pyramidal cells make extensive associational connections onto other pyramidal cells throughout the olfactory cortex. Together these connections create a network of spatially distributed overlapping ensembles of cells capable of integrating inputs from several different receptor types.

Exposure to an odor would activate specific activity patterns encoding odorant feature information within the bulb. These patterns would then converge on subsets of pyramidal neurons within the PC. Through experience, these features would be bound together into unique odor objects, much like the facial recognition cells in visual inferotemporal cortex (Haberly, 2001; Wilson, 2001a; Wilson, 2003; Wilson and Stevenson, 2003).

In addition to odor identity coding, the PC may participate in odor intensity coding as well. As stated above, more superficially located tufted cells project mainly to more rostral regions of the AOC and PC. In addition, these cells appear to have lower activation thresholds than mitral/tufted cells projecting to more caudal regions of cortex. Based on this, it has been hypothesized that the rostro-caudal connectivity patterns may provide the basis for intensity coding within the olfactory system. Recent support for this view has come through optical imaging studies of odor-evoked activity showing that odorants at lower

concentrations activated more rostral areas of the APC (Sugai et al., 2005). Given that odorants elicit broadly overlapping activity patterns across the APC, it appears that the PC may not only provide information about odor identity, but simultaneously provide information about the odor's intensity as well.

Chapter 2

Olfactory Bulb Mitral-Tufted Cell Plasticity: Odorant-Specific Tuning Reflects Previous Odorant Exposure[1]

Abstract

Olfactory system second-order neurons, mitral-tufted cells, have odorant receptive fields (ORFs) (molecular receptive ranges in odorant space for carbon chain length in organic odorant molecules). This study quantified several dimensions of these excitatory odorant receptive fields to novel odorants in rats and then examined the effects of passive odorant exposure on the shape of the ORF-tuning curve. ORFs for carbon chain length of novel ethyl esters (pure odorants that the animals had not been exposed to previously) were determined before and after a 50 sec prolonged exposure to one of the odorants. In response to novel odorants, quantitative analysis of mitral-tufted cell excitatory ORFs revealed that the median ORF width spanned 3-4 carbons, generally with a single-most excitatory odorant. Exposure to either the most excitatory odorant (ON-PEAK) or an odorant that was two carbons longer (OFF-PEAK) for 50 sec produced whole ORF suppression immediately after the end of the prolonged exposure, with the ON-PEAK exposure producing the greatest suppression. These results are consistent with a feature-detecting function for mitral-tufted cells. Redetermination of the ORF 15 and 60 min after the exposure revealed that OFF-PEAK exposure produced a reduction in responsiveness to the best odorant and an increase in responsiveness to the exposed odorant. In contrast, exposure to the ON-PEAK odorant or no odorant did not affect ORFs. Given that mitral-tufted cells receive exclusively excitatory input from olfactory receptor neurons expressing identical receptor proteins, it is hypothesized that experience-induced mitral-tufted cell ORF changes reflect modulation of lateral and centrifugal olfactory bulb circuits.

Introduction

Experience can influence both behavioral and physiological responses to sensory input. Both associative conditioning and, in certain circumstances, stimulus exposure alone can modify cortical sensory neuron receptive fields (RFs) and, consequently, behavioral sensory abilities (Gilbert et al., 2001). In thalamocortical sensory systems, RF plasticity is believed to be dependent on the heterogeneity and plasticity of afferent and association inputs (Hebb, 1949; Weinberger, 1995; Buonomano and Merzenich, 1998).

Similarly, mammalian olfactory system responses to odors can change with experience. For example, associative conditioning can alter olfactory bulb (OB) glomerular activity patterns (Leon, 1987; Wilson and Sullivan, 1994), OB output neuron (mitral-tufted cell) responses (Leon, 1987; Wilson and Sullivan, 1994; Faber et al., 1999), and local field potential oscillations (Freeman and Schneider, 1982; Kendrick et al., 1992; Ravel et al., 2003). OB odor response patterns can also be modified by simple odor exposure (Buonviso and Chaput, 2000; Spors and Grinvald, 2002) and by odor deprivation (Guthrie et al., 1990; Wilson and Sullivan, 1995). Experience can also modify odor response patterns in olfactory cortical neurons (Litaudon et al., 1997; McCollum et al., 1991; Schoenbaum et al., 1999; Wilson, 2000a). These changes in olfactory system response patterns may underlie both the memory for odors with acquired significance (Freeman and Schneider, 1982; Kendrick et al., 1992; Wilson and Sullivan, 1994; Ravel et al., 2003) and learned changes in behavioral olfactory acuity (Wilson and Stevenson, 2003).

Although changes in mitral-tufted cell responses to learned odors have been reported previously, the effects of odor experience on mitral-tufted cell odorant receptive fields (ORFs) have not. Mitral-tufted cell ORFs (molecular receptive range; Imamura et al., 1992; Mori and Yoshihara, 1995) are believed to primarily reflect the excitatory input that mitral-tufted cells receive on their apical dendritic tuft from a homogenous population of olfactory receptor neurons (ORNs), all expressing the same olfactory receptor protein (Vassar et al., 1994; Tsuboi et al., 1999). In mammals, individual mitral-tufted cells receive input from a single glomerulus and thus should have ORFs that primarily reflect the ORFs of their afferent receptor neurons (Bozza and Kauer, 1998; Luo and Katz, 2001). In addition to this excitatory receptor neuron input to the apical dendrite, mitral-tufted cell ORFs are also influenced by inputs to their extensive lateral dendrites. The inputs to lateral dendrites are primarily inhibitory (Yokoi et al., 1995; Shepherd and Greer, 1998), although there is evidence of excitatory (Isaacson, 1999) and autoexcitatory (Aroniadou-Anderjaska et al., 1999) activity.

On the basis of hypothesized mechanisms of experience-induced change in RFs of cortical neurons in other sensory systems (Gilbert et al., 2001), the unique anatomy of the olfactory receptor neuron-glomerulus-mitral-tufted cell circuit might suggest unique consequences of experience on mitral-tufted cell ORFs. For example, given that mitral-tufted cells receive homogenous afferent receptor input, does this preclude experience-induced ORF shifts? The present experiment aimed at better understanding mitral-tufted cell ORFs and ORF plasticity. Mitral-tufted cell single-unit ORFs to a homologous series of ethyl

esters were quantitatively characterized both before and after simple prolonged exposure to one of the odors. The results suggest that mitral-tufted cell ORFs to novel odorants can be shaped by previous exposure.

Materials and Methods

Subjects. Adult male Long-Evans hooded rats (Harlan Bioproducts for Science, Indianapolis, IN) were used as subjects. Rats were housed in polypropylene cages with water and food available ad libitum. Lights were maintained on a 12 hr light/dark cycle with testing taking place during the light hours. Animal care and protocols were approved by the University of Oklahoma Institutional Animal Care and Use Committee in accordance with National Institutes of Health guidelines. ORFs were mapped from a total of 72 cells in 56 animals with no more than three cells from each animal. Only cells that showed excitatory responses to at least one of the ethyl esters presented were used in this study.

Electrophysiology. Animals were anesthetized with urethane (1.5 gm/kg) and placed in a stereotaxic apparatus. After exposing the skull, a small hole was drilled over the left OB. Another hole was drilled over the lateral olfactory tract (LOT) posterior to the OB, allowing a tungsten-stimulating electrode to be inserted into the LOT. Respiratory activity was monitored throughout the experiment using a piezoelectric monitor strapped around the animals' chest. This output was then sent through a window discriminator allowing odorant pulse delivery to be timed to the transition of the inspiration-expiration cycle as reported previously (Wilson, 2000a).

For single-unit mitral-tufted cell recordings, a tungsten microelectrode (5-12 M) was lowered into the dorsal region of the left OB normal to the dorsal surface. Recordings were made in the dorsomedial region of the OB known to be responsive to ethyl esters of differing hydrocarbon chains (Imamura et al., 1992; Uchida et al., 2000). Confirmation of recording electrode placement was verified by LOT electrical stimulation and histological confirmation of the recording electrode tip location. Unfortunately, given the superficial location of these recordings, most recording sites could not be reconstructed. Single units were amplified and bandpass filtered (300 Hz to 10 kHz) and then either directly isolated or extracted through template matching using Spike 2 software (Cambridge Electronics Design, Cambridge, UK).

Odorant receptive fields. The term receptive field is generally defined as that portion of the sensory epithelium or stimulus space to which a sensory neuron responds. In some systems, this corresponds to a precise spatial dimension in a description of the RF [e.g., somatosensory system (Mountcastle, 1957) or early stages of the visual pathway (Hubel and Weisel, 1959)], whereas in other systems, descriptions of RFs do not necessarily include a spatial dimension [e.g., frequency tuning in the central auditory system (Diamond and Weinberger, 1986; Weinberger, 1995) and object-oriented RFs of higher order visual system (Rolls et al., 2003)]. Although central olfactory system neurons can also display spatial RFs [e.g., mitral-tufted cells (Kauer and Moulton, 1974; Jiang and Holley, 1992) and piriform cortex neurons (Wilson, 1997)], a variety of terms have been used to describe the odorant stimulus tuning properties of these

35

neurons and their underlying anatomy. These terms include odotopy (Shepherd and Greer, 1998), rhinotopy (Clancy et al., 1994), molecular receptive range (Mori and Yoshihara, 1995), and odorant receptive field (Wilson, 2000b; Luo and Katz, 2001; Sanchez-Montanes and Pearce, 2002). The two latter terms are generally considered analogous (Mori and Yoshihara, 1995; Luo and Katz, 2001) and refer to that region of odorant space to which an olfactory neuron responds. The ORF of a single unit in the central olfactory system is dependent on both the type of olfactory receptor neuron input it receives (influenced by precise anatomical projections from the receptor sheet) and central circuit processing (Kauer, 1991; Mori and Yoshihara, 1995; Luo and Katz, 2001). One dimension that has been routinely used to partially describe (map) ORFs is carbon chain length (Imamura et al., 1992). The present study uses the ORF terminology as described here to enhance comparison with published work from other sensory systems.

Odor stimulation. Odorants were delivered by passing a stream of humidified charcoal-filtered air through syringe filters saturated with specific odorants using a flow dilution olfactometer (1:10 dilution). Although higher odorant concentrations are known to elicit broader ORFs than lower concentrations, previous studies found the best (most effective) odorant of the ORF to be the same, regardless of concentration (Imamura et al., 1992, Sato et al., 1994). Odorants used were ethyl formate (E1), ethyl acetate (E2), ethyl propionate (E3), ethyl butyrate (E4), ethyl valerate (E5), ethyl hexanoate (E6), ethyl heptanoate, ethyl octanoate (E8), and isoamyl acetate (AA) (Sigma, St.

36

Louis, MO). For all ORF determination, animals were given 2 sec odor pulses delivered in pseudorandom order. Odorant habituation (exposure) consisted of a single 50 sec odorant presentation to either the BEST-ODORANT (ON-PEAK) or the odorant that was two carbons longer in chain length than the BEST-ODORANT (OFF-PEAK). In all cases, odorants used for the 50 sec exposure were E3, E4, E5, or E6. All odorants were initially novel to the animals tested, and no animal received more than one 50 sec odorant exposure to allow examination of the effects of the initial odorant exposure on mitral-tufted cell ORFs, a design similar to our previous work (Wilson, 2000a).

Odor response analysis. A variety of quantification and classification schemes exist for odorant responses (Pager et al., 1972; Mair, 1982; Harrison and Scott, 1986; Meredith, 1986; Hamilton and Kauer, 1989; Wellis et al., 1989; Imamura et al., 1992; Buonviso and Chaput, 2000; Wilson, 2000b). Using these schemes, it has been shown that both the number of evoked spikes and temporal patterning of spike occurrence can vary with odorant stimulus quality and intensity. As a first approach to detecting ORF changes with exposure, we chose to focus on stimulus-evoked spike counts to facilitate comparison with results from other sensory systems (Weinberger et al., 1993; Rolls et al., 2003).

For the description of mitral-tufted cell ORFs to novel odorants, we used two different measures, one highly inclusive and liberal and one more conservative. Response magnitudes were calculated by subtracting the number of spikes during a 4 sec prestimulus period from the number of spikes during each 4 sec odorant presentation. Partial ORFs for the esters used here could

then be mapped on the basis of changes in raw spike counts. For the more liberal response definition, cells were considered to show an excitatory response to an odorant if the mean response magnitude for that odorant was >0. This allowed characterization of ORFs with very inclusive criteria. The more conservative ORF measure involved statistical analysis of response magnitudes for each odorant response. For statistical ORF comparisons, cells were considered to respond to an odorant if the mean number of spikes during the 4 sec period beginning with the odorant presentation was significantly greater (0.25 sec bin width; t test; $p < 0.05$) than the number of spikes during the 4 sec prestimulus baseline activity.

For comparisons of individual ORFs as well as exposure-induced (i.e., 50 sec exposure) changes, it was necessary to normalize the ORFs relative to the response magnitude to the most excitatory (best) odorant. This allowed for comparisons of overall ORF-tuning curve shape. Normalized ORFs were obtained by calculating response magnitudes for each odorant as a percentage of the BEST-ODORANT response magnitude. The BEST-ODORANT was defined as the odorant that produced the largest response relative to the other odorants in the series at that time point. By normalizing responses, potential shifts in BEST-ODORANT could be seen by a shift in the postexperience ORF peak away from the preexperience ORF peak while canceling simple changes in the overall firing rate to odorant presentations. Experience might not only shift the ORF toward a different peak odorant but also change the overall shape of the

38

ORF. With ORFs normalized, a more precise relationship between odorant responses could be observed.

ORFs were remapped immediately, 15 and 60 min after the 50 sec odorant exposure stimulation. For preexposure, 15 min postexposure, and 60 min postexposure ORFs, response magnitudes were averaged across two presentations of each odorant. Because of time constraints of presenting eight odorants, ORFs immediately after the 50 sec exposure were based on responses to a single presentation of each odorant. The respiration rate, which could be indicative of changes in anesthetic level or animal condition over the course of the 60 min experiment, did not significantly change in the animals used for long-term testing [$t(18) = 0.10$; not significant].

For each cell, the 50 sec exposure odorant was chosen as either the BEST-ODORANT within the baseline ORF of that cell or an odorant that was two carbons longer in chain length than the BEST-ODORANT. Response magnitudes to each of the odorants were calculated for each time point in the same manner as the initial normalized ORFs. ORFs mapped before exposure, immediately after exposure, and 60 min after the 50 sec exposure were compared with three-way repeated measure ANOVA and post hoc comparisons.

Results

Odorant ORF mapping

Single-unit ORFs were mapped in odorant space along the carbon chain length dimension from 72 mitral-tufted cells to a homologous series of novel ethyl esters. Figure 1 shows a typical example of a single-unit excitatory ORF to ethyl esters. The recording in Figure 1A shows the spike discharge of the mitral-tufted cell before, during, and after a 2 sec odorant presentation. In this case, the cell responded to four of the eight ethyl esters presented, with vigorous firing to three of the odorants. For ORF determination along the dimension of carbon chain length, averaged single-unit responses were expressed for each odorant (Fig. 1B). To make comparisons between individual ORFs and potential experience-induced changes, all single-unit ORFs were also expressed as a percentage of the odorant eliciting the largest response for each cell (BEST-ODORANT) (Fig. 1C). Because the second phase of this study was concerned with comparing individual ORF changes, normalizing the ORF fields allowed for better comparisons of overall ORF-tuning curve shape over time. Expressing ORFs as a percentage of the BEST-ODORANT does not change the overall shape of the ORF, as shown in Figure 1.
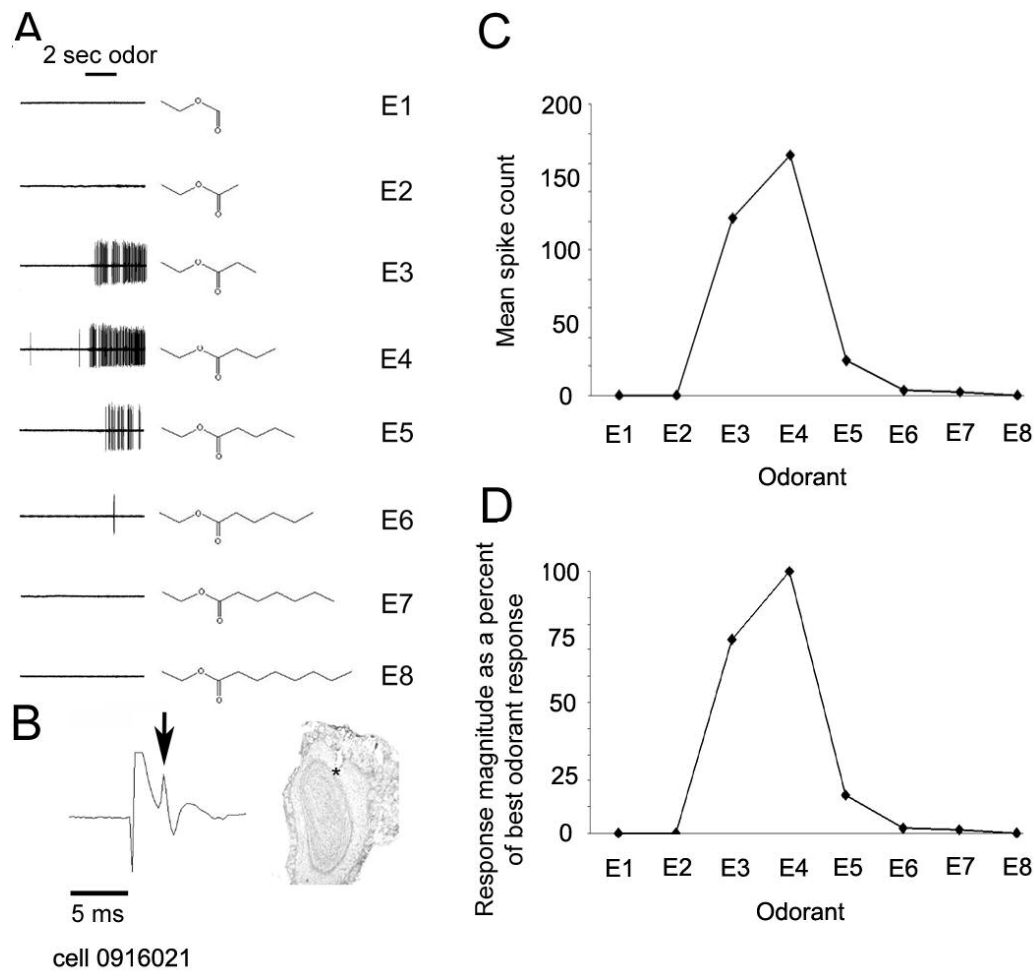
Figure 1. Representative example of single-unit mitral-tufted cell responses to a novel series of ethyl esters. A, Sample traces of spike activity before, during, and after 2 sec odorant presentations of a homologous series of ethyl esters differing in carbon chain length B, Antidromic LOT-evoked spike recorded from the neuron shown in A (arrow, evoked spike) and histological verification of electrode location near the mitral-tufted cell layer (asterisk, recording site). The time scale for antidromic response is 5 msec. C, ORF for cell in A is based on mean odorant-evoked changes in cell firing for each odorant. D, ORF of same cell remapped as a percentage of the BEST-ODORANT response (normalized). Replotting the ORF as a percentage of BEST-ODORANT response does not change overall ORF shape.

41

Representative ORFs to novel odorants from four different cells are shown in Figure 2. Individual cells differed in their ORFs to the esters presented. Differences between cells were observed in responses to odorants within the series, with most cells excited by only a subset of odorant chain lengths in the series. For example, the cell in Figure 2A responded to odorants E3-E5, with chain lengths outside of this range being ineffective. The cell in Figure 2B had a broader ORF with stronger responses to odorants E3-E6. This cell also displayed excitatory responses to isoamyl acetate (AA), whereas AA appeared to be ineffective in exciting the cell in Figure 2A. Figure 2C shows an example of a cell with a sharper ORF, with the cell only responding to two of the chain lengths. This cell was somewhat inhibited by chain lengths immediately outside the range of excitatory odorants. Similarly, Figure 2D shows a cell with a very narrow ORF characterized by a single excitatory odorant and suppression to neighboring chain lengths.

The mean odor-evoked spike counts of all cells (n = 72) to all odorants were combined in Figure 3A. As a population, this group of cells responded most strongly to E3 and E4 with a slight skew toward longer chains (Fig. 3A). Using the liberal definition of excitatory odorant response as a simple increase in spike count during the stimulus compared with prestimulus count, most individual cells also responded to E3 and E4 (Fig. 3B). A majority of the cells tested also had excitatory responses when presented with isoamyl acetate (Fig. 3B). Furthermore, using the liberal definition of excitatory odorant responses, the
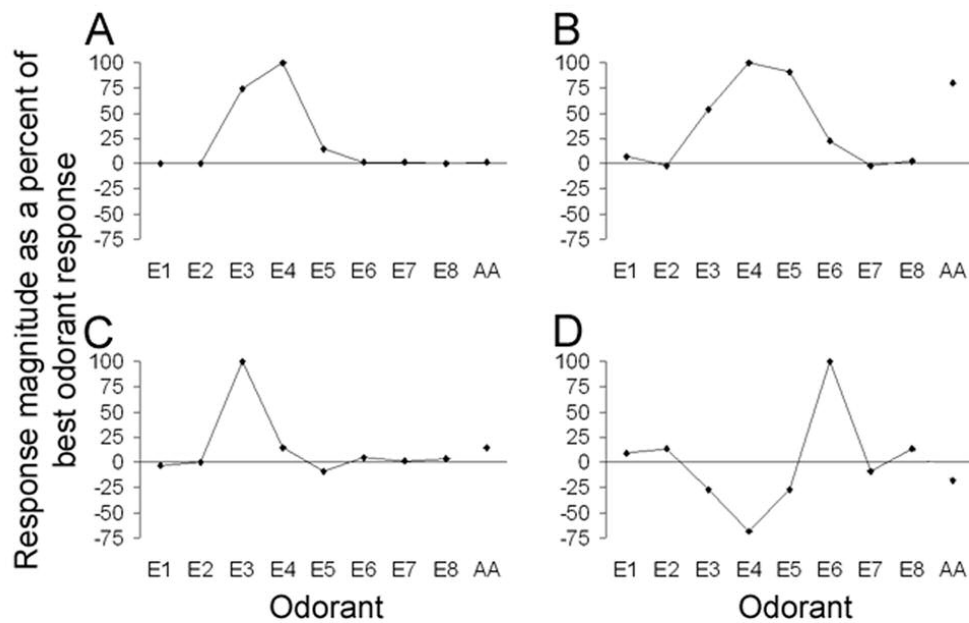
Figure 2. A--D, Individual examples of mitral-tufted cell ORFs to novel ethyl esters. Normalized ORFs were mapped as a percentage of the BEST-ODORANT response for each cell. Individual cells show differences in ORF shape and some have suppressive responses to odorants with longer and shorter chains surrounding excitatory stimuli. Responses to AA were also mapped. Some cells that responded to ethyl esters were also responsive to AA stimulation.

majority of cells had excitatory ORF widths between four and seven odorants (Fig. 3C).

When the ORF responses were analyzed more conservatively on the basis of statistically significant changes in spike count, a slightly different picture of ORFs to novel odorants emerged. As might be expected, cells responded to substantially fewer odorants of the set than compared with the liberal response definition (Fig. 4). Furthermore, the majority of cells had ORF widths between one and four odorants (Fig. 4B).

The conservative definition of odorant responses was also used to quantitatively characterize mitral-tufted cell ORFs by examining the conditional probability of responses to a particular odorant by a single cell, given that that same cell responds to another odorant. Thus, for example, we wanted to determine whether a cell that responds to an ester with a carbon chain length of four is equally likely to respond to esters with longer (E5) and shorter (E3) chain lengths, or whether there is an asymmetry in mitral-tufted cell ORFs for chain length. Data from olfactory receptor neuron recordings (Gaillard et al., 2002) and mitral-tufted cell cross-habituation studies (Wilson, 2000b) suggest that an asymmetry or bias exists in ORFs for chain length. Figure 5 shows probabilities of responses to ethyl esters on the basis of ORFs to novel odorants. Given the low response probability to E1 and E2, only data for E3-E8 are included. As shown, individual cells tend to respond to odorants of similar carbon chain length, although there is an asymmetry in relationship to carbon chain length preference.
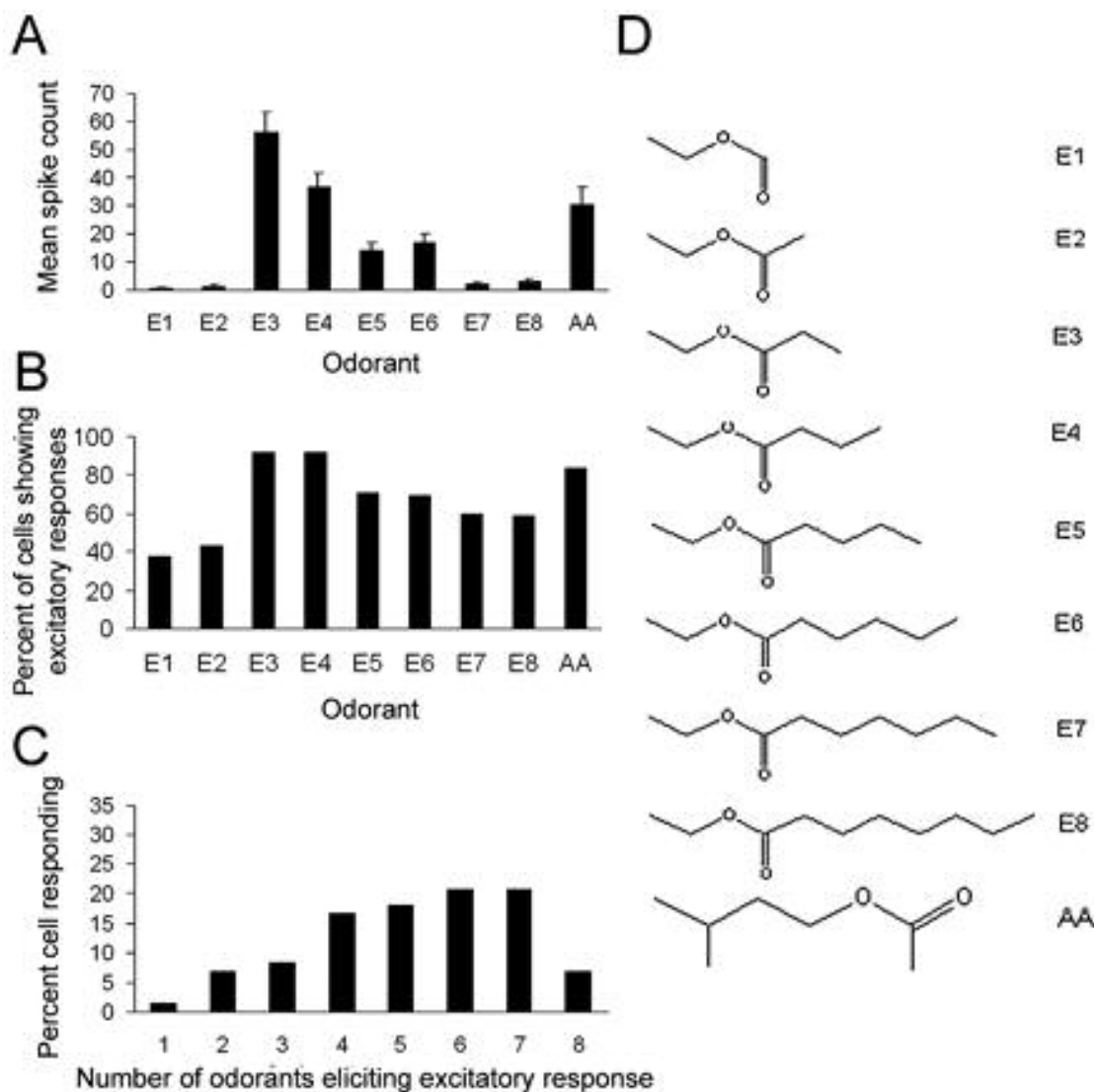
Figure 3. Response specificities of mitral-tufted cells to novel ethyl esters. A cell was considered to respond to an odorant if the odorant-evoked activity was >0 (see Materials and Methods). *A*, Mean novel responses for all cells (*n* = 72) based on odorant-evoked changes in cell firing to each ethyl ester and AA. *B*, Percentage of excitatory responses evoked by each odorant for all cells tested. *C*, Mean number of odorants eliciting responses in each cell. On the basis of excitatory responses alone, most cells displayed relatively broad RFs. *D*, Molecular structure and name of all odorants used.
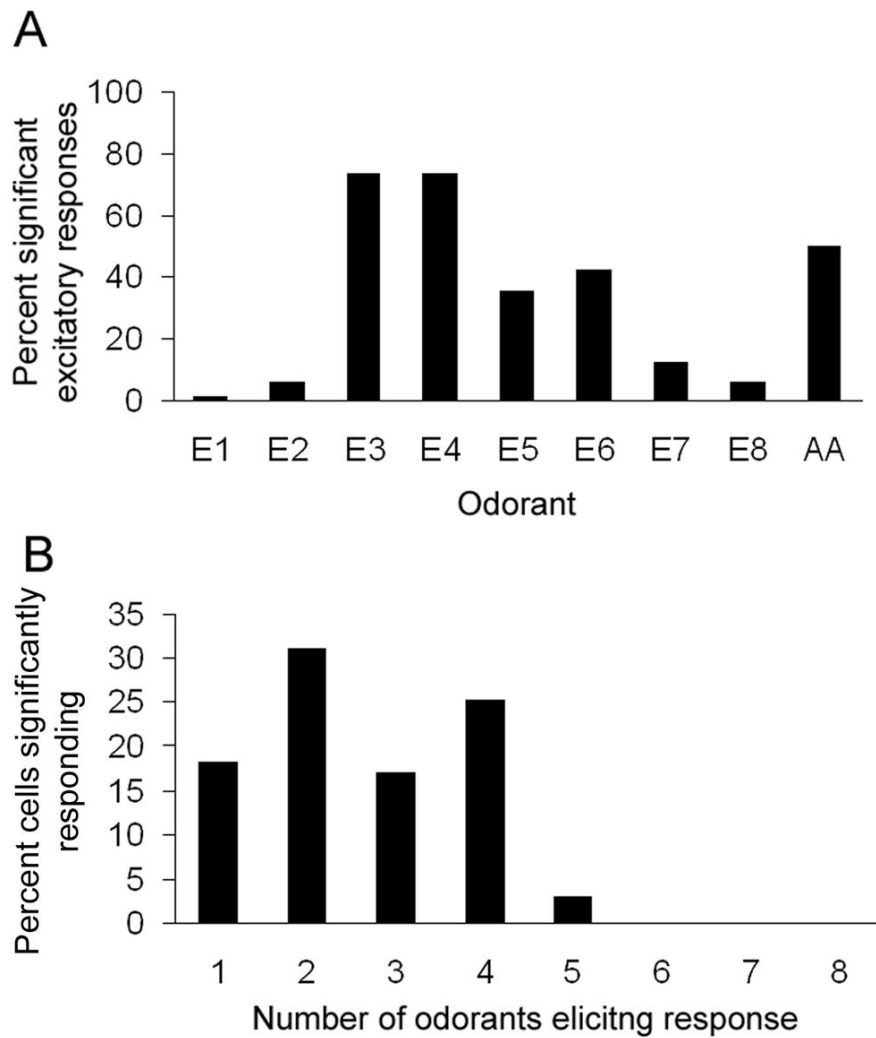
Figure 4. Response specificities of mitral-tufted cells based on statistically defined responses (see Materials and Methods). Responses were considered significant only if the odorant-evoked firing was statistically different from baseline activity. *A*, Mean novel responses for all cells based on significant odorant-evoked changes in cell firing to each ethyl ester and AA. *B*, Mean number of odorants eliciting responses in each cell. On the basis of significant response, most cells displayed more narrow ORFs with fewer odorants eliciting responses.

Thus, assuming a cell responds to a given chain length, it has a higher probability of responding to odorants with a shorter chain length than to odorants with a longerchain length. For example, of the cells that responded to E4, 80% also responded to E3, whereas only 40% responded to E5. In contrast, of the cells that responded to E5, 80% also responded to E4, whereas only 50% responded to E6.

These results suggest that a conservative estimate of mitral-tufted cell excitatory ORFs for novel esters includes odorants varying in length by a median of three carbons. Furthermore, a conditional probability analysis suggests that if a cell responds to an odorant of a particular carbon chain length, it is more likely to respond also to shorter chain odorants than longer chain odorants. The following analyses examined the effect of previous experience on these ORFs.

Odorant ORF short-term plasticity

After ORF determination to novel odorants, a subset of cells received a 50 sec odorant exposure to either the BEST-ODORANT for that cell (ON-PEAK; n = 20) or the odorant that was two carbons longer in chain length than the BEST-ODORANT for that cell (OFF-PEAK; n = 28). Given that most cells recorded here had BEST-ODORANTs of E3 or E4 and very few cells responded to E1 and E2, examination of the effects of exposure to shorter chain lengths was not possible. Immediately after the 50 sec exposure, ORFs were remapped. ORFs were normalized to the maximal response, as described in Materials and Methods, and aligned across cells to the BEST-ODORANT for each cell as determined during
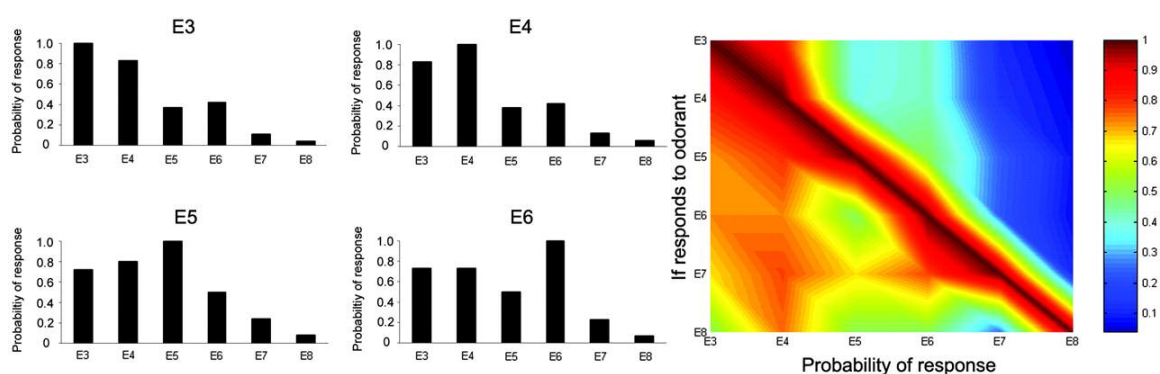
Figure 5. Conditional probability of an individual cell responding to specific odorants on the basis of all ORFs determined in this experiment (n = 72). Assuming a response to a given odorant (listed as the ordinate in the pseudocolor graph on the right), the probability of response to other odorants is displayed with higher probabilities (red). A histogram representation of the same data is shown on the left (odorant that the cell responds to is labeled above each histogram). If a given cell responded to an odorant of specific carbon chain length, it had a high probability of responding to shorter chained-related odorants. Response probabilities were based on odorant-induced responses that were statistically significant different from baseline activity.

the preexposure mapping. Figure 6 shows the effects of a single 50 sec odorant stimulus on mitral-tufted cell raw spike-count ORFs mapped immediately after the termination of the prolonged exposure. Responses to the odorants after the 50 sec exposure were suppressed in both the ON-PEAK (Fig. 6A) and OFF-PEAK exposed (Fig. 6B) groups (ANOVA; main effect of trial, $F(1,228) = 52.1$; $p < 0.01$), with postexposure responses being suppressed more in the ON-PEAK group (ANOVA; trial x group interaction, $F(1,228) = 3.94$; $p < 0.05$). Post hoc Fisher tests revealed a significant difference between the ON-PEAK and OFF-PEAK postexposure responses to the BEST-ODORANT ($p < 0.05$), with responses in the ON-PEAK group showing greater suppression. The results show that immediately after a 50 sec exposure to an odorant within the ORF, responses across the ORF in both groups were suppressed.

By normalizing both preexposure and immediately postexposure ORFs, effects on the shape of the ORF can be better examined. Normalizing the pre-ORFs and post-ORFs again showed that a 50 sec odorant stimulus suppressed both the ON-PEAK and OFF-PEAK exposed ORFs (ANOVA; main effect of trial, $F(1,228) = 21.5$; $p < 0.01$) (Fig. 7). Again, post hoc Fisher tests revealed a significant difference between the ON-PEAK and OFF-PEAK postexposure responses to the BEST-ODORANT ($p < 0.05$) with responses in the ON-PEAK group being lower. In the normalized ORFs, no significant difference in the amount of habituation was found between groups (ANOVA; significant trial x group interaction; $F(1,228) = 2.37$; not significant) or within odorant responses
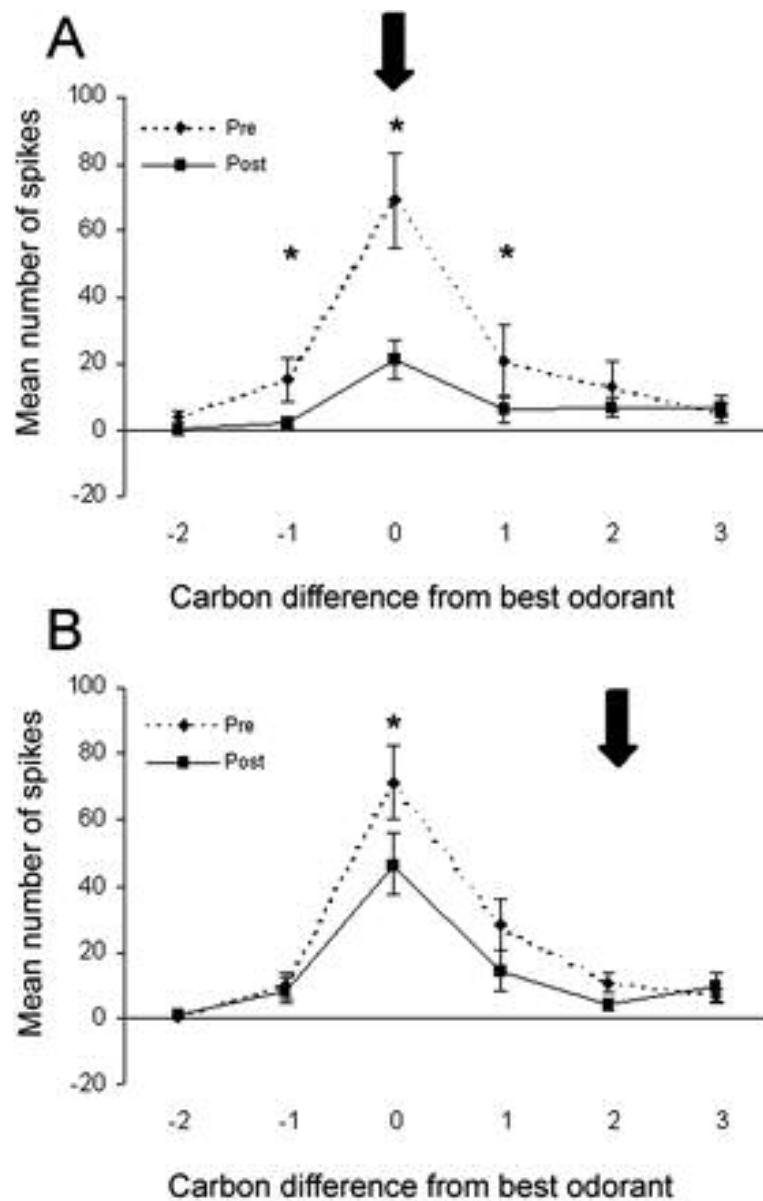
Figure 6. Mean single-unit ORF changes (odor-evoked spikes) immediately after 50 sec odorant exposure. *A*, Mean single-unit changes immediately after exposure to the ON-PEAK odorant (n = 20). *B*, Mean single-unit changes immediately after exposure to the OFF-PEAK odorant (n = 28). Arrows represent the carbon chain length of odorant presented during exposure. Asterisks represent a significant difference between postexposure odorant responses and preexposure responses (p < 0.05).
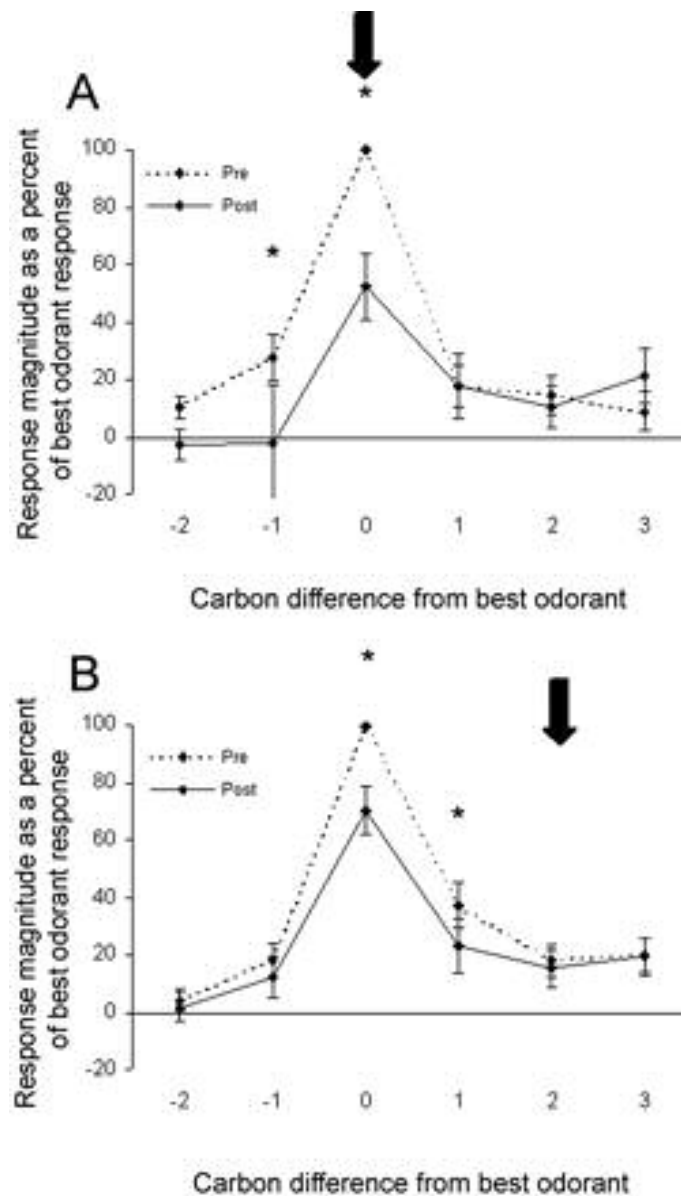
Figure 7. Mean normalized single-unit ORF changes immediately after 50 sec odorant exposure. ORFs from Figure 6 were normalized as a percentage of the preexposure BEST-ODORANT response. *A*, Mean single-unit changes immediately after exposure to the ON-PEAK odorant (*n* = 20). *B*, Mean single-unit changes immediately after exposure to the OFF-PEAK odorant (*n* = 28). Arrows represent the carbon chain length of odorant presented during exposure. Asterisks represent a significant difference between postexposure odorant responses and preexposure responses ($p < 0.05$).

(ANOVA; trial x group x odor interaction; $F_{(4,228)} = 2.04$; not significant). These results show that although there is a postexposure decrease in the response of both groups, no significant overall change in the shape of the ORF can be observed.

Odorant ORF long-term plasticity

In a subset of the animals used to describe short-term effects of odorant exposure, ORFs were remapped 15 and 60 min after the 50 sec odorant exposure. Figure 8 shows examples of individual normalized ORFs mapped before and 60 min after 50 sec exposure. The cell in Figure 8A was exposed to its BEST-ODORANT (ON-PEAK), whereas the cell in Figure 8B was exposed to the OFF-PEAK odorant. The ON-PEAK exposed cell shows no change in ORF BEST-ODORANT 60 min after exposure but does appear to narrow with the appearance of enhanced suppressive responses to longer and shorter odorant chains (Fig. 8A). In contrast, the OFF-PEAK exposed cell shows a marked shift ORF BEST-ODORANT away from the original BEST-ODORANT toward the exposure stimulus (Fig. 8B).

Mean ORF changes over time are shown in Figures 9 and 10. In the ON-PEAK exposed group (n = 11), little change occurs in the shape of the ORF over time (Figs. 9A, 10A). Although the ORF seems broader 15 min after the odorant exposure, within 1 hr the shape of the ORF is relatively unchanged. This suggests that odorant ORFs under the conditions here can be highly stable after exposure to the BEST-ODORANT.
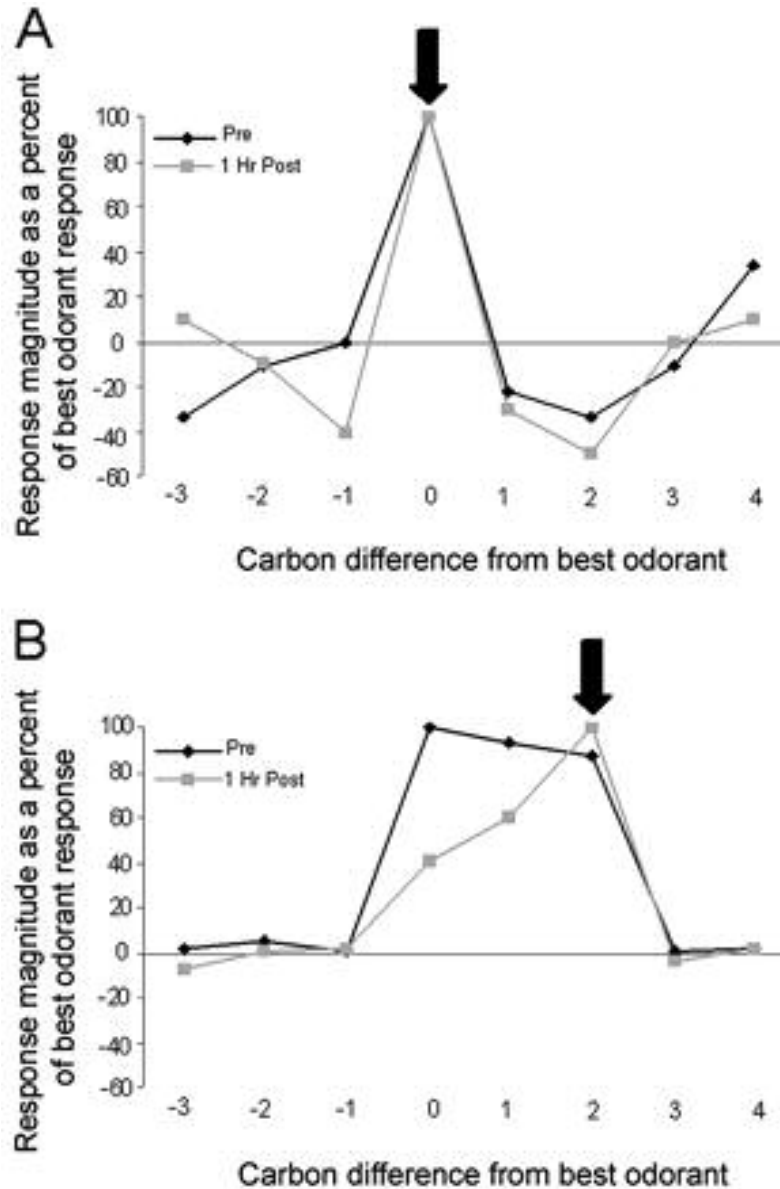
Figure 8. Examples of individual mitral-tufted cell odorant ORFs before and 60 min after a single 50 sec odorant exposure. ORFs are normalized on the basis of the preexposure BEST-ODORANT response. *A*, ORF changes in a mitral-tufted cell after ON-PEAK odorant exposure. In this case, the overall ORF shows little change, although with enhanced suppression of odorants similar to the BEST-ODORANT. *B*, ORF changes in a mitral-tufted cell with OFF-PEAK odorant exposure. In this cell, ORF changes were seen with an overall shift of the ORF toward the experienced odorant as well as suppression of the BEST-ODORANT response. Arrows represent the carbon chain length of the odorant presented during the 50 sec exposure.
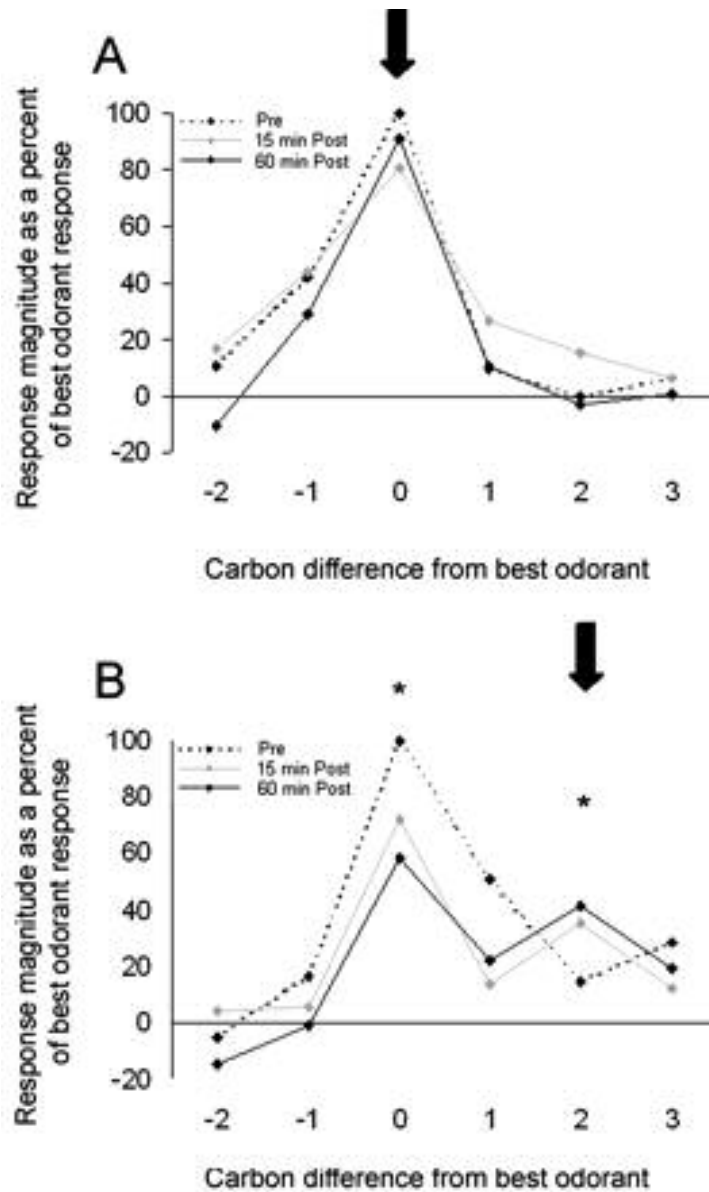
Figure 9. Mean single-unit odorant ORF changes after a single 50 sec odorant exposure. ORFs were normalized as a percentage of the preexposure BEST-ODORANT response. *A*, Mean single-unit changes 15 min and 1 hr after exposure to the ON-PEAK odorant (*n* = 11). *B*, Mean single-unit changes 15 min and 1 hr after experience to the OFF-PEAK odorant (*n* = 10). Arrows represent the carbon chain length of odorant presented during exposure. Asterisks represent a significant difference between postexposure odorant responses and preexposure responses (*p* < 0.05).

As an additional test of odorant ORF stability, the odorant ORFs of a small number of additional cells were monitored over repeated (range, 4-9) stimulation over the course of up to 60 min without an intervening 50 sec odorant exposure. In those cells, normalized ORFs did not significantly change over time (n = 5; repeated measures ANOVA; $F_{(2,24)} = 1.27$; not significant).

In contrast to the stability of odorant ORFs after ON-PEAK odorant exposure, in the OFF-PEAK exposed group (n = 10), there was a significant change in the overall odorant ORF shape with a shift in the peak toward the experienced odorant (ANOVA; trial x group x odorant interaction; $F_{(1,57)} = 3.87$; $p < 0.05$). Post hoc Fisher tests revealed a significant drop in the BEST-ODORANT response and a significant increase in the exposure odorant response 60 min after odor exposure ($p < 0.05$) (Figs. 9B,10B). These ORF shape changes after OFF-PEAK odorant exposure can develop over time with the ORF after 15 min of being intermediate between the pre-ORF and 60 min post-ORF (Fig. 9). Given the stability of odorant ORFs in ON-PEAK exposed animals and nonexposed CONTROL animals described above, the shifts in odorant ORF after OFF-PEAK exposure appear to be exposure-induced In addition to changes in BEST-ODORANT, selectivity of the exposed cells as a whole was also modified. As shown in Figure 11, as a population, mitral-tufted cells exposed to an ester for 50 sec showed a significant narrowing of responsiveness to other esters.
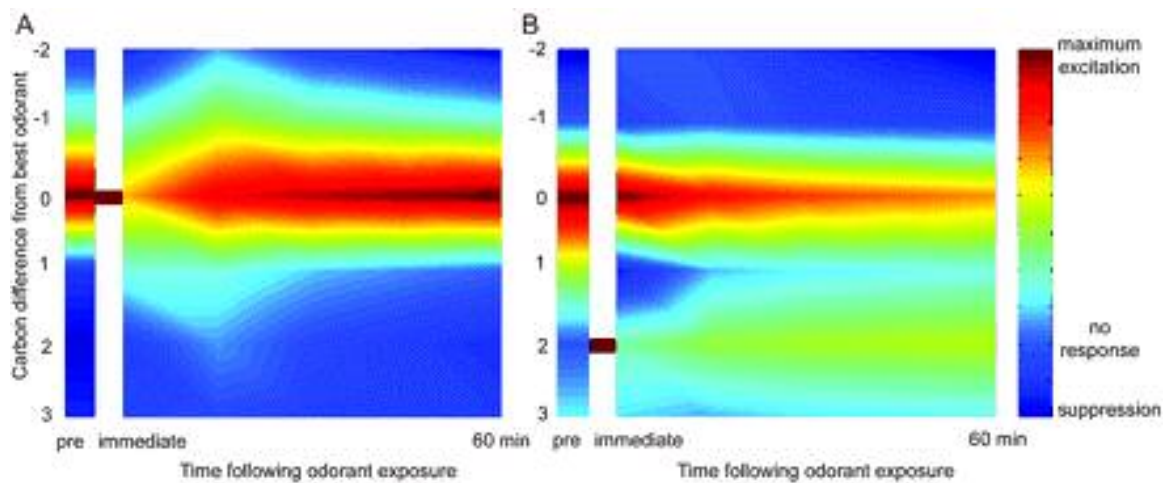
Figure 10. Pseudocolor representation of ORF changes over the course of 60 min after a single 50 sec odorant exposure. *A*, Mean single-unit changes after exposure to the ON-PEAK odorant (*n* = 11). Immediately after exposure, the ORF is suppressed but appears to recover within 15 min. After this, the ORF remains relatively stable over time, with no apparent shift, and the BEST-ODORANT remains the same. *B*, Mean single-unit changes after exposure to the OFF-PEAK odorant (*n* = 10). In contrast to the ON-PEAK exposed cells, after the initial suppression was brought about through OFF-PEAK exposure, the ORF displays major changes throughout the 60 min. The ORF shape changes with the responses to the BEST-ODORANT being suppressed, and responses to the experienced odorant being enhanced. The horizontal bar represents the carbon chain length of odorant presented during exposure. The color bar represents the amount of odorant-induced activity, with red being excitatory odorant responses and blue being suppression relative to baseline.

56
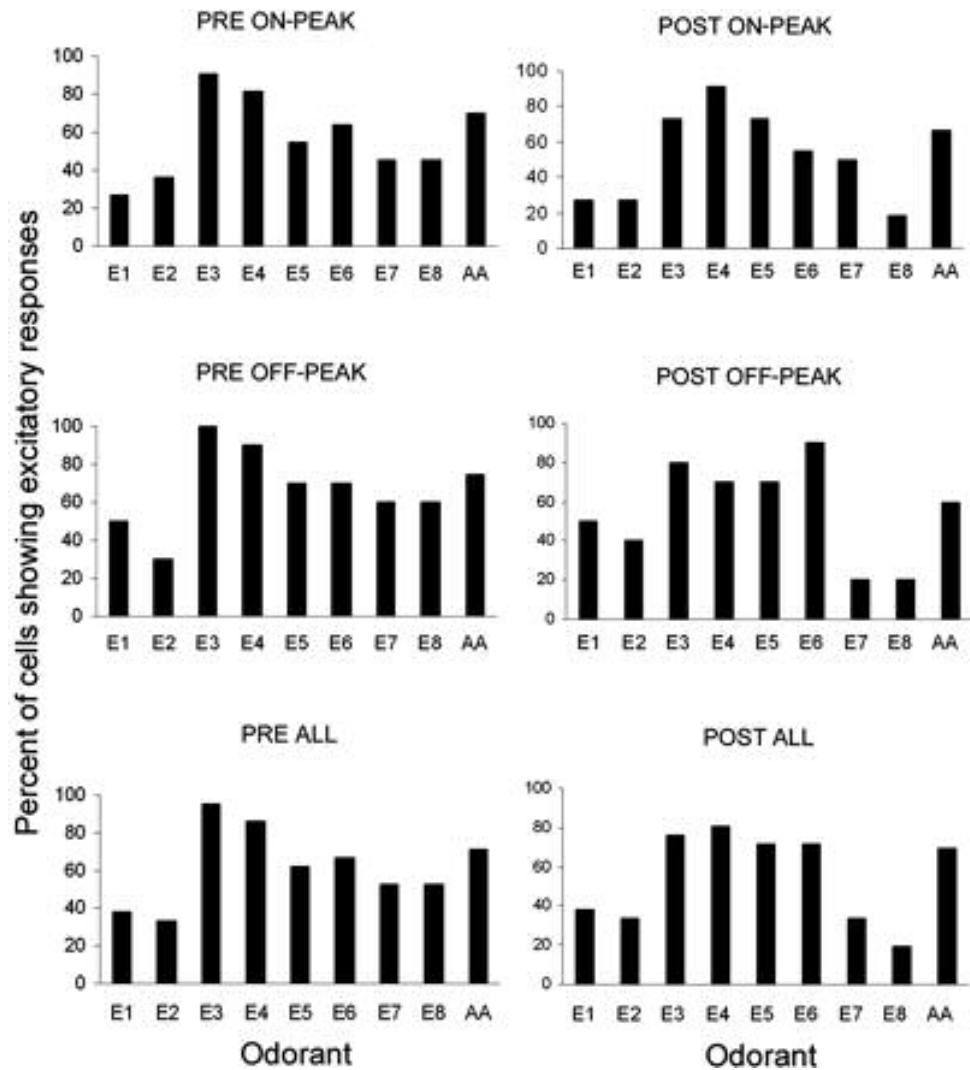
Figure 11. Mitral-tufted cells show narrowing of responsiveness to all esters after 50 sec of exposure with one of the esters in the series. As a population, both ON-PEAK- and OFF-PEAK exposed groups showed ORF narrowing with a significant decrease in the percentage of cells showing excitatory responses to the esters 60 min after the 50 sec odorant exposure. A statistical comparison revealed a significant difference between preexposure and postexposure for all cells ($p < 0.05$).

A comparison of the percentage of cells responding to each odor for all cells combined showed a significant change 60 min after the 50 sec exposure (2; df(8) = 18.91; $p < 0.05$).

In some animals, the response to isoamyl acetate was also measured after the odorant exposure. Similar to the other odorants immediately after a 50 sec exposure to one of the ethyl esters, responses to isoamyl acetate were significantly suppressed [$t(12) = 2.28$; $p < 0.05$]. The response to isoamyl acetate recovered over the course of the experiment, with responses returning to baseline within 60 min (ANOVA; $F(3,36) = 0.64$; not significant) (Fig. 12).

Discussion

The current study quantified excitatory mitral-tufted ORFs to a homologous series of novel ethyl esters to investigate exposure-induced ORF plasticity. As described previously (Imamura et al., 1992; Mori et al., 1992), mitral-tufted cell responsiveness varied along the dimension of carbon chain length, generally showing a maximal responsiveness to a single carbon chain length (BEST-ODORANT). Median mitral-tufted cell excitatory ORFs spanned three to five of eight esters presented. There appeared to be an asymmetric conditional probability response bias, with cells more likely to respond to a given odorant and shorter carbon chain lengths than to longer chain lengths. Mitral-tufted cell ORFs to novel odorants demonstrated both long- and short-term plasticity after a 50 sec odorant exposure characterized by an immediate
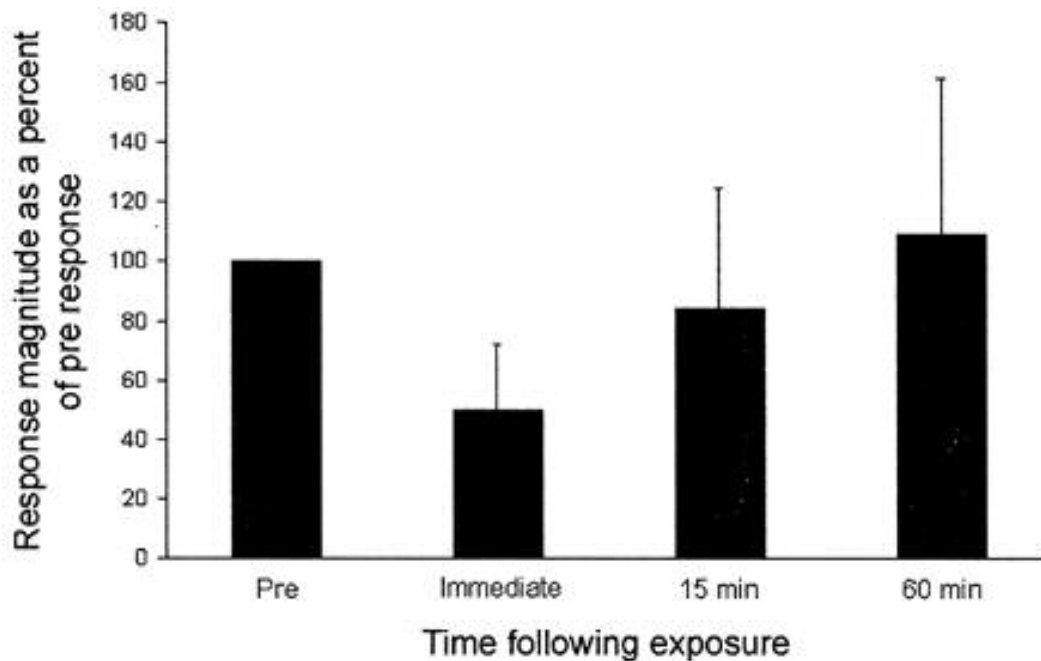
Figure 12. Responses to isoamyl acetate before and after experience with ethyl esters. Response magnitudes are expressed as a percentage of the initial isoamyl acetate response. Similar to the other odorants, adaptation to one of the ethyl esters caused responses to be significantly suppressed. The responses seemed to recover over the course of the experiment and being similar to baseline after 60 min (n = 13).

suppression across the ORF and followed by recovery and a long-term ORF shift toward the experienced odorant. These latter findings are very similar to RF plasticity in thalamocortical sensory systems (Weinberger, 1995; Buonomano and Merzenich, 1998; Gilbert et al., 2001), despite the unusual anatomy of afferent input to mitral-tufted cells.

Olfactory bulb odorant ORFs

These results are consistent with previously reported studies of mitral-tufted cell responses to odorants differing in carbon chain length (Imamura et al., 1992). In addition, a majority of cells activated by ethyl esters also showed excitatory responses to isoamyl acetate (Fig. 3), which shares some structural similarities with ethyl esters used here. Note that the ORFs of the mitral-tufted cells recorded in this study have only been partially sampled and are presumably much larger, containing many more odorants differing not only in carbon chain length but possibly in type and position of functional groups within the odorant molecule as well (Hamilton and Kauer, 1989; Wellis et al., 1989; Imamura et al., 1992).

Mitral-tufted cell ORFs reflect both afferent input and central processing. Olfactory receptor neurons expressing homologous receptor genes project their axons to a small set of neighboring OB glomeruli, with individual glomeruli receiving exclusive input from receptor neurons expressing the same receptor gene (Vassar et al., 1994; Tsuboi et al., 1999). In turn, apical dendrites of rat mitral-tufted cells receive excitatory input from a single glomerulus (Shepherd and Greer, 1998). Thus, in the absence of local circuit inputs, excitatory ORFs of

mitral-tufted cells to novel odorants should primarily reflect the ORF of the receptor neurons that innervate them. In fact, the quantified mitral-tufted cell excitatory ORFs described here, showing a median carbon chain length span of three to five, match well with qualitative and quantitative descriptions of olfactory receptor neuron ORFs for carbon chain length. Specifically, the mouse OR912-93 receptor only binds aliphatic odorants with a straight carbon chain length of more than four and with maximal specificity to a seven carbon chain (Gaillard et al., 2002). Many other studies have reported ORNs that are responsive to a series of homologous odorants spanning less than five carbons in chain length difference (Sato et al., 1994; Malnic et al., 1999; Araneda et al., 2000).

One surprising characteristic of the mitral-tufted cell excitatory ORFs described here was the asymmetry in conditional probability of responding to chain length. Within the sampled population, if a cell responded to a particular carbon chain length, it was more likely to also respond to shorter chains than longer chains. Similar phenomena have been reported for olfactory receptor neuron ORFs, in which, for example, a receptor may respond maximally to a given chain length but also to shorter chains (Gaillard et al., 2002). This type of receptor response could account for the asymmetry described here. However, there are several examples in the literature of the opposite effect, in which a receptor does not respond until a certain chain length is reached and then continues to respond as the chain length is increased (Malnic et al., 1999); although, these responses were not analyzed in detail. A more quantitative analysis of olfactory receptor neuron ORFs for carbon chain length, perhaps

combined with mitral-tufted cell ORF mapping for the same odorant set and concentration, appears necessary to help isolate characteristics of mitral-tufted cell ORFs that result purely from OB processing, as opposed to those that primarily reflect afferent input.

Of course, mitral-tufted cell ORFs not only passively reflect excitatory olfactory receptor input but also reflect extensive lateral and feedback input to mitral-tufted cells from interneurons and centrifugal input from the rest of the brain (Shepherd and Greer, 1998; Mori et al., 1999). Through mechanisms such as lateral inhibition and centrifugal feedback, mitral-tufted cell ORFs can be sharpened to possibly enhance tuning specificities to odorant responses (Yokoi et al., 1995; Luo and Katz, 2001). Although previous reports have demonstrated that responses to particular odorants can be modified on the basis of behavioral state (Pager et al., 1972; Jiang et al., 1996) and past experience (Freeman and Schneider, 1982; Wilson and Sullivan, 1994, 1995; Brennan and Keverne, 1997; Kay and Laurent, 1999; Buonviso and Chaput, 2000), presumably through changes in central processing, the effects of experience on mitral-tufted cell ORFs have not been examined until now.

Odorant ORF plasticity: short-term effects of odorant exposure

As reported previously (Wilson 2000b), exposure to an odorant within a mitral-tufted cell ORF produced a widespread depression (habituation) of the odorant ORF, whereas the general shape of the ORF-tuning curve remained constant. Exposure to the BEST-ODORANT produced greater generalized habituation than exposure to an odorant near the edge of the ORF. These results

are consistent with a feature detection model of mitral-tufted cell function in which habituation to one odorant (feature) within the ORF suppresses responses to all odorants sharing that feature (Mori and Yoshihara, 1995; Wilson 2000b). An odorant feature, perhaps less effective at stimulating the relevant receptors (OFF-PEAK), thus may produce less overall suppression, similar to the pharmacological concept of a partial agonist.

Odorant ORF plasticity: long-term effects of odorant exposure

The consequences of odorant exposure continued to emerge over the course of at least 60 min, as demonstrated by the OFF-PEAK exposed cells. In OFF-PEAK exposed cells, ORFs 60 min after exposure showed a decrease in responsiveness to the previously BEST-ODORANT and an increase in responsiveness to the exposed odorant. In some cells, these changes produced a complete shift in ORF peak toward the exposed odorant (Fig. 8B). In cells exposed to the BEST-ODORANT, ORFs maintained their preexposure BEST-ODORANT (Fig. 9A). In addition to changes in ORF peak, exposure to either the ON-PEAK or OFF-PEAK odorant produced a narrowing of the ORF. Thus, simple exposure to a novel odorant can focus mitral-tufted cell ORFs on the exposed odorant, conceivably enhancing odorant feature discrimination.

The experience-induced ORF changes reported here are similar to those found in other sensory systems in which experience can modify single-unit RFs and cortical representations (Weinberger, 1995; Buonomano and Merzenich, 1998; Gilbert et al., 2001) to enhance encoding of learned stimuli. The changes observed in the present study did not require specific associative training but

used stimuli that the animals had never encountered before. Similar ORF changes may not occur in response to the exposure to well learned or familiar stimuli. The changes observed may represent an initial fine tuning of response patterns to novel stimuli and the first stage of olfactory perceptual learning. In both rats (Fletcher and Wilson, 2002) and humans (Rabin, 1988; Stevenson, 2001), discrimination of novel odorants can be enhanced through experience with those odorants. Although perceptual learning is thought to be primarily a cortical event in most sensory systems (Gilbert et al., 2001; Wilson and Stevenson, 2003), the mitral-tufted cell ORF changes shown here could also contribute to this behavioral change.

Potential mechanisms of ORF change

Experience-induced changes in mitral-tufted cell excitatory ORFs is somewhat surprising, given that the afferent input to rat mitral-tufted cells is believed to be from a homogeneous population of olfactory receptor neurons. Although the receptor neuron-to-mitral-tufted cell synapse is capable of long-term potentiation (Ennis et al., 1998) and may contribute to the ORF changes seen here (C. Linster, M. L. Fletcher, and D. A. Wilson, unpublished observations), we hypothesize that plasticity in synaptic strength of interneuron connections and cortical feedback may be the major forces shaping mitral-tufted cell ORF experience-induced changes, as hypothesized for olfactory associative learning-induced OB changes (Freeman and Schneider, 1982; Gray et al., 1986; Sullivan et al., 1989; Ravel et al., 1990; McLean et al., 1993; Wilson and Sullivan, 1994;

Brennan and Keverne, 1997; Kay and Laurent, 1999; Linster and Cleland 2002; Yuan et al., 2003).

The majority of centrifugal inputs to the OB terminate on inhibitory interneurons (Haberly and Price, 1978; Shepherd and Greer, 1998). Thus, we propose that experience-induced changes in mitral-tufted cell ORFs primarily reflect a change in inhibitory interneuron modulation of the olfactory receptor neuron-driven excitatory ORF. In this way, the BEST-ODORANT of an excitatory ORF of an individual mitral-tufted cell could be shifted between several odorants dependent on past experience. However, it is predicted that the extent of a possible shift will be entirely limited by the ORFs of the receptor neurons targeting the apical glomerulus and dendrite of that mitral-tufted cell. This dependence of coding plasticity on local "horizontal" circuits and descending input from higher processing centers is again highly reminiscent of plasticity in thalamocortical sensory systems (Gilbert et al., 2001).

In summary, mitral-tufted cell odorant ORFs, and thus OB output, are dynamic and can be modulated by odor experience. These ORF changes could affect OB spatiotemporal dynamics as well as cortical odor processing, ultimately resulting in modified perception of familiar odorants.

Chapter 3

High Frequency Oscillations Are Not Necessary For Simple Olfactory Discriminations In Young Rats[2]

Abstract

Individual olfactory bulb mitral/tufted cells respond preferentially to groups of molecularly similar odorants. Bulbar interneurons such as peri-glomerular and granule cells are thought to influence mitral/tufted odorant receptive fields through mechanisms such as lateral inhibition. The mitral-granule cell circuit is also important in the generation of the odor-evoked fast oscillations seen in the olfactory bulb local field potentials and hypothesized to be an important indicator of odor quality coding. Infant rats, however, lack a majority of these inhibitory interneurons until the second week of life. It is unclear if these developmental differences affect olfactory bulb odor coding or behavioral odor discrimination. The following experiments aimed at better understanding odor coding and behavioral odor discrimination in the developing olfactory system. Single-unit recordings from mitral/tufted cells and local field potential recordings from both the olfactory bulb and anterior piriform cortex were performed in freely breathing urethane-anesthetized rats (postnatal day 7 – adult). Age-dependent behavioral odor discrimination to a homologous series of ethyl esters was also examined using a cross-habituation paradigm. Odorants were equated in all experiments for concentration (150 PPM) using a flow dilution olfactometer. In concordance with the reduced interneuron population, local field potentials in neonates lacked detectable odor-evoked gamma frequency oscillations that were observed in mature animals. However, mitral/tufted cell odorant receptive fields and behavioral odor discrimination did not significantly change, despite known substantial changes in local circuitry and neuronal populations, over the age range examined. The results suggest that high frequency local field potential oscillations do not reflect processes critical for simple odor discrimination.

67

Introduction

The olfactory bulb is thought to function as a combinatorial odorant feature detector in which different parts of odor molecules activate specific subsets of bulbar output neurons. This code is then sent to higher cortical centers involved in integrating this information into perceptual wholes (odor objects) involved in sensory discrimination and memory (Wilson and Stevenson, 2003).

Two views of olfactory bulb combinatorial coding exist. First, glomeruli and their corresponding mitral/tufted cells respond preferentially to groups of molecularly similar odorants (Uchida et al., 2000; Leon and Johnson, 2003), resulting in odor-specific spatial patterns of glomerular activity and associated mitral/tufted cell output. Through mechanisms such as glomerular and granule cell layer lateral inhibition, inhibitory interneurons could shape the spatiotemporal activity pattern to enhance contrast between similar odorant features, as well as begin the process of feature synthesis.

A second proposed coding mechanism involves coincident firing of groups of mitral/tufted cells precisely synchronized to oscillatory local field potentials (LFP's). Oscillatory activity has been found in the olfactory systems of many species (Adrian, 1952; Bressler and Freeman, 1980; Laurent and Davidowitz, 1994; Lam et al., 2000). In some invertebrates, odor discrimination is thought to rely on the precise oscillatory synchronization of dynamic olfactory bulb assemblies in which coincident firing of projection cells would form the basis of feature synthesis and odor coding (Laurent, 2002), although other studies have shown that projection cell synchronization is not dependent on these oscillations

(Christensen et al., 2003). In this model, the role of inhibitory interneurons in the shaping of individual projection cell tuning curves is less important than their role in precisely synchronizing subsets of active cells to the global oscillatory dynamics of the bulb (Laurent, 1999).

Odors elicit both beta (15-40Hz) and gamma frequency (40-75 Hz) oscillations in the mammalian olfactory bulb although their strict relationship to odor quality coding is unclear (Adrian, 1952; Bressler and Freeman, 1980; Chabaud et al., 2000; Neville and Haberly, 2003). Oscillations in mammalian olfactory bulb may reflect odor quality coding (Nusser et al., 2001), but have also been linked to memory (Ravel et al., 2003) and experience-dependent phenomena such as expectancy (Kay et al., 1996). In this latter view, inhibitory neurons such as granule cells serve as the target of cortical feedback circuits to modify bulb activity based on changes in expectation and state (Freeman, 1978). In this model, therefore, disruption of normal inhibitory interneuron function may not be expected to produce drastic effects on simple odor discrimination.

Infant rats offer an excellent system for investigating olfactory bulb odor coding mechanisms in that they possess a morphologically and physiologically immature olfactory system and yet are capable of, and in fact are dependent on, olfactory learning and odor-guided behaviors (Wilson and Sullivan, 1994). For example, neonatal rats lack a majority of bulbar inhibitory interneurons thought to be involved in generating fast oscillations (Rosselli-Austin and Altman, 1979; Mair et al., 1982), and thus lack adult-like spontaneous local oscillatory activity (Almli et al., 1985). However, it is unclear if these developmental differences

affect olfactory bulb coding necessary for simple behavioral odor discrimination. The following experiments were aimed at better understanding olfactory bulb oscillatory activity, mitral/tufted cell olfactory receptive fields (ORF's), and how they relate to odor coding and odor discrimination in the developing olfactory system.

Methods

Subjects. Male and female Long-Evans hooded rats (Harlan Bioproducts for Science, Indianapolis, IN) were used. Rats were housed in polypropylene cages with food and water available *ad libitum*. Lights were maintained on a 12 hr light/dark cycle with all testing during the light hour cycle. Animal care and protocols were approved by the University of Oklahoma Institutional Animal Care and Use Committee in accordance with National Institutes of Health guidelines. Postnatal day 7 (PN 7) (mean weight: 16.6 ± 0.3 g), postnatal day 14 (PN 14) (mean weight: 32.3 ± 0.8 g) and mature rats (mean weight: 264.4 ± 31.3 g) were compared. Day of birth was considered postnatal day 0 (PN 0). PN 7 rats were chosen as they have previously been shown to have dramatically reduced numbers of granule cells and reduced numbers of juxtaglomerular neurons, although relatively normal numbers of mitral cells (Brunjes and Frazier, 1986). Many mitral cells at this age, however, have multiple apical dendrites extending into more than one glomerulus (Malun and Brunjes, 1996). Similar results have been described in mice, with the addition that some classes of olfactory receptor neuron axons extend to more than one glomerulus at this age, before being pruned back in older mice (Zou et al., 2004).

Olfactory bulb physiology. For local field potential (LFP) and single-unit mitral/tufted cell recordings, animals were anesthetized with urethane (1.5gm/kg) and placed in a stereotaxic apparatus. Upon exposure of the skull, a small hole was drilled over the left olfactory bulb for bulbar recordings or over the left anterior piriform cortex (aPCX) for cortical recordings. LFP and single-unit recordings at all ages were aimed at a similar dorsomedial region of the olfactory bulb. Another small hole was drilled posterior to the bulb allowing a tungsten stimulating electrode to be placed in the ipsilateral lateral olfactory tract for identification of mitral/tufted cells through antidromic activation. A piezoelectric monitor strapped around the animal's chest monitored respiratory activity throughout the experiment. The output was then sent to a window discriminator allowing the odorant pulse to be delivered on the transition of the inspiration–expiration cycle. Animals were placed on a heating pad to maintain constant body temperature.

Field potential recordings were made with tungsten microelectrodes (bulb) (5 Mohms, A-M Systems, Carlsburg, WA) or stainless steel wire (cortex) (0.3mm, Teflon coated, A-M Systems, Carlsburg, WA). All penetrations were approximately perpendicular to the brain surface. Signals were amplified 1000x, band pass filtered (0.1-10,000 Hz), acquired at 500Hz, and analyzed using Spike 2 software (Cambridge Electronic Design, Cambridge, UK). Spectral analysis was performed on 3-sec windows of data immediately prior to and following odorant onset using fast Fourier transforms following application of a Hanning window. Odor-evoked power spectra were normalized to the baseline pre-odor

power for each frequency to facilitate comparisons of relative odor-evoked power increases for each frequency band for each age.

A small number of animals were also used to confirm that differences in local field potential activity across age did not simply reflect differences in anesthetic state. Animals (PN7) were anesthetized with pentobarbital and had chronic indwelling stainless steel electrodes implanted into the olfactory bulb, and were allowed to recover (Wilson and Sullivan, 1990). Odor-evoked local field potential activity was analyzed as described for anesthetized animals.

Single-unit recordings were made with tungsten microelectrodes (5 Mohms, A-M Systems, Carlsburg, WA). Signals were amplified, band pass filtered (300Hz-10kHz), acquired at 25kHz and analyzed using Spike 2 software (Cambridge Electronic Design, Cambridge, UK). Responses to a homologous series of ethyl esters were compared in a total of 77 cells from PN 7 and mature rats. Only cells showing excitatory responses to at least 1 of the ethyl esters presented were used in this study. For all RF mapping, animals were given 2-second odor pulses delivered in pseudo-random order. Response magnitudes were calculated by subtracting the number of spikes during a 4-second pre-stimulus period from the number of spikes during each 4-second odorant presentation. In most animals, odorants were presented at least twice and the mean response for each odorant was used. To allow for comparisons of overall RF shape, normalized RF's were obtained by calculating response magnitudes for each odorant as a percentage of the best-odorant response magnitude as previously described (Fletcher & Wilson, 2003).

Mean single-unit spontaneous activity was calculated from the spontaneous firing rate of each cell for each 4-second period immediately preceding all odor presentations. Odor-evoked mitral/tufted cell mean maximum instantaneous firing frequency was calculated from the maximum firing rate of each cell for each 4-second period immediately following odor onset. Analysis for relating spike activity to respiratory cycle was calculated by constructing phase histograms of unit activity relative to the respiratory cycle for 4 seconds following each odor onset. Mean vectors describing unit activity and respiratory cycle phase relationships were determined and compared across ages, as described in (Wilson, 1998), with a vector length of 0 representing no phase relationship between unit activity and respiration and a vector length of 1 representing phase lock between respiration and unit activity.

Odor discrimination. Postnatal day 7 (n=7), postnatal day 14 (n=11), or mature rats were used (n=9). For PN 14 and mature animals, telemetry devices were used to measure heart-rate (Data Sciences International, St. Paul, MN). The devices were implanted subcutaneously on the dorsal surface under sodium pentobarbital anesthesia (50mg/kg). Upon recovery from the anesthetic, the PN 14 pups were placed back with their mothers for 2 days. For PN 7 rats, subcutaneous electrodes were implanted under isoflurane anesthesia as described previously (Fletcher and Wilson, 2001). Upon recovery pups were placed in the testing chamber and allowed a 15 min. recovery period before testing. Animals were given 4 sec presentations of the odorants. Only animals displaying heart-rate drops to at least 2 odors were used. In these animals, one

odor was chosen as the habituating odor. Habituation consisted of 20, 4 sec odor presentations given every 10 sec. Upon habituation, the other odors were presented again. The final habituation and cross-habituation magnitudes were calculated as a percentage of the initial heart-rate drop for that odor.

Odorant stimulation. For all experiments, odorant concentrations were 150 parts per million (ppm). Odorants were delivered by passing a stream of humidified, charcoal-filtered air through vials containing each odorant using a flow dilution olfactometer. Odorants used were ethyl acetate, ethyl propionate, ethyl butyrate, ethyl valerate, ethyl hexanoate, ethyl heptanoate, ethyl octanoate, methyl butyrate, propyl butyrate, and isoamyl acetate (Sigma, St. Louis, MO).

RESULTS

Odor stimulation evoked quite different oscillatory activity in the olfactory bulbs of 7 day-old as compared with mature rats. As can be seen in Figure 1A, the majority of odor-evoked activity seen in the olfactory bulb of PN 7 rats consisted of the same low frequency oscillations seen before odor onset as well as a minimal beta band (15-40 Hz) response and essentially no detectable gamma band (40-75 Hz) activity (Figure 1B). The odor-evoked LFP recorded in the mature olfactory bulb showed much greater oscillatory bursts per respiratory cycle (Figure 1A). These oscillatory bursts contained greater beta (15-40 Hz) and gamma (40-75 Hz) band activity in the mature olfactory bulb (Figure 1B).
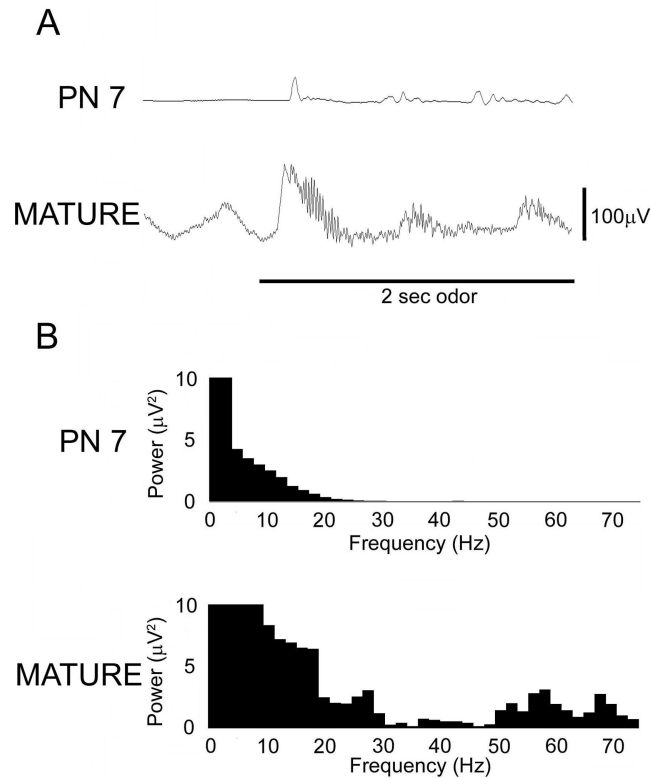
Figure 1. Examples of olfactory bulb local field potentials (LFP) recorded before and during a 2 second presentation of isoamyl acetate (150 ppm dilution). A, Raw signal recorded from the olfactory bulb of a 7 day-old and a mature rat respectively. The horizontal bar indicates odor presentation. B, Power spectra for the odor-evoked oscillations taken from LFP examples above. Note that the majority of odor-evoked activity in the PN 7 rat is in the lower frequency ranges with a minimal beta band (15-40 Hz) response and no gamma band (40-75 Hz) activity as compared to the mature rat analysis showing a relatively large increase in both beta and gamma band odor-evoked activity.

Mean raw power spectra (Figure 2A) for the odor-evoked oscillations demonstrate that the majority of odor-evoked activity in the PN 7 rat is in the lower frequency ranges. This consisted of a minimal beta band response and very little gamma band activity as compared to the mature rats in which there was a relatively large increase in both beta and gamma band odor-evoked activity. Mean raw power spectra were normalized to account for differences in overall baseline power across age. The normalized data again showed the overall trend of increases in both odor-evoked beta band and gamma band power in mature rats, whereas the PN 7 rats had a slight increase in odor-evoked beta band activity with a very large relative increase in lower frequency oscillations (Figure 2B).

Time-frequency comparisons of total beta and gamma band activity by respiratory cycle showed much greater odor-evoked oscillatory activity in mature rats as compared to PN 7 rats (Figure 3). In PN 7 rats, odor stimulation induced a slight, but significant increase in the beta frequency range power (ANOVA: odor evoked beta, $F_{(7,63)}=2.1$, $p=0.05$) with no significant increase in odor-evoked gamma activity (ANOVA: odor-evoked gamma, $F_{(7,63)}=1.4$, ns) (Figure 3A). In contrast, odor stimulation in the mature rats elicited a strong increase in beta band oscillations (ANOVA: odor-evoked beta, $F_{(7,63)}=5.3$, $p < 0.05$) as well as an increase in gamma frequencies not seen in the young animals (ANOVA: odor-evoked gamma, $F_{(7,63)}=2.5$, $p<0.05$) (Figure 3B). There was significantly
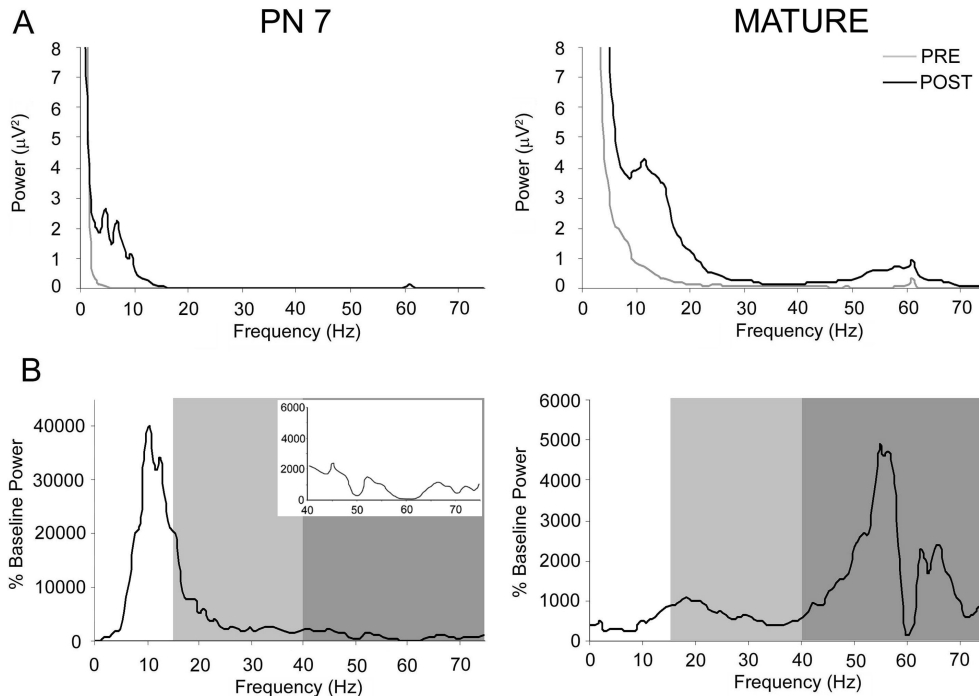
Figure 2. Comparison of olfactory bulb LFP activity in infant and mature rats presented with isoamyl acetate (150 ppm dilution). A, Mean power spectra of odor-evoked LFP oscillations in the olfactory bulb of 7 day-old and mature rats. Mean power spectra before (pre: thin line) and during (thick line) a 2 sec odor stimulus (post). Note the increase in odor-evoked beta and gamma band oscillations in mature rats as compared to 7 day-old rats. B, Mean relative power spectra of odor-evoked LFP oscillations in the olfactory bulb of 7 day-old and mature rats. Mean change in power spectra during a 2 sec odor stimulus relative to pre-odor was expressed for each frequency band relative to the mean baseline power for each frequency within each animal to emphasize difference in odor-evoked power spectra between ages. Mean odor-evoked oscillations increase in the beta (light gray) and gamma (dark gray) bands in the mature rats as opposed to the theta/low beta activity seen in pups. Inset depicts an enlargement of gamma power for PN 7 rats plot on the same power scale as the mature data.
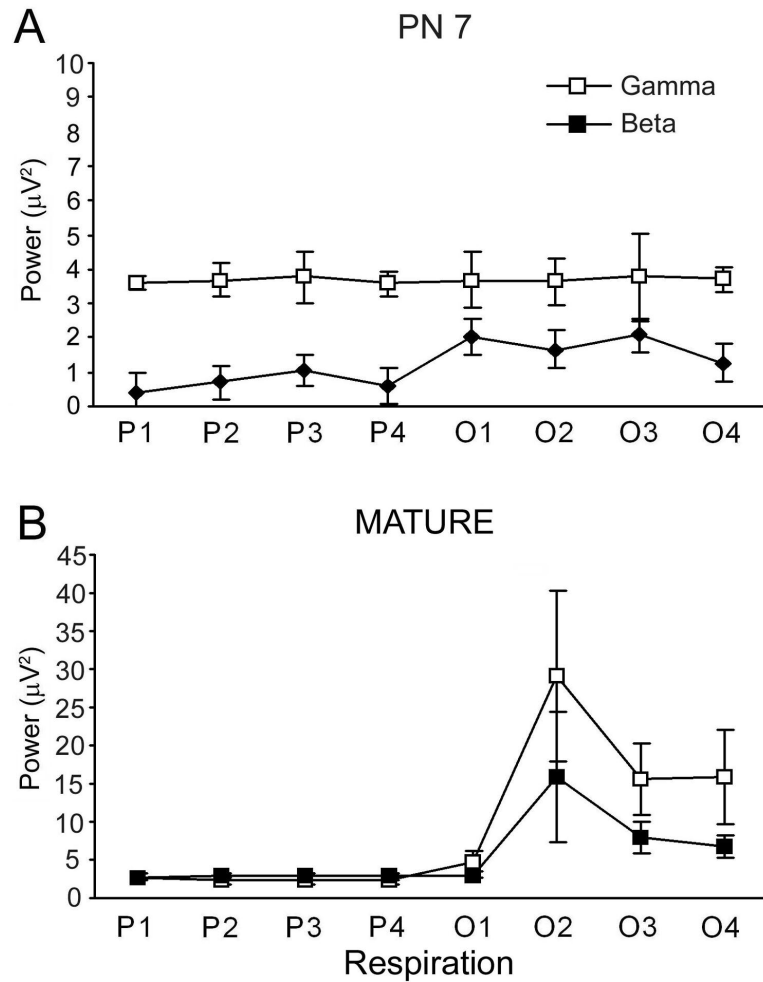
Figure 3.
Comparison of the total mean power in the beta (15-40 Hz) and gamma (40-75 Hz) frequency bands for each respiratory cycle during odor stimulation in PN 7 and mature rats. P1-P4: represents 4 respiratory cycles immediately before odor onset; O1-O4: represents 4 respiratory cycles during odor stimulation. Mean baseline (pre-odor) power spectra were calculated over 4 sniff cycles (P1-P4) with power spectra before and during (O1-O4) a 2 sec odor stimulus expressed as a percent of this baseline activity. Odor stimulation elicits stronger beta and gamma frequency responses in the mature rats. Error bars denote ± standard error.

greater odor-evoked beta and gamma power in the mature rats as compared to the PN 7 rats (ANOVA: main effect of age, $F_{(1,36)}=9.4$, $p<0.05$).

Differences in odor-evoked LFP activity across age were also seen in the piriform cortex. The majority of odor-evoked activity seen in the piriform cortex of PN 7 rats consisted of beta band (15-40 Hz) response and no detectable gamma band (40-75 Hz) activity (Figure 4A). Time-frequency comparisons show oscillatory bursts contained much more odor-evoked beta band oscillatory activity and no significant detectable odor-evoked gamma band activity in both PN 7 (ANOVA: odor-evoked beta, $F_{(7,49)}=4.9$, $p<0.05$; odor-evoked gamma: $F_{(7,49)}=2.1$, ns) (Figure 4C) and mature rats (ANOVA: odor-evoked beta, $F_{(7,49)}=3.3$, $p<0.05$; odor-evoked gamma: $F_{(7,49)}=1.7$, ns) (Figure 4D). The odor-evoked LFP's seen in the mature piriform cortex showed much greater oscillatory bursts per respiratory cycle than that seen in the PN 7 piriform cortex and there was significantly greater odor-evoked beta band power in the mature rats as compared to the PN 7 rats (ANOVA: main effect of age, $F_{(1,28)}=8.9$, $p<0.05$).

Comparisons of single-unit mitral/tufted cell spontaneous and odor-evoked activity revealed differences across age (Figure 5). Of the 77 total cells recorded, 15 cells in each age group responded to at least one ethyl ester and thus are included in the analysis here. Mean single-unit spontaneous activity was significantly greater in the mature rats than in PN 7 rats (mean spontaneous activity: mature = 10.0 ± 1.3 Hz; PN 7 = 0.4 ± 0.2 Hz; unpaired t- test: $t_{(28)}=-7.6$, $p<0.05$) (Figure 5A). Overall, odorants appeared to elicit more robust responses

Figure 4. Examples of piriform cortex local field potentials (LFP) recorded before and during a 2 second presentation of isoamyl acetate (150 ppm dilution). A, Raw signal recorded from the piriform cortex of a 7 day-old rat. B, Raw signal recorded from the pir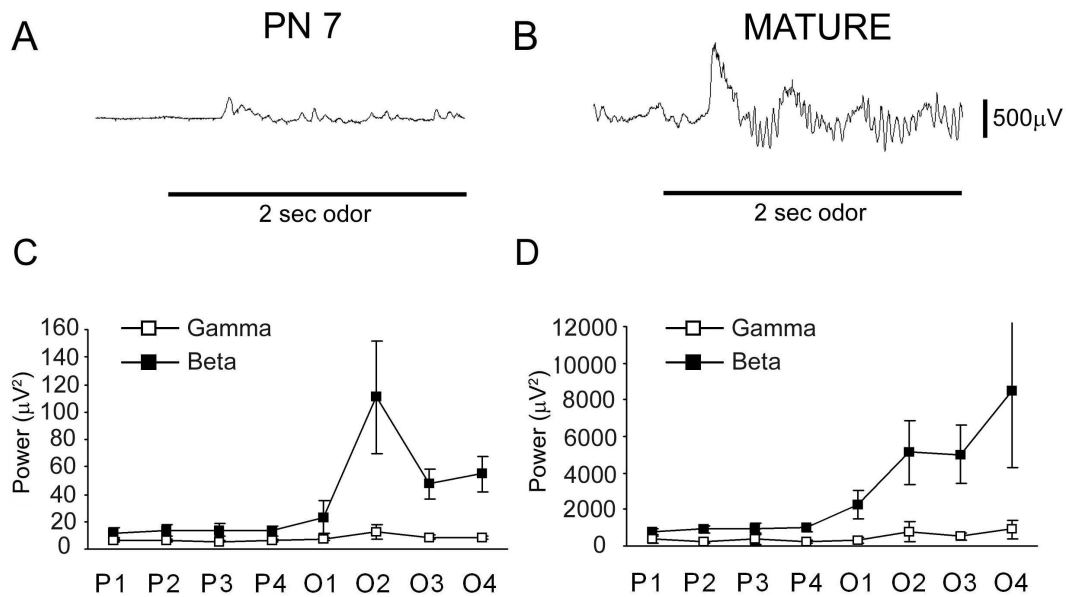iform cortex of a mature rat. The horizontal bar indicates odor presentation. C, D, Comparison of the total power in the beta (15-40 Hz) and gamma (40-75 Hz) frequency bands for each respiratory cycle during odor stimulation in PN 7 and mature rats. Mean baseline (pre-odor) power spectra were calculated over 4 sniff cycles (P1-P4) with power spectra before and during (O1-O4) a 2 sec odor stimulus expressed as a percent of this baseline activity. The majority of odor-evoked piriform cortex activity in PN 7 and mature rats is in the beta (15-40 Hz) frequency ranges with minimal gamma band (40-75 Hz) activity.

in the mature rats (mitral/tufted cell mean odor-evoked maximum instantaneous firing rate: mature = 242.3±30.8 Hz; PN 7 = 39.0±11.7 Hz) (Figure 5B). At PN 7, mitral/tufted activity was significantly more strongly in phase with respiration than mature mitral/tufted cell activity (mean vector length: PN 7=0.30±0.05, mature=0.15±0.06, Mann Whitney: U=44.0, p<0.05) (Figure 5C). Thus, mitral/tufted cells in PN7 rats displayed low levels of spontaneous activity, less robust odor-evoked activity, and activity more tightly in phase with respiration than cells in mature rats. Surprisingly, no significant differences were detected in the normalized mitral/tufted cell receptive fields (Figure 5D) to a homologous series of equal concentration ethyl esters between age groups (ANOVA: main effect of odor, F(4,109)=18.6, p<0.05; main effect of age, F(1,109)=1.2, ns; odor by age, F(4,109)=1.5, ns).

In spite of the significant differences seen in odor-evoked activity in both the olfactory bulb and piriform cortex of PN 7 and mature rats, animals at all ages tested were able to discriminate ethyl esters using a heart-rate orienting response habituation/cross-habituation paradigm (Figure 6). Animals of all ages habituated to a single ethyl ester were able to discriminate structurally similar ethyl esters (ANOVA: main effect of age, F(2,84)=0.24, ns; main effect of odor: F(2,84)=15.78, p< 0.05, no significant age x odor interaction). *Post hoc* Fisher's analysis revealed a significant difference between the response magnitude to the habituated odor and to ethyl esters 1 and 2 carbons longer for each age, p<0.05.

Since this study compared odor-evoked LFP activity in urethane-anesthetized animals to odor acuity in awake animals, a small number of awake
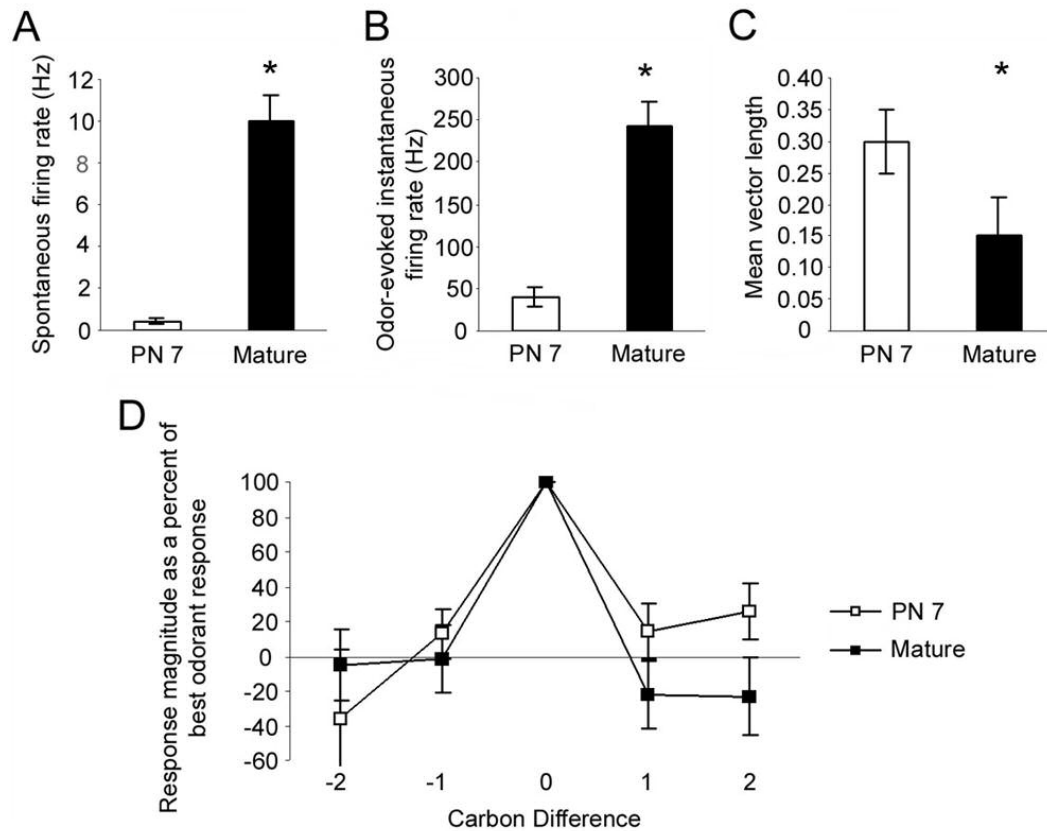
Figure 5. Mitral/tufted cell single unit activity in PN 7 and mature rats. **A**, Spontaneous activity was significantly elevated in adult rats compared to cells in PN 7 rats. **B**. Odor-evoked activity induced significantly higher firing rates in mature rats compared to PN 7 cells. **C**, Single-unit activity was significantly more tightly in phase with respiration in PN 7 rats than cells in mature rats. **D**, Mitral/tufted cell single-unit odorant receptive fields to a homologous series of ethyl esters (150 ppm) were not significantly different between cells in PN 7 and mature rats. Asterisks indicate significantly greater mean spontaneous activity in mature rats. Error bars represent standard error.

olfactory bulb LFP recordings in PN 7 rats (n=3) were also performed under temperature and odor-stimulation conditions identical to the behavioral odor discrimination task. This was done to investigate any possible differences in LFP power in awake animals as well as differences related to body temperature. Although olfactory bulb LFPs from awake animals showed greater odor-evoked beta band oscillatory power than the anesthetized animals, no differences in odor-evoked gamma band activity were seen between anesthetized and awake PN7 rats (ANOVA: condition x frequency, $F_{(1,22)}=10.5$, $p<0.05$; *post hoc* Fisher's test for beta power, $p<0.05$, gamma, ns).

Discussion

Olfactory bulbs with reduced local interneurons may be expected to have poor odor quality coding according to either the spatial or temporal odor coding hypotheses. Together, these two often diametrically opposed hypotheses should predict that infant rats would be deficient in odor discrimination as compared to mature animals, given the anatomical and functional immaturity of the infant rat olfactory system. This, however, was not the case. Based on data presented here, infant rats discriminate similar odors just as well as mature rats despite the restricted number of local interneurons and lack of odor-induced gamma oscillations compared to adults. These results raise questions as to the role of both local olfactory bulb interneurons and olfactory bulb LFP high frequency oscillations in odor discrimination.

Figure 6. Discrimination of novel ethyl esters of different carbon chain length by
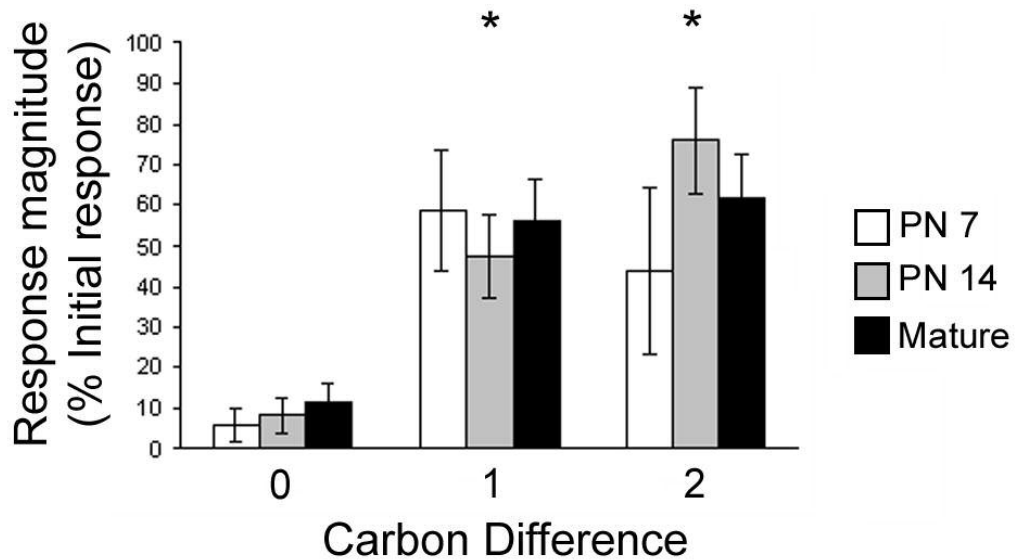
PN 7, PN 14, and mature rats using a heart-rate orienting response habituation/cross-habituation paradigm. The amount of habituation (0 carbon difference) as well as the response magnitude to the cross-habituated odors is expressed as a percentage of the initial heart-rate drop for that odor. Animals at all ages can discriminate ethyl esters differing by a single carbon at the 150ppm concentrations. Asterisks represent significant difference from habituated odor response. Error bars represent standard error.

Odor-evoked olfactory bulb local field potential oscillations differ with age.

Odor-evoked LFP oscillations showed a strong age-dependent change in dominant frequencies between infant and mature rats. In PN 7 rats, odor stimulation evoked a small increase in lower end beta band activity but no detectable increase in gamma oscillations, whereas in mature animals, odor stimulation evoked significantly larger beta and gamma responses (Figure 2). The lack of odor-evoked gamma oscillations was observed in both urethane anesthetized and awake pups. Similar results were seen in a previous study of spontaneous olfactory bulb LFPs in awake rats in that infants displayed a dominant frequency at ~11Hz on PN 6 with very little beta and gamma frequency oscillations and adults were found to have dominant frequencies well within the beta and gamma frequency ranges (Almli et al., 1985).

Since olfactory bulb gamma oscillations are generated by mitral/tufted-granule cell reciprocal interactions (Rall and Shepherd, 1968; Eeckman and Freeman, 1990; Neville and Haberly, 2003; Lagier et al., 2004), it is not surprising that infant rats would exhibit reduced odor-evoked oscillations considering that the number of granule cells is only about 40% of the adult number (Rosselli-Austin and Altman, 1979; Bayer, 1983) and most do not reach adult-like morphology until the third postnatal week (Mair et al., 1982; Frazier-Cierpial and Brunjes, 1989). The immature granule cell population combined with largely unmyelinated mitral cell axons at this age (Schwob et al., 1984) could lead to a greatly reduced olfactory circuit that is incapable of generating the fast oscillations seen in the adult.

Differences in odor-evoked beta and gamma band activity were also seen in the piriform cortex (Figure 4). Although there was no age-dependent change in dominant frequency, odor-evoked changes between ages were seen. Most notably, adult rats showed stronger odor-evoked beta band power as compared to the infants. This could be due to slower conduction velocities of unmyelinated mitral cell axons and delayed maturation of cortical inhibition seen in infant rats (Schwob et al., 1984).

Olfactory bulb mitral/tufted cell activity differs between ages, yet ORFs remain similar.

Single-unit mitral/tufted cell spontaneous and odor-evoked activity differed between ages (Figure 5). Spontaneous activity was much greater in mature rats than in infants. This is consistent with other reports of mitral/tufted cell activity increasing with age (Math and Davrainville, 1980; Shafa et al., 1981; Mair and Gesteland, 1982; Wilson and Leon, 1986). Similarly, odorants appeared to elicit more robust responses in mature rats as measured by instantaneous firing rates. Mitral/tufted cell firing in relation to the respiratory cycle also differed between ages. At PN 7, mitral/tufted activity was significantly more in phase with respiration than mature mitral/tufted cell activity. These results suggest that the temporal response patterns of infant mitral/tufted cells more closely reflect olfactory receptor input than that of mature animals, perhaps due to reduced local circuit and cortical feedback activity in neonates.

Despite differences in spontaneous activity and odor-evoked instantaneous firing rates, no dramatic differences were observed between infant

and mature single-unit mitral/tufted ORFs. Infant and adult rat mitral/tufted cell ORFs had a single best odorant with similar odorants evoking relatively smaller responses. This suggests that mitral/tufted cell responses to a particular odorant in relation to other related odorants are similar in infants and mature animals, again despite major differences in local circuit anatomy across ages.

Discrimination of structurally similar esters is similar in infants and mature rats.

Despite the differences in olfactory bulb odor-evoked activity, no difference in discriminatory ability was observed, with animals at all ages capable of discriminating 1- and 2-carbon odorants at 150 ppm concentration. These results show infant rats' olfactory acuity to be equal to that of mature animals in a simple odor discrimination task. In light of the differences between infant and mature rat olfactory bulb odor-evoked oscillatory activity, these results raise questions as to the role of granule cells and gamma frequency oscillations in olfactory odor coding.

Odor coding and odor discrimination in neonates.

Our results support the view that changes in firing rates of spatially defined mitral/tufted cells may be sufficient for simple odor quality coding in the mammalian olfactory bulb. In this view the olfactory bulb acts as an odorant feature detector in which different features of a specific odorant activate specific sets of glomeruli and their corresponding mitral/tufted cells (Mori et al., 1999; Leon and Johnson, 2003). The piriform cortex then integrates these subsets of active cells (features) into perceptual wholes (Wilson and Stevenson, 2003), thus

enabling the animal to discriminate a variety of odorants. This basic circuitry is relatively intact by PN7 in the rat, as is simple odor discrimination of similar odorants. Large populations of local interneurons, and the LFP high frequency oscillations dependent on those interneurons, are not present at PN 7, and yet there is no corresponding deficit in behavioral or mitral/tufted cell odorant discrimination. These results are consistent with findings in both Manduca moths (Christensen et al., 1998) and zebrafish (Friedrich et al., 2004) that odor-evoked synchronous output neuron oscillatory activity is not required for odor identity coding.

Odor-specific spatial patterns of glomerular activity are apparent at birth and do not change dramatically over the postnatal period, while spatial patterns of mitral cell activity are more diffuse early in development and then become spatially restricted with maturation (Astic and Saucier, 1981; Guthrie and Gall, 2003). The restriction of spatial patterns of mitral cell activity may reflect the increased numbers of inhibitory interneurons (Brunjes and Frazier, 1986) and/or the pruning of olfactory receptor axons (Zou et al., 2004) and mitral cell apical dendrites during the first and second postnatal weeks (Malun and Brunjes, 1996). Nonetheless, the present results suggest that spatial coding alone may be sufficient for discrimination between monomolecular compounds in the absence of background stimuli, intensity shifts, or complex odor plume dynamics. LFP high frequency oscillations, on the other hand, may indicate processing that is not required for simple discrimination.

Furthermore, work from a variety of behavioral paradigms has suggested that olfactory bulb LFP oscillations, rather than simply reflecting odor quality encoding, may reflect behavioral state, past experience and odor expectancy (Freeman and Schneider, 1982; Gray and Skinner, 1988; Ravel et al., 2003). For example, in highly trained animals, gamma frequency oscillatory activity is often most pronounced prior to odor onset, at a time when the animal is preparing to sample the odor (Ravel et al., 2003). Similarly, Freeman has demonstrated that olfactory bulb spatial patterns of LFP oscillations (largely reflecting mitral-granule cell interactions) are not odor-specific, but rather reflect past associations and memory (Freeman and Schneider, 1982).

These data suggest strong top-down influences on olfactory bulb LFP oscillations, which may not be expected to dramatically affect simple discrimination of novel odorants. Freeman suggests this cortical feedback may create expectancy-based templates of local interneuron (granule cell) activity, upon which the receptor afferent activity is imposed (Freeman and Schneider, 1982). In situations such as the well-learned tasks described above, this feedback could then facilitate odor recognition and discrimination. In other situations, such as the simple discrimination of novel odorants used here, such feedback (and the resulting high frequency oscillations) may be less critical for optimal discrimination performance. Current work is focused on applying this model to investigate the effects of expectation and attention on odor discrimination in infant rats, with the hypothesis that neonates may be specifically impaired in expectancy based effects on olfactory behavior.

The results observed here are reminiscent of the extensive literature on the effects of olfactory bulb lesions on simple odor discrimination by Slotnick and co-workers (e.g., (Slotnick and Bisulco, 2003; Slotnick et al., 2004). There is clear evidence that odorants evoke unique spatial patterns of glomerular layer activity in the olfactory bulb, but that large lesions within these patterns have no detectable effect on simple discrimination. These findings suggest that discrimination between monomolecular compounds, in the absence of background stimuli, intensity shifts or complex odor plume dynamics, is a remarkably simple task for the vertebrate olfactory system – a task easily solved by even a greatly reduced system (ontogenetically or experimentally).

The question remains then, given that the olfactory system can function apparently well despite restricted numbers of interneurons and associated LFP oscillations compared to the mature system, what is the role of these additional cells? It should be noted that in the mature mammalian olfactory bulb, the ratio of numbers of output neurons to juxtaglomerular neurons is 1:20 and output neurons to granule cells is 1:50 or higher (Shepherd, 1998). These ratios are extremely different than what is found in the mammalian thalamus (Shepherd, 1998) and mammalian neocortex (Shepherd, 1998), which all express the reversed ratio of output neurons to local interneurons of approximately 3:1. The mammalian olfactory bulb appears to be an extreme outlier in terms of local interneuron numbers, though it clearly functions relatively well on simple tasks with many fewer interneurons. The apparent robust redundancy and complexity of the mature olfactory system, therefore, may reflect the fact that odor-guided

behavior normally requires much more sophisticated computation than is required for simple odor discrimination.

Chapter 4

Ontogeny Of Odor Discrimination: Intensity Modulation Of Olfactory Acuity

Abstract

Olfactory acuity can be modulated by several factors including past experience, expectation and stimulus intensity. Although imaging data appear to predict reduced olfactory acuity as stimulus intensity increases, behavioral data suggest just the opposite – enhanced odorant discrimination with increasing intensity. In light of these data, it has been argued that olfactory bulb local interneuron function may modulate olfactory acuity with respect to intensity. If this is the case, then neonatal rats, with severely limited numbers of periglomerular and granule interneurons, should exhibit predictably different patterns of intensity modulation of olfactory acuity than mature rats. To investigate this, odor discrimination was compared in week-old and post-weaning rats.

Odorant discrimination was determined using a cross-habituation task with odor-evoked heart-rate orienting responses as the behavioral measure. This task requires no prior training, and can be expressed by animals during the first postnatal week; thus it is ideal for the study of odor discrimination ontogeny. A homologous series of ethyl esters were used as stimuli at 75, 150 and 300 ppm. In post-weaning rats, olfactory acuity increased with moderate stimulus intensity, but decreased as intensity increased to 300 ppm. In week-old rats, however, acuity was greatest at the lowest intensity and was reduced as odor intensity increased.

Introduction

One of the central tasks of the olfactory system is to selectively discriminate between olfactory stimuli. In any environment, a given odorant may be present at different concentrations or intensities at different times and locations. For example, odorant concentrations may be very high at their source, yet relatively weak some distance away. Thus, for animals dependent upon olfaction, it is necessary to be able to reliably discriminate many odorants at a variety of concentrations.

Odor perception begins with odorants binding to several different olfactory receptor neurons in the epithelium (Araneda et al., 2000; Mombaerts, 2004). This subset of activated sensory neurons forms the basis of the combinatorial odor code that is mapped onto the glomerular layer of the olfactory bulb. In this way, the pattern of glomerular activation would represent a collection of odor features that represent the odor percept. Odor-evoked glomerular activity maps have been found to be similar for perceptually similar odorants yet individually distinct for any given odorant (Linster et al., 2001; Leon and Johnson, 2003). Imaging of glomerular activity at different intensities has shown an increasing degree of representational overlap as odorant concentration increases. Therefore, increased odor representational overlap within the olfactory bulb could possibly lead to reduced olfactory acuity as stimulus intensity increases (Johnson and Leon, 2000; Xu et al., 2000; Bozza et al., 2004).

Behavioral data, however, suggests just the opposite – enhanced odorant discrimination with increasing intensity (Cleland and Narla, 2003; Wright and

Smith, 2004). These studies imply that the increasing overlap among glomerular activation patterns at higher concentrations does not adversely affect perceptual acuity. In light of these data, it has been argued that contrast enhancement in the olfactory system is dynamic, depending on olfactory bulb interneuron function to modulate olfactory acuity with respect to intensity (Fletcher et al., 2005a).   In this model, at high odorant concentrations, the most active glomerular columns would inhibit neighboring glomerular columns through inhibitory periglomerular cells or deeper granule cell populations (Luo and Katz, 2001; Aungst et al., 2003).

Neonatal rats provide an excellent system for testing this model in that they possess limited numbers of periglomerular and granule interneurons in the first week of life (Brunjes et al., 1982; Bayer, 1983; Frazier and Brunjes, 1988), yet display adult-like mitral/tufted cell odor receptive fields (Fletcher et al., 2005b). Due to their lower number of interneurons, and thus lack of adult-like inhibition, infant rats would be expected to exhibit predictably different patterns of intensity modulation of olfactory acuity than mature rats. To investigate this, odor discrimination was compared in week-old and post-weaning rats using a homologous series of ethyl esters at three different intensities.

Methods

Subjects. Male and female Long-Evans hooded rats were tested at either the end of the first postnatal week (PN6-7) (n=23) or postweaning (PN 21-24) (n=26). Subcutaneous telemetry devices or recording electrodes were implanted under anesthesia as previously described (Fletcher and Wilson, 2001; Fletcher et al., 2005b). Upon recovery pups were placed in the testing chamber and allowed a 15 min. recovery period before testing.

Odor discrimination. Animals were given 4-sec presentations of the odorants. Only animals displaying heart-rate drops to at least 2 odorants were used. In these animals, one odorant was pseudorandomly chosen as the habituating odorant. Habituation consisted of 20, 4 -sec odorant presentations given every 10 sec. Upon habituation, each of the odorants was presented again. The final habituation and cross-habituation magnitudes were calculated as a percentage of the initial heart-rate drop for that odor.   For comparison across concentrations, a discrimination index was calculated by subtracting the habituated response magnitude from the cross-habituated response magnitude.

Odorants. Odorants were delivered at 75 ppm, 150 ppm, or 300ppm by passing a stream of humidified, charcoal filtered air through vials containing each odorant using a flow dilution olfactometer. Odorants used were ethyl acetate, ethyl propionate, ethyl butyrate, ethyl valerate, ethyl hexanoate, and ethyl heptanoate.
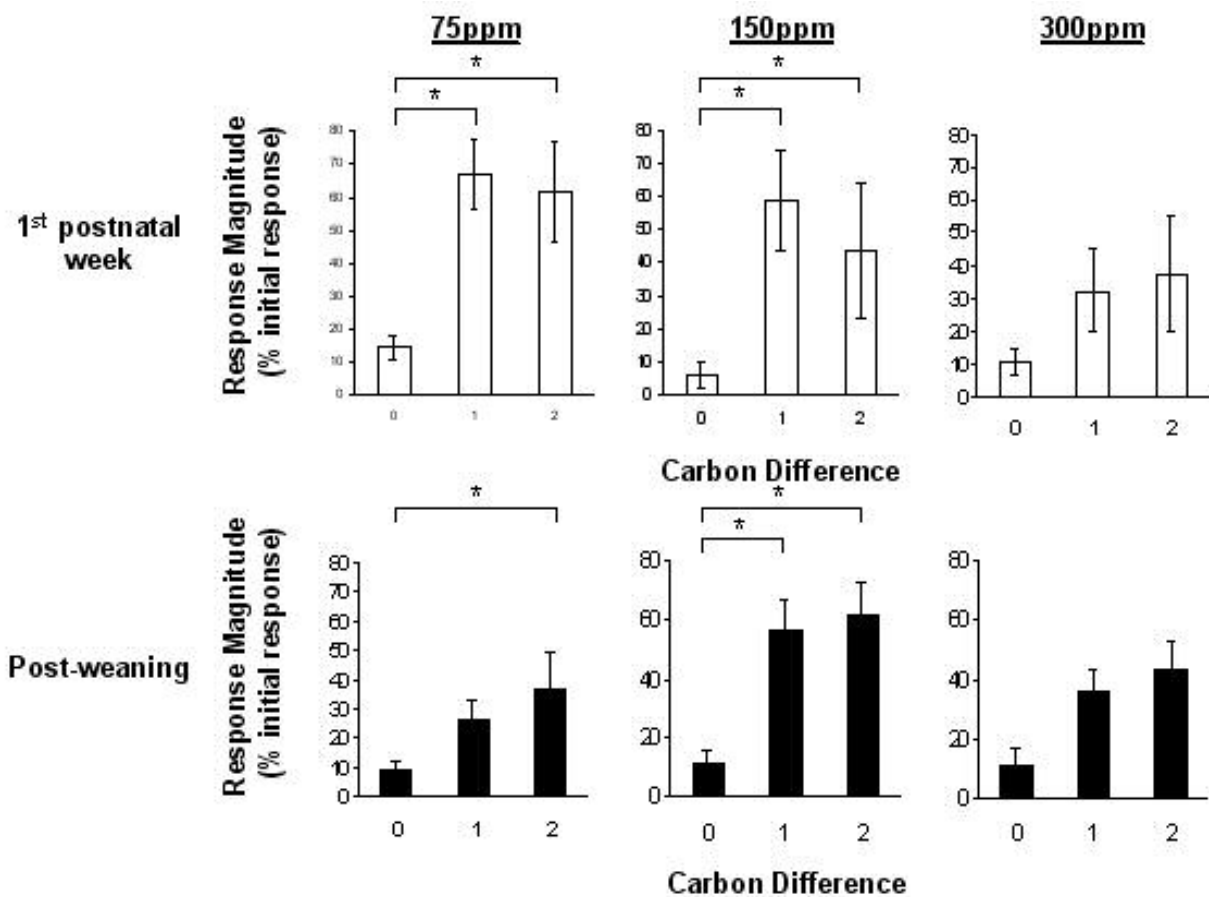
Results

Discrimination of novel ethyl esters of different carbon chain length by week old and post-weanling rats was investigated by using a heart rate-orienting response habituation/cross-habituation paradigm. On average, the magnitude of self-habituation was independent of age or concentration across range used here.

Examination of cross-habituation between novel esters revealed that animals at both ages could discriminate ethyl esters at the 150 ppm concentration (ANOVA: main effect of odor, $F_{(2, 144)}$ = 23.8, p < 0.05; *posthoc* Fisher's tests revealed significant differences between the self- and cross-habituated odor response magnitudes for the 1-carbon and 2-carbon difference, *p* < 0.05) (Figure 1).

Interestingly, there appears to be age-related differences in discriminating ethyl esters at the low concentration, 75 ppm. While both ages could make 2-carbon discriminations at 75 ppm, only the younger animals were capable of making a 1-carbon discrimination, suggesting greater acuity at lower concentrations (ANOVA: concentration x age, $F_{(2, 144)}$ = 4.4, p < 0.05; *posthoc* Fisher's test for week old 1-carbon discrimination: p < 0.05; week old 2-carbon discrimination: p < 0.05; for weanling 1-carbon discrimination: NS; weanling 2-carbon discrimination: p < 0.05) (Figure 1). Neither age group could reliably discriminate a 1- or 2-carbon difference at 300ppm (ANOVA: main effect of odor, $F_{(2, 144)}$ = 23.8, p < 0.05; *posthoc* Fisher's tests revealed no differences between

the self- and cross-habituated odor response magnitudes for the 1-carbon and 2-carbon difference, NS) (Figure 1).

As stated above, there were no significant differences in self-habituation between either age at any concentration (ANOVA: concentration x age, $F_{(2,44)}$ = 0.87, NS) (Figure 2A). To facilitate comparison across ages and concentrations, a discrimination index was calculated by subtracting the habituated response magnitude from the cross-habituated response magnitude. Since the main differences in acuity between the ages were seen for the 1-carbon discrimination, only the discrimination indices for 1-carbon differences are presented here (Figure 2B). As can be seen, odor acuity in neonates decreased at the highest odorant intensity only, while mature rats showed an initial increase in acuity with increasing stimulus intensity but a decrease in acuity at the highest intensity (ANOVA: main effect of concentration, $F_{(2, 65)}$ = 4.2, $p < 0.05$; *posthoc* Fisher's tests revealed significant differences in acuity at 150 ppm in the postweanling age group, $p < 0.05$; as well as significant differences in acuity at 300 ppm for the week-old animals, $p < 0.05$). Overall, these results suggest differences in olfactory acuity as a function of age and odorant intensity with young animals capable of making fine odor discriminations at lower odorant intensities.

Figure 1. Discrimination of novel ethyl esters of different carbon chain length by week old and post-weanling rats using a heart rate-orienting response habituation/cross-habituation paradigm. The amount of self-habituation (0 carbon difference) as well as the response magnitude to the cross-habituated odors is expressed as a percentage of the initial heart rate drop for that odor. Animals at all ages can discriminate ethyl esters differing by a single carbon at the 150 ppm concentration. However, only the younger animals were capable of making a 1-carbon discrimination at 75 ppm, suggesting greater acuity at lower concentrations. Neither age group could reliably discriminate a 1- or 2-carbon difference at 300ppm. Asterisks represent significant difference from habituated odor response. Error bars represent SE.
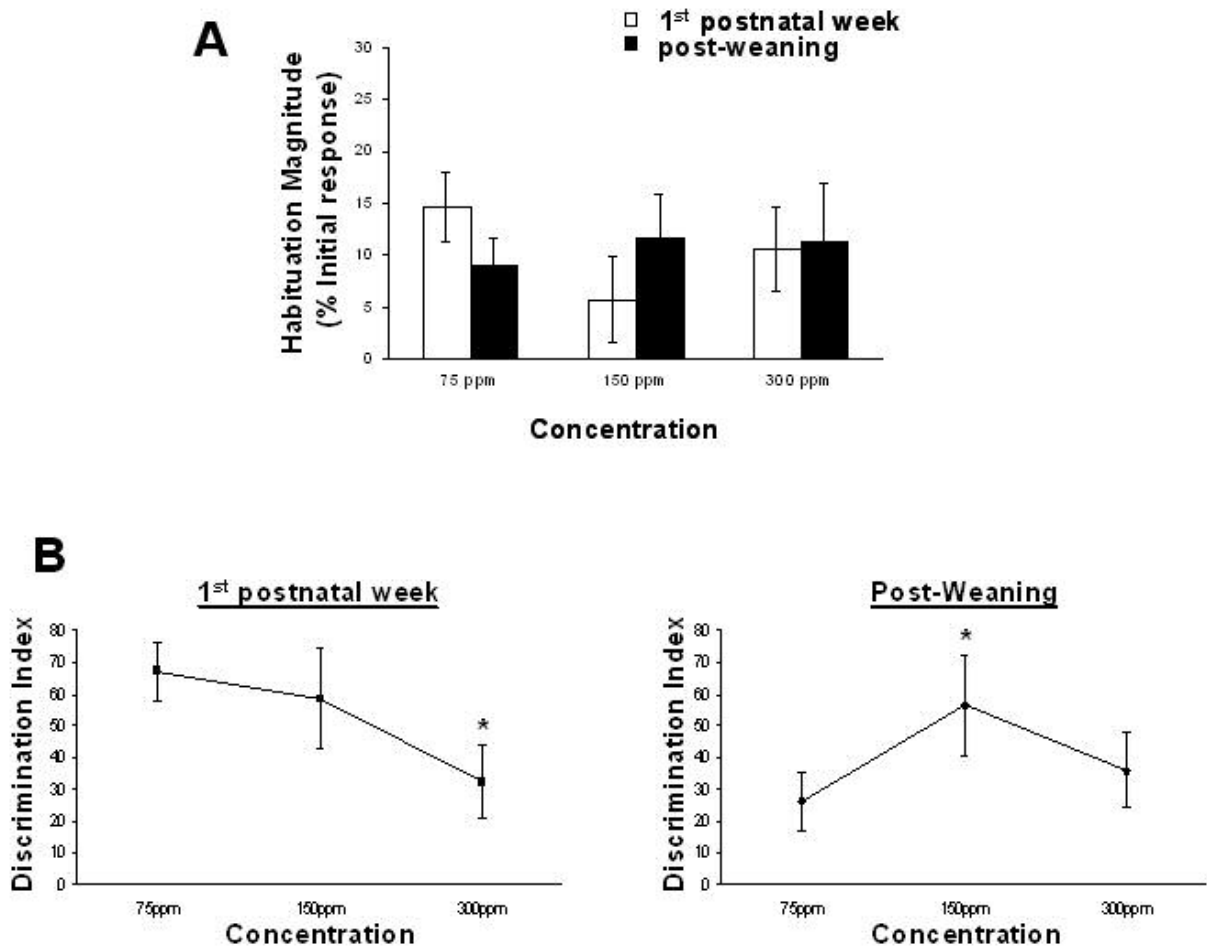
Figure 2. Self- and cross-habituation magnitudes for each concentration for both ages. A. The magnitude of self-habituation was independent of age or concentration across range used here. There were no significant differences in self-habituation between any group. B. Thus, the magnitude of cross-habituation for each intensity is shown below to facilitate visual comparisons across intensities. Though the absolute maximal levels of cross-habituation varied across ages, odor acuity in neonates decrease with increasing odorant intensity, while mature rats showed an initial increase in acuity with increasing stimulus intensity. At the highest intensity used here, however, even mature rats showed decreased acuity (increased cross-habituation). Asterisks represent significant difference from other discrimination indices. Error bars represent SE.

Discussion

In this study, olfactory acuity for young and older animals was dependent upon odor intensity. Over the intensity range tested here, older rats showed an inverted-U shaped relationship between acuity and stimulus intensity.   As stimulus intensity increased, olfactory acuity initially increased then decreased at the highest intensity.   In contrast, neonates showed a decrease in acuity as intensity increased. These results are similar to other studies investigating odor acuity at different intensities. In these studies using adult animals, odor acuity increased with increased intensity (Cleland and Narla, 2003; Wright and Smith, 2004). Our results for the older, post-weanling animals fit well with these reports; however, odor acuity-intensity relationships appear quite different in the neonates.

Several mechanisms could account for the differences seen in acuity at different intensities. For example, increasing concentration could lead to a larger population of cells responsible for the odor code. Imaging studies of glomerular activation by odorants at different concentrations have shown increased glomerular representations with increased concentration (Johnson and Leon, 2000; Uchida et al., 2000; Meister and Bonhoeffer, 2001; Fried et al., 2002; Bozza et al., 2004). These larger representations for each odorant could help enhance odor differences and thus facilitate discrimination.

However, since glomerular activity maps reflect mainly presynaptic activity, it is not known whether the increased glomerular representations seen at higher concentrations lead to increased mitral/tufted cell recruitment. Inhibitory interneurons such as periglomerular cells have been shown to modulate

101

glomerular activity through mechanisms similar to lateral inhibition (Aungst et al., 2003). In this way, highly active glomeruli could suppress other active glomeruli to maintain representational fidelity even at higher concentrations. This is in line with psychophysical and animal studies indicating that many odorants maintain their perceptual qualities within a wide range of concentrations (Gross-Isseroff and Lancet, 1988; Wright and Smith, 2004). However, this mechanism may only function well within a certain range of concentrations. This may potentially explain why the animals displayed decreased acuity at the highest concentrations.

This shifting odor-evoked glomerular representation size in relation to odor intensity could also account for the deficits seen in the older animals at the lowest concentration. At very low intensities, the glomerular maps may be too sparse to effectively code for an odor. In this way the patterns of activity may be too similar for an animal to distinguish very similar odorants, such as those differing by a single carbon.

This ability to discriminate a 1-carbon difference at the lowest intensity in the neonates cannot be fully accounted for by changes in presynaptic activity patterns. However, anatomical and physiological differences between neonatal and mature rats may be able to account for the differences seen. For example, neonates have less than half of the adult numbers of periglomerular and granule cells (Bayer, 1983; Frazier and Brunjes, 1988). Given the extensive interglomerular inhibitory circuitry the periglomerular cells participate in, it is possible that interglomerular inhibition would be drastically reduced in neonatal

rats, leading to larger odor representations within the glomerular layer, and thus facilitate odorant discrimination.

Since a majority of periglomerular cells participate in postsynaptic inhibition of mitral/tufted cell dendrites within each glomerulus (Toida et al., 1998; Hayar et al., 2004), interglomerular inhibition may not be represented in odor-evoked glomerular activation maps that are based on imaging studies of presynaptic input. Thus, at the glomerular level, odor representations should be similar across age. C-fos imaging studies support this idea, as neonatal odor-evoked glomerular activity patterns are sharply defined, odor specific, and similar to older animals (Guthrie and Gall, 2003).

Based on this, one may expect the majority of age-related differences in odor-evoked responses to be seen at the level of the olfactory bulb output neurons, the mitral/tufted cells. Although most mitral/tufted cells appear anatomically mature by PN 7 (Malun and Brunjes, 1996; Matsutani and Yamamoto, 2000), their physiological properties are distinct from mature animals (Math and Davrainville, 1980; Shafa et al., 1981; Mair and Gesteland, 1982; Fletcher et al., 2005b). For example, both mitral/tufted cell spontaneous activity and odor-evoked activity are much lower in neonatal animals as compared to adults (Math and Davrainville, 1980; Fletcher et al., 2005b). Assuming odor coding relies, at least somewhat, on firing rate, neonatal mitral/tufted cells may be more efficient in responding to weaker olfactory nerve input because their baseline spontaneous activity levels are near zero. In this way, very low intensity odorants would result in higher signal-to-noise ratios in neonatal animals. This

could result in increased acuity at low concentrations as compared to older animals.

In addition, although granule cell inhibition of mitral cell activity is present in the first week of life (Wilson and Leon, 1986), it is certainly reduced as infant rats lack the high frequency oscillatory activity seen in adults that is associated with mitral-granule cell reciprocal interactions (Salas et al., 1969; Iwahara et al., 1973; Almli et al., 1985; Fletcher et al., 2005b). At this point it is unclear if this reduced inhibition contributes to the increased neonatal odor acuity at the lowest intensity as compared to older animals.

Based on the results reported here, it appears that neonatal animals posses greater olfactory acuity at low odor intensities as compared to more mature animals. This ability may stem from the developmental differences seen between the two ages, although the exact mechanism responsible for the differences is not known. Overall, these results suggest that neonatal rats show no deficits in simple olfactory acuity tasks despite a somewhat reduced olfactory circuit.

Chapter 5

Conclusions

In summary, the research presented here extends my previous work in both perceptual learning and ontogeny of olfactory coding and discrimination (Fletcher and Wilson, 2001; Fletcher and Wilson, 2002). Olfactory bulb mitral/tufted cell odorant receptive fields were found to shift toward the experienced odorant within one hour following exposure. These results suggest that odorant experience can shape olfactory bulb odor coding and may be partly responsible for the increased acuity seen in the behavioral perceptual learning experiments above.

At this point, it is still unclear if the experience-induced shifts in mitral/tufted cell RFs represent plasticity solely occurring within the olfactory bulb, or if changes are occurring in multiple areas along the olfactory pathway. Given the extensive centrifugal input from olfactory cortex that terminates within the granule cell layer of the olfactory bulb, it would not be surprising if the RF changes seen are mediated through feedback from olfactory cortex. This hypothesis could be further investigated by blocking centrifugal input to the olfactory bulb during the 50-sec odor-exposure. Another interesting question is do the RF shifts seen in the anesthetized animals actually correlate with the improved acuity seen in the awake animals? This could be addressed by comparing mitral/tufted cell RFs in both trained and untrained animals. Presumably, one might expect to find more mitral/tufted cells RFs shifted toward the learned odor in the trained animals.

The second project detailed an examination of the ontogeny of odor discrimination as well as the role of odor-evoked oscillations in odor coding.

Recent work in invertebrates has suggested that high frequency oscillations may play an important role in odor coding (Laurent, 1999). Infant rats, which lack a majority of the circuitry involved in generating these oscillations, were found to have no detectable odor-evoked gamma frequency activity as compared to adults, while mitral/tufted cell odorant receptive fields were nearly identical across age. In addition, infant rats were similar to adults in discriminating ethyl esters differing by as little as a single carbon at 150 ppm concentration. These results showed that despite a lack of odor-evoked gamma oscillations seen in the adult, infant rats showed no deficits in simple odor discrimination tasks. This suggests that high frequency oscillations may not be required for simple, novel odor discrimination.

It would be interesting to further investigate the role high frequency oscillations play in olfactory system odor coding. Studies in adult mammals have shown olfactory bulb gamma oscillations are correlated with behavioral context and can increase prior to odor sampling in animals trained in more complex odor discrimination tasks (Freeman and Schneider, 1982; Gray and Skinner, 1988; Ravel et al., 2003). Based on this, it is possible that patterns of bulbar oscillatory activity could be influenced by centrifugal input from olfactory cortical areas as well as other modulatory regions. These higher centers could prime the bulb for odors having behavioral relevance based upon prior experience, expectation, and attention. Based on this, neonatal animals may show deficits in behavioral discrimination tasks involving expectation or attention.

The final project of this dissertation further investigated the ontogeny of odor acuity by comparing odor discrimination in weanling and neonatal rats. In this experiment, odor acuity was examined at different odor concentrations. Overall, the results showed that, unlike older animals, neonatal rats are capable of making fine odor discriminations at low odor concentrations; while animals at both ages could not make 1- or 2-carbon discriminations at the highest intensity tested. Many mechanisms could explain the differences seen between the two ages. For example, lower odor-evoked mitral/tufted cell signal-to-noise ratios could contribute to the increased acuity at lower concentrations in neonatal animals. Further experiments involving different ages, especially younger animals, and a broader range of concentrations may help further understand the differences seen.

Overall, the developmental studies outlined above provide evidence that key olfactory questions may be better understood by comparing neonatal and adult olfactory capabilities. By correlating know developmental and anatomical insufficiencies with odor discrimination-related behavioral deficits, a better understanding of the true mechanisms underlying odor coding can be elucidated. In conclusion, the research outlined here provides evidence of a very dynamic olfactory system in which physiological and anatomical changes brought on through development and experience can have profound effects on olfactory bulb odor coding and acuity.

References

Adrian ED (1938) Nervous Discharges from the Olfactory Organs of Fish. J Physiol 94:441-460.

Adrian ED (1942) Olfactory reactions in the brain of the hedgehog. J Physiol 100:459-473.

Adrian ED (1950) The electrical activity of the mammalian olfactory bulb. Electroen Clinical Neuro l 2:377-388.

Adrian ED (1952) The electrical activity of the mammalian olfactory bulb.

Almli CR, Henault MA, Velozo CA, Morgane PJ (1985) Ontogeny of electrical activity of main olfactory bulb in freely-moving normal and malnurished rats. Develop Brain Res 18:1-12.

Araneda RC, Kini AD, Firestein S (2000) The molecular receptive range of an odorant receptor. Nat Neuroscience 3:1248-1255.

Aroniadou-Anderjaska V, Ennis M, Shipley MT (1997) Glomerular synaptic responses to olfactory nerve input in rat olfactory bulb slices. Neuroscience 79:425-434.

Aroniadou-Anderjaska V, Ennis M, Shipley MT (1999) Dendrodendritic recurrent excitation in mitral-tufted cells of the rat olfactory bulb. J Neurosci 82: 489-494.

Aroniadou-Anderjaska V, Zhou FM, Priest CA, Ennis M, Shipley MT (2000) Tonic and synaptically evoked presynaptic inhibition of sensory input to the rat olfactory bulb via GABA(B) heteroreceptors. J Neurophysiol 84:1194-1203.

Astic L, Saucier D (1981) Ontogenesis of the functional activity of rat olfactory bulb: autoradiographic study with the 2-deoxyglucose method. Brain Res 254:243-256.

Aungst JL, Heyward PM, Puche AC, Karnup SV, Hayar A, Szabo G, Shipley MT (2003) Centre-surround inhibition among olfactory bulb glomeruli. Nature 426:623-629.

Bayer SA (1983) 3H-thymidine-radiographic studies of neurogenesis in the rat olfactory bulb. Exp Brain Res 50:329-340.

Becker CJ, Freeman WJ (1968) Prepyriform electrical activity after loss of peripheral and central input, or both. Physiol Behav 3:597-599.

Belluscio L, Lodovichi C, Feinstein P, Mombaerts P, Katz LC (2002) Odorant receptors instruct functional circuitry in the mouse olfactory bulb. Nature 419:296-300.

Bischofberger J, Jonas P (1997) Action potential propagation into the presynaptic dendrites of rat mitral cells. J Physiol 504 (Pt 2):359-365.

Boulet M, Daval G, Leveteau J (1978) Qualitative and quantitative odour discrimation by mitral cells as compared to anterior olfactory nucleus cells. Brain Res 142:123-134.

Bowery NG, Hudson AL, Price GW (1987) GABAA and GABAB receptor site distribution in the rat central nervous system. Neuroscience 20:365-383.

Bozza T, Feinstein P, Zheng C, Mombaerts P (2002) Odorant receptor expression defines functional units in the mouse olfactory system. J Neurosci 22:3033-3043.

Bozza T, McGann JP, Mombaerts P, Wachowiak M (2004) In vivo imaging of neuronal activity by targeted expression of a genetically encoded probe in the mouse. Neuron 42:9-21.

Bozza TC, Kauer JS (1998) Odorant response properties of convergent olfactory receptor neurons. J Neurosci 18:4560-4569.

Breer H, Boekhoff I (1991) Odorants of the same odor class activate different second messenger pathways. Chem Senses 16:19-29.

Brennan PA, Keverne EB (1997) Neural mechanisms of mammalian olfactory learning. Prog Neurobiol 51: 457-481.

Bressler SL (1984) Spatial organization of EEGs from olfactory bulb and cortex. Electroen Clinical Neuro 57:270-276.

Bressler SL, Freeman WJ (1980) Frequency analysis of olfactory system EEG in cat, rabbit, and rat. Electroencephalogr Clin Neurophysiol 50:19-24.

Brunet LJ, Gold GH, Ngai J (1996) General anosmia caused by a targeted disruption of the mouse olfactory cyclic nucleotide-gated cation channel. Neuron 17:681-693.

Brunjes P, Schwark HD, Greenough WT (1982) Olfactory granule cell development in normal and hyperthyroid rats. Developmental Brain Research 5:149-159.

Brunjes PC, Frazier LL (1986) Maturation and plasticity in the olfactory system of vertebrates. Brain Res 396:1-45.

Buck L, Axel R (1991) A novel multigene family may encode odorant receptors: a molecular basis for odor recognition. Cell 65:175-187.

Buck LB (1996) Information coding in the vertebrate olfactory system. Annu Rev Neurosci 19:517-544.

Buonomano DV, Merzenich MM (1998) Cortical plasticity: from synapses to maps. Annu Rev Neurosci 21: 149-186.

Buonviso N, Chaput M (2000) Olfactory experience decreases responsiveness of the olfactory bulb in the adult rat. Neuroscience 95: 325-332.

Buonviso N, Revial MF, Jourdan F (1991) The Projections of Mitral Cells from Small Local Regions of the Olfactory Bulb: An Anterograde Tracing Study Using PHA-L (Phaseolus vulgaris Leucoagglutinin). Eur J Neurosci 3:493-500.

Chabaud P, Ravel N, Wilson DA, Mouly AM, Vigouroux M, Farget V, Gervais R (2000) Exposure to behaviourally relevant odour reveals differential characteristics in rat central olfactory pathways as studied through oscillatory activities. Chem Senses 25:561-573.

Chaput MA, Holley A (1985) Responses of olfactory bulb neurons to repeated odor stimulations in awake freely-breathing rabbits. Physiol Behav 34:249-258.

Chen WR, Midtgaard J, Shepherd GM (1997) Forward and backward propagation of dendritic impulses and their synaptic control in mitral cells. Science 278:463-467.

Chen WR, Shen GY, Shepherd GM, Hines ML, Midtgaard J (2002) Multiple modes of action potential initiation and propagation in mitral cell primary dendrite. J Neurophysiol 88:2755-2764.

Chen WR, Shepherd GM (1997) Membrane and synaptic properties of mitral cells in slices of rat olfactory bulb. Brain Res 745:189-196.

Chen WR, Xiong W, Shepherd GM (2000) Analysis of relations between NMDA receptors and GABA release at olfactory bulb reciprocal synapses. Neuron 25:625-633.

Christensen TA, Lei H, Hildebrand JG (2003) Coordination of central odor representations through transient, non-oscillatory synchronization of glomerular output neurons. Proc Natl Acad Sci USA 100:11076-11081.

Christensen TA, Waldrop BR, Hildebrand JG (1998) Multitasking in the olfactory system: context-dependent responses to odors reveal dual GABA-regulated coding mechanisms in single olfactory projection neurons. J Neurosci 18:5999-6008.

Christie JM, Schoppa NE, Westbrook GL (2001) Tufted cell dendrodendritic inhibition in the olfactory bulb is dependent on NMDA receptor activity. J Neurophysiol 85:169-173.

Christie JM, Westbrook GL (2003) Regulation of backpropagating action potentials in mitral cell lateral dendrites by A-type potassium currents. J Neurophysiol 89:2466-2472.

Clancy AN, Schoenfeld TA, Forbes WB, Macrides F (1994) The spatial organization of the peripheral olfactory system of the hamster. Part II: receptor surfaces and odorant passageways within the nasal cavity. Brain Res Bull 34: 211-241.

Cleland TA, Narla VA (2003) Intensity modulation of olfactory acuity. Behav Neurosci 117:1434-1440.

Davis BJ, Macrides F (1981) The organization of centrifugal projections from the anterior olfactory nucleus, ventral hippocampal rudiment, and piriform cortex to the main olfactory bulb in the hamster: an autoradiographic study. J Comp Neurol 203:475-493.

Davis BJ, Macrides F (1982) Tyrosine hydroxylase immunoreactive neurons and fibers in the olfactory system of the hamster. J Comp Neurol 214:427-440S.

De Carlos JA, Lopez-Mascaraque L, Valverde F (1989) Connections of the olfactory bulb and nucleus olfactorius anterior in the hedgehog (Erinaceus europaeus): fluorescent tracers and HRP study. J Comp Neurol 279:601-618.

De Olmos J, Hardy H, Heimer L (1978) The afferent connections of the main and accessory olfactory bulb formations in the rat: an experimental HRP-study. J Comp Neurol 181:213-244.

Diamond DM, Weinberger NM (1986) Classical conditioning rapidly induces specific changes in frequency receptive fields of single neurons in secondary and ventral ectosylvian auditory cortical fields. Brain Res 372: 357-260.

Dionne VE (1992) Chemosensory responses in isolated olfactory receptor neurons from Necturus maculosus. J Gen Physiol 99:415-433.

Duchamp-Viret P, Duchamp A, Chaput MA (2003) Single olfactory sensory neurons simultaneously integrate the components of an odour mixture. Eur J Neurosci 18:2690-2696.

Eeckman FH, Freeman WJ (1990) Correlations between unit firing and EEG in the rat olfactory system. Brain Res 528:238-244.

Egger V, Svoboda K, Mainen ZF (2003) Mechanisms of lateral inhibition in the olfactory bulb: efficiency and modulation of spike-evoked calcium influx into granule cells. J Neurosci 23:7551-7558.

Ekstrand JJ, Domroese ME, Feig SL, Illig KR, Haberly LB (2001) Immunocytochemical analysis of basket cells in rat piriform cortex. J Comp Neurol 434:308-328.

Ennis M, Linster C, Aroniadou-Anderjaska V, Ciombor K, Shipley MT (1998) Glutamate and synaptic plasticity at mammalian primary olfactory synapses. Ann NY Acad Sci USA 855: 457-466.

Ennis M, Zhou FM, Ciombor KJ, Aroniadou-Anderjaska V, Hayar A, Borrelli E, Zimmer LA, Margolis F, Shipley MT (2001) Dopamine D2 receptor-mediated presynaptic inhibition of olfactory nerve terminals. J Neurophysiol 86:2986-2997.

Faber T, Joerges J, Menzel R (1999) Associative learning modifies neural representations of odors in the insect brain. Nat Neurosci 2: 74-78.

Firestein S, Werblin F (1989) Odor-induced membrane currents in vertebrate-olfactory receptor neurons. Science 244:79-82.

Fletcher M, Wilson DA (2001) Ontogeny of odor discrimination: a method to assess novel odor discrimination in neonatal rats. Physiol Behav 74:589-593.

Fletcher ML, Smith AM, Best AR, Wilson DA (2005b) High-frequency oscillations are not necessary for simple olfactory discriminations in young rats. J Neurosci 25:792-798.

Fletcher ML, Wilson DA (2002) Experience modifies olfactory acuity: acetylcholine-dependent learning decreases behavioral generalization between similar odorants. J Neurosci 22: RC201.

Fletcher ML, Wilson DA (2003) Olfactory bulb mitral-tufted cell plasticity: odorant-specific tuning reflects previous odorant exposure. J Neurosci 23:6946-6955.

Fletcher ML, Wilson DA, Cleland TA (2005a) Ontogeny of odor discrimination: intensity modulation of olfactory acuity emerges postnatally. In: The Association for Chemoreception Sciences. Sarasota, FL.

Frazier LL, Brunjes PC (1988) Unilateral odor deprivation: early postnatal changes in olfactory bulb cell density and number. J Comp Neurol 269:355-370.

Frazier-Cierpial LL, Brunjes PC (1989) Early postnatal differentiation of granule cell dendrites in the olfactory bulbs of normal and unilaterally odor-deprived rats. Dev Brain Res 47:129-136.

Freeman WJ (1959) Distribution in time and space of prepyriform electrical activtiy. J Neurophsyiol 22:644-665.

Freeman WJ (1968) Relations between unit activity and evoked potentials in prepyriform cortex of cats. J Neurophysiol 31:337-348.

Freeman WJ (1972) Measurement of oscillatory responses to electrical stimulation in olfactory bulb of cat. J Neurophysiol 35:762-779.

Freeman WJ (1978) Spatial properties of an EEG event in the olfactory bulb and cortex. Electroen Clinical Neurol 44:586-605.

Freeman WJ, Schneider W (1982) Changes in spatial patterns of rabbit olfactory EEG with conditioning to odors. Psychophysiology 19:44-56.

Fried HU, Fuss SH, Korsching SI (2002) Selective imaging of presynaptic activity in the mouse olfactory bulb shows concentration and structure dependence of odor responses in identified glomeruli. Proc Natl Acad Sci USA 99:3222-3227.

Friedrich RW, Habermann CJ, Laurent G (2004) Multiplexing using synchrony in the zebrafish olfactory bulb. Nat Neurosci 7:862-871.

Friedrich RW, Korsching SI (1997) Combinatorial and chemotopic odorant coding in the zebrafish olfactory bulb visualized by optical imaging. Neuron 18:737-752.

Friedrich RW, Laurent G (2001) Dynamic optimization of odor representations by slow temporal patterning of mitral cell activity. Science 291:889-894.

Fujita SC, Mori K, Imamura K, Obata K (1985) Subclasses of olfactory receptor cells and their segregated central projections demonstrated by a monoclonal antibody. Brain Res 326:192-196.

Gaillard I, Rouquier S, Pin J, Molard P, Sylvain R, Barnabe C, Demaille J, Giorgi D (2002) A single olfactory receptor specifically binds a set of odorant molecules. Eur J Neurosci 15: 409-418.

Getchell TV (1986) Functional properties of vertebrate olfactory receptor neurons. Physiol Rev 66:772-818.

Getchell TV, Shepherd GM (1978a) Adaptive properties of olfactory receptors analysed with odour pulses of varying durations. J Physiol 282:541-560.

Getchell TV, Shepherd GM (1978b) Responses of olfactory receptor cells to step pulses of odour at different concentrations in the salamander. J Physiol 282:521-540.

Gilbert CD, Sigman M, Crist RE (2001) The neural basis of perceptual learning. Neuron 31: 681-697.

Goldman AL, Van der Goes van Naters W, Lessing D, Warr CG, Carlson JR (2005) Coexpression of two functional odor receptors in one neuron. Neuron 45:661-666.

Gray CM, Freeman WJ, Skinner JE (1986) Chemical dependencies of learning in the rabbit olfactory bulb: acquisition of the transient spatial pattern change depends on norepinephrine. Behav Neurosci 100: 585-596.

Gray CM, Skinner JE (1988) Field potential response changes in the rabbit olfactory bulb accompany behavioral habituation during the repeated presentation of unreinforced odors. Exp Brain Res 73:189-197.

Greer CA (1987) Golgi analyses of dendritic organization among denervated olfactory bulb granule cells. J Comp Neurol 257:442-452.

Gross-Isseroff R, Lancet D (1988) Concentration-dependent changes of perceived odor quality. Chem Senses 13:191-204.

Guthrie KM, Anderson AJ, Leon M, Gall C (1993) Odor-induced increases in c-fos mRNA expression reveal an anatomical "unit" for odor processing in olfactory bulb. Proc Natl Acad Sci U S A 90:3329-3333.

Guthrie KM, Gall C (2003) Anatomic mapping of neuronal odor responses in the developing rat olfactory bulb. J Comp Neurol 455:56-71.

Guthrie KM, Wilson DA, Leon M (1990) Early unilateral deprivation modifies olfactory bulb function. J Neurosci 10: 3402-3412.

Haberly LB (1983) Structure of the piriform cortex of the opossum. I. Description of neuron types with Golgi methods. J Comp Neurol 213:163-187.

Haberly LB (1985) Neuronal circuitry in olfactory cortex: anatomy and functional implications. Chemical Senses 10:219-238.

Haberly LB (2001) Parallel-distributed processing in olfactory cortex: new insights from morphological and physiological analysis of neuronal circuitry. Chem Senses 26:551-576.

Haberly LB, Bower JM (1989) Olfactory cortex: model circuit for study of associative memory? Trends Neurosci 12:258-264.

Haberly LB, Hansen DJ, Feig SL, Presto S (1987) Distribution and ultrastructure of neurons in opossum piriform cortex displaying immunoreactivity to GABA and GAD and high-affinity tritiated GABA uptake. J Comp Neurol 266:269-290.

Haberly LB, Presto S (1986) Ultrastructural analysis of synaptic relationships of intracellularly stained pyramidal cell axons in piriform cortex. J Comp Neurol 248:464-474.

Haberly LB, Price JL (1977) The axonal projection patterns of the mitral and tufted cells of the olfactory bulb in the rat. Brain Res 129:152-157.

Haberly LB, Price JL (1978a) Association and commissural fiber system of the olfactory cortex of the rat. I. Systems originating in the piriform cortex and adjacent areas. J Comp Neurol 178: 711-740.

Haberly LB, Price JL (1978b) Association and commissural fiber systems of the olfactory cortex of the rat. II. Systems originating in the olfactory peduncle. J Comp Neurol 181:781-807.

Halabisky B, Friedman D, Radojicic M, Strowbridge BW (2000) Calcium influx through NMDA receptors directly evokes GABA release in olfactory bulb granule cells. J Neurosci 20:5124-5134.

Halasz N, Ljungdahl A, Hokfelt T, Johansson O, Goldstein M, Park D, Biberfeld P (1977) Transmitter histochemistry of the rat olfactory bulb. I. Immunohistochemical localization of monoamine synthesizing enzymes. Support for intrabulbar, periglomerular dopamine neurons. Brain Res 126:455-474.

Hamilton K, Kauer JS (1989) Patterns of intracellular potentials in salamander mitral-tufted cells in response to odor stimulation. J Neurophysiol 62: 609-625.

Harrison TA, Scott JW (1986) Olfactory bulb responses to odor stimulation: analysis of response pattern and intensity relationships. J Neurophysiol 56: 1571-1590.

Hayar A, Karnup S, Ennis M, Shipley MT (2004) External tufted cells: a major excitatory element that coordinates glomerular activity. J Neurosci 24:6676-6685.

Hayar A, Karnup S, Ennis M, Shipley MT (2004a) External tufted cells: a major excitatory element that coordinates glomerular activity. J Neurosci 24:6676-6685.

Hayar A, Karnup S, Shipley MT, Ennis M (2004b) Olfactory bulb glomeruli: external tufted cells intrinsically burst at theta frequency and are entrained by patterned olfactory input. J Neurosci 24:1190-1199.

Hebb DO (1949) The organization of behavior. New York: Wiley.

Herrick CJ (1924) The nucleus olfactorius anterior of the oppusum. Journal of Comparative Neurology 37:217-259.

Heyward P, Ennis M, Keller A, Shipley MT (2001) Membrane bistability in olfactory bulb mitral cells. J Neurosci 21:5311-5320.

Hubel DH, Weisel TN (1959) Receptive fields of single neurons in the cat's striate cortex. J Physiol (Lond) 148: 574-591.

Illig KR, Haberly LB (2003) Odor-evoked activity is spatially distributed in piriform cortex. J Comp Neurol 457:361-373.

Imamura K, Mataga N, Mori K (1992) Coding of odor molecules by mitral/tufted cells in rabbit olfactory bulb. I. Aliphatic compounds. J Neurophysiol 68:1986-2002.

Inaki K, Takahashi YK, Nagayama S, Mori K (2002) Molecular-feature domains with posterodorsal-anteroventral polarity in the symmetrical sensory maps of the mouse olfactory bulb: mapping of odourant-induced Zif268 expression. Eur J Neurosci 15:1563-1574.

Isaacson JS (1999) Glutamate spillover mediates excitatory transmission in the rat olfactory bulb. Neuron 23: 377-384.

Isaacson JS (2001) Mechanisms governing dendritic gamma-aminobutyric acid (GABA) release in the rat olfactory bulb. Proc Natl Acad Sci USA 98:337-342.

Isaacson JS, Strowbridge BW (1998) Olfactory reciprocal synapses: dendritic signaling in the CNS. Neuron 20:749-761.

Iwahara S, Oishi H, Sano K, Yang K-m, Takahashi T (1973) Electrical activity of the olfactory bulb in the postnatal rat. Japan Journal of Physiology 23:361-370.

Jahr CE, Nicoll RA (1980) Dendrodendritic inhibition: demonstration with intracellular recording. Science 207:1473-1475.

Jahr CE, Nicoll RA (1982) An intracellular analysis of dendrodendritic inhibition in the turtle in vitro olfactory bulb. J Physiol 326:213-234.

Jiang M, Griff ER, Ennis M, Zimmer LA, Shipley MT (1996) Activation of locus coeruleus enhances the responses of olfactory bulb mitral-tufted cells to weak olfactory nerve input. J Neurosci 16: 6319-6329.

Jiang T, Holley A (1992) Some properties of receptive fields of olfactory mitral-tufted cells in the frog. J Neurophysiol 68: 726-733.

Johnson BA, Leon M (2000) Modular representations of odorants in the glomerular layer of the rat olfactory bulb and the effects of stimulus concentration. J Comp Neurol 422:496-509.

Johnson DM, Illig KR, Behan M, Haberly LB (2000) New features of connectivity in piriform cortex visualized by intracellular injection of pyramidal cells suggest that "primary" olfactory cortex functions like "association" cortex in other sensory systems. J Neurosci 20:6974-6982.

Kajiya K, Inaki K, Tanaka M, Haga T, Kataoka H, Touhara K (2001) Molecular bases of odor discrimination: reconstitution of olfactory receptors that recognize overlapping sets of odorants. J Neurosci 21:6018-6025.

Kashiwadani H, Sasaki YF, Uchida N, Mori K (1999) Synchronized oscillatory discharges of mitral/tufted cells with different molecular receptive ranges in the rabbit olfactory bulb. J Neurophysiol 82:1786-1792.

Kasowski HJ, Kim H, Greer CA (1999) Compartmental organization of the olfactory bulb glomerulus. J Comp Neurol 407:261-274.

Katoh K, Koshimoto H, Tani A, Mori K (1993) Coding of odor molecules by mitral/tufted cells in rabbit olfactory bulb. II. Aromatic compounds. J Neurophysiol 70:2161-2175.

Kauer JS (1991) Contributions of topography and parallel processing to odor coding in the vertebrate olfactory pathway. Trends Neurosci 14: 79-85.

Kauer JS, Moulton DG (1974) Responses of olfactory bulb neurons to odour stimulation of small nasal areas in the salamander. J Physiol (Lond) 243: 717-737.

Kay LM (2005) Theta oscillations and sensorimotor performance. Proc Natl Acad Sci USA 102:3863-3868.

Kay LM, Freeman WJ (1998) Bidirectional processing in the olfactory-limbic axis during olfactory behavior. Behav Neurosci 112:541-553.

Kay LM, Lancaster LR, Freeman WJ (1996) Reafference and attractors in the olfactory system during odor recognition. Int J Neural Syst 7:489-495.

Kay LM, Laurent G (1999) Odor- and context-dependent modulation of mitral cell activity in behaving rats. Nat Neurosci 2:1003-1009.

Kendrick KM, Levy F, Keverne EB (1992) Changes in the sensory processing of olfactory signals induced by birth in sheep. Science 256: 833-836.

Kishi K, Mori K, Ojima H (1984) Distribution of local axon collaterals of mitral, displaced mitral, and tufted cells in the rabbit olfactory bulb. J Comp Neurol 225:511-526.

Kosaka K, Toida K, Margolis FL, Kosaka T (1997) Chemically defined neuron groups and their subpopulations in the glomerular layer of the rat main olfactory bulb--II. Prominent differences in the intraglomerular dendritic arborization and their relationship to olfactory nerve terminals. Neuroscience 76:775-786.

Koster NL, Norman AB, Richtand NM, Nickell WT, Puche AC, Pixley SK, Shipley MT (1999) Olfactory receptor neurons express D2 dopamine receptors. J Comp Neurol 411:666-673.

Lagier S, Carleton A, Lledo PM (2004) Interplay between local GABAergic interneurons and relay neurons generates gamma oscillations in the rat olfactory bulb. J Neurosci 24:4382-4392.

Lam YW, Cohen LB, Wachowiak M, Zochowski MR (2000) Odors elicit three different oscillations in the turtle olfactory bulb. J Neurosci 20:749-762.

Laurent G (1999) A systems perspective on early olfactory coding. Science 286:723-728.

Laurent G (2002) Olfactory network dynamics and the coding of multidimensional signals. Nat Rev Neurosci 3:884-895.

Laurent G, Davidowitz H (1994) Encoding of olfactory information with oscillatory neural assemblies. Science 265:1872-1875.

Laurent G, Stopfer M, Friedrich RW, Rabinovich MI, Volkovskii A, Abarbanel HD (2001) Odor encoding as an active, dynamical process: experiments, computation, and theory. Annu Rev Neurosci 24:263-297.

Leon M (1987) Plasticity of olfactory output circuits related to early olfactory learning. Trends Neurosci 10: 434-438.

Leon M, Johnson BA (2003) Olfactory coding in the mammalian olfactory bulb. Brain Res Brain Res Rev 42:23-32.

Lin DM, Wang F, Lowe G, Gold GH, Axel R, Ngai J, Brunet L (2000) Formation of precise connections in the olfactory bulb occurs in the absence of odorant-evoked neuronal activity. Neuron 26:69-80.

Linster C, Cleland TA (2002) Cholinergic modulation of sensory representations in the olfactory bulb. Neural Netw 15: 709-717.

Linster C, Johnson BA, Yue E, Morse A, Xu Z, Hingco EE, Choi Y, Choi M, Messiha A, Leon M (2001) Perceptual correlates of neural representations evoked by odorant enantiomers. J Neurosci 21:9837-9843.

Litaudon P, Mouly AM, Sullivan RM, Gervais R, Catarelli M (1997) Learning-induced changes in rat piriform cortex activity mapped using multisite recording with voltage-sensitive dye. Eur J Neurosci 9: 1593-1602.

Liu WL, Shipley MT (1994) Intrabulbar associational system in the rat olfactory bulb comprises cholecystokinin-containing tufted cells that synapse onto the dendrites of GABAergic granule cells. J Comp Neurol 346:541-558.

Lowe G (2002) Inhibition of backpropagating action potentials in mitral cell secondary dendrites. J Neurophysiol 88:64-85.

Luo M, Katz LC (2001) Response correlation maps of neurons in the mammalian olfactory bulb. Neuron 32:1165-1179.

Luskin MB, Price JL (1983a) The topographic organization of associational fibers of the olfactory system in the rat, including centrifugal fibers to the olfactory bulb. J Comp Neurol 216:264-291.

Luskin MB, Price JL (1983b) The laminar distribution of intracortical fibers originating in the olfactory cortex of the rat. J Comp Neurol 216:292-302.

Macrides F, Schoenfeld TA, Marchand JE, Clancy AN (1985) Evidence for morphologically, neurochemically and functionally heterogeneous classes of mitral and tufted cells in the olfactory bulb. Chem Senses 10:175-202.

Mair RG (1982) Response properties of rat olfactory neurons. J Physiol (Lond) 326: 241-359.

Mair RG, Gellman RL, Gesteland RC (1982) Postnatal proliferation and maturation of olfactory bulb neurons in the rat. Neurosci 7:3105-3116.

Mair RG, Gesteland RC (1982) Response properties of mitral cells in the olfactory bulb of the neonatal rat. Neurosci 7:3117-3125.

Malnic B, Hirono J, Sato T, Buck LB (1999) Combinatorial receptor codes for odors. Cell 96:713-723.

Malun D, Brunjes PC (1996) Development of olfactory glomeruli: temporal and spatial interactions between olfactory receptor axons and mitral cells in opossums and rats. J Comp Neurol 368:1-16.

Margrie TW, Sakmann B, Urban NN (2001) Action potential propagation in mitral cell lateral dendrites is decremental and controls recurrent and lateral inhibition in the mammalian olfactory bulb. Proc Natl Acad Sci USA 98:319-324.

Math F, Davrainville JL (1980) Electrophysiological study on the postnatal development of mitral cell activity in the rat olfactory bulb. Brain Res 190:243-247.

Matsutani S, Yamamoto N (2000) Differentiation of mitral cell dendrites in the developing main olfactory bulbs of normal and naris-occluded rats. The J Comp Neurol 418:402-410.

McCollum J, Larson J, Otto T, Schottler F, Granger R, Lynch G (1991) Short-latency single-unit processing in olfactory cortex. J Cognit Neurosci 3: 293-299.

McLean JH, Darby-King A, Sullivan RM, King SR (1993) Serotonergic influence on olfactory learning in the neonate rat. Behav Neural Biol 60: 152-162.

McLean JH, Shipley MT (1987) Serotonergic afferents to the rat olfactory bulb: I. Origins and laminar specificity of serotonergic inputs in the adult rat. J Neurosci 7:3016-3028.

McLean JH, Shipley MT (1988) Postmitotic, postmigrational expression of tyrosine hydroxylase in olfactory bulb dopaminergic neurons. J Neurosci 8:3658-3669.

McLean JH, Shipley MT (1991) Postnatal development of the noradrenergic projection from locus coeruleus to the olfactory bulb in the rat. J Comp Neurol 304:467-477.

Meister M, Bonhoeffer T (2001) Tuning and topography in an odor map on the rat olfactory bulb. J Neurosci 21:1351-1360.

Meredith M (1986) Patterned response to odor in mammalian olfactory bulb: the influence of intensity. J Neurophysiol 56: 572-597.

Mombaerts P (1999) Molecular biology of odorant receptors in vertebrates. Annu Rev Neurosci 22:487-509.

Mombaerts P (2004) Genes and ligands for odorant, vomeronasal and taste receptors. Nat Rev Neurosci 5:263-278.

Mombaerts P (2004) Odorant receptor gene choice in olfactory sensory neurons: the one receptor-one neuron hypothesis revisited. Curr Opin Neurobiol 14:31-36.

Mombaerts P, Wang F, Dulac C, Chao SK, Nemes A, Mendelsohn M, Edmondson J, Axel R (1996) Visualizing an olfactory sensory map. Cell 87:675-686.

Mori K, Fujita SC, Imamura K, Obata K (1985) Immunohistochemical study of subclasses of olfactory nerve fibers and their projections to the olfactory bulb in the rabbit. J Comp Neurol 242:214-229.

Mori K, Kishi K (1982) The morphology and physiology of the granule cells in the rabbit olfactory bulb revealed by intracellular recording and HRP injection. Brain Res 247:129-133.

Mori K, Kishi K, Ojima H (1983) Distribution of dendrites of mitral, displaced mitral, tufted, and granule cells in the rabbit olfactory bulb. J Comp Neurol 219:339-355.

Mori K, Mataga N, Imamura K (1992) Differential specificities of single mitral-tufted cells in rabbit olfactory bulb for a homologous series of fatty acid odor molecules. J Neurophysiol 67: 786-789.

Mori K, Nagao H, Yoshihara Y (1999) The olfactory bulb: coding and processing of odor molecule information. Science 286: 711-715.

Mori K, Takagi SF (1978) An intracellular study of dendrodendritic inhibitory synapses on mitral cells in the rabbit olfactory bulb. J Physiol 279:569-588.

Mori K, Yoshihara Y (1995) Molecular recognition and olfactory processing in the mammalian olfactory bulb. Prog Neurobiol 45: 585-619.

Mountcastle VB (1957) Modality and topographic properties of single neurons of the cat's somatic sensory cortex. J Neurophysiol 20: 408-434.

Nagao H, Yoshihara Y, Mitsui S, Fujisawa H, Mori K (2000) Two mirror-image sensory maps with domain organization in the mouse main olfactory bulb. Neuroreport 11:3023-3027.

Nagayama S, Takahashi YK, Yoshihara Y, Mori K (2004) Mitral and tufted cells differ in the decoding manner of odor maps in the rat olfactory bulb. J Neurophysiol.

Nakamura T, Gold GH (1987) A cyclic nucleotide-gated conductance in olfactory receptor cilia. Nature 325:442-444.

Nakashima M, Mori K, Takagi SF (1978) Centrifugal influence on olfactory bulb activity in the rabbit. Brain Res 154:301-316.

Neville KR, Haberly LB (2003) Beta and gamma oscillations in the olfactory system of the urethane-anesthetized rat. J Neurophysiol 90:3921-3930.

Neville KR, Haberly LB (2004) Olfactory Cortex. In: The synaptic organization of the brain, 5th Edition (Shepherd GM, ed), pp 415-454. New York: Oxford University Press.

Nickell WT, Behbehani MM, Shipley MT (1994) Evidence for GABAB-mediated inhibition of transmission from the olfactory nerve to mitral cells in the rat olfactory bulb. Brain Res Bull 35:119-123.

Nickell WT, Norman AB, Wyatt LM, Shipley MT (1991) Olfactory bulb DA receptors may be located on terminals of the olfactory nerve. Neuroreport 2:9-12.

Nowycky MC, Mori K, Shepherd GM (1981) GABAergic mechanisms of dendrodendritic synapses in isolated turtle olfactory bulb. J Neurophysiol 46:639-648.

Nusser Z, Kay LM, Laurent G, Homanics GE, Mody I (2001) Disruption of GABA(A) receptors on GABAergic interneurons leads to increased oscillatory power in the olfactory bulb network. J Neurophysiol 86:2823-2833.

Orona E, Rainer EC, Scott JW (1984) Dendritic and axonal organization of mitral and tufted cells in the rat olfactory bulb. J Comp Neurol 226:346-356.

Orona E, Scott JW, Ranier EC (1983) Different granule cell populations innervate superficial and deep regions of the external plexiform layer in rat olfactory bulb. Journal of Comparative Neurology 217:227-237.

Pace U, Hanski E, Salomon Y, Lancet D (1985) Odorant-sensitive adenylate cyclase may mediate olfactory reception. Nature 316:255-258.

Pager J, Giachetti I, Holley A, LeMagnen J (1972) A selective control of olfactory bulb electrical activity in relation to food deprivation and satiety in rats. Physiol Behav 9: 573-579.

Philpot BD, Foster TC, Brunjes PC (1997) Mitral/tufted cell activity is attenuated and becomes uncoupled from respiration following naris closure. J Neurobiol 33:374-386.

Pinching AJ, Powell TPS (1971a) The neuropil of the glomeruli of the olfactory bulb. J Cell Sci 9:347-377.

Pinching AJ, Powell TPS (1971b) The neuron types of the glomerular layer of the olfactory bulb. J Cell Sci 9:305-345.

Pinching AJ, Powell TPS (1971c) The neuropile of the periglomerular region of the olfactory bulb. J Cell Sci 9:379-409.

Price JL (1973) An autoradiographic study of complementary laminar patterns of termination of afferent fibers to the olfactory cortex. J Comp Neurol 150:87-108.

Price JL, Powell TP (1970a) The morphology of the granule cells of the olfactory bulb. J Cell Sci 7:91-123.

Price JL, Powell TPS (1970b) The synaptology of the granule cells of the olfactory bulb. J Cell Sci 7:125-155.

Price JL, Powell TP (1970c) An experimental study of the origin and the course of the centrifugal fibres to the olfactory bulb in the rat. J Anat 107:215-237.

Price JL, Powell TP (1970d) The mitral and short axon cells of the olfactory bulb. J Cell Sci 7:631-651.

Price JL, Slotnick BM, Revial MF (1991) Olfactory projections to the hypothalamus. The Journal of Comparative Neurology 306:447-461.

Rabin MD (1988) Experience facilitates olfactory quality discrimination. Percept Psychophys 44: 532-540.

Rall W, Shepherd GM (1968) Theoretical reconstruction of field potentials and dendrodendritic synaptic interactions in olfactory bulb. J Neurophysiol 31:884-915.

Rall W, Shepherd GM, Reese TS, Brightman MW (1966) Dendrodendritic synaptic pathway for inhibition in the olfactory bulb. Exp Neurol 14:44-56.

Ravel N, Akaoka H, Gervais R, Chouvet G (1990) The effect of acetylcholine on rat olfactory bulb unit activity. Brain Res Bull 24: 151-155.

Ravel N, Chabaud P, Martin C, Gaveau V, Hugues E, Tallon-Baudr C, Bertrand O, Gervais R (2003) Olfactory learning modifies the expression of odour-induced oscillatory responses in the gamma (60-90 Hz) and beta (15-40 Hz) bands in the rat olfactory bulb. Eur J Neurosci 17: 350-358.

Ravel N, Pager J (1990) Respiratory patterning of the rat olfactory bulb unit activity: nasal versus tracheal breathing. Neurosci Lett 115:213-218.

Ressler KJ, Sullivan SL, Buck LB (1993) A zonal organization of odorant receptor gene expression in the olfactory epithelium. Cell 73:597-609.

Ressler KJ, Sullivan SL, Buck LB (1994) Information coding in the olfactory system: evidence for a stereotyped and highly organized epitope map in the olfactory bulb. Cell 79:1245-1255.

Reyher CK, Lubke J, Larsen WJ, Hendrix GM, Shipley MT, Baumgarten HG (1991) Olfactory bulb granule cell aggregates: morphological evidence for interperikaryal electrotonic coupling via gap junctions. J Neurosci 11:1485-1495.

Ribak CE, Vaughn JE, Saito K, Barber R, Roberts E (1977) Glutamate decarboxylase localization in neurons of the olfactory bulb. Brain Res 126:1-18.

Rolls ET, Aggelopoulos NC, Zheng F (2003) The receptive fields of inferior temporal cortex neurons in natural scenes. J Neurosci 23: 339-348.

Rosselli-Austin L, Altman J (1979) The postnatal development of the main olfactory bulb of the rat. J Dev Physiol 1:295-313.

Rubin BD, Katz LC (1999) Optical imaging of odorant representations in the mammalian olfactory bulb. Neuron 23:499-511.

Salas M, Guzman-Flores C, Schapiro S (1969) An ontogenic study of olfactory bulb electrical activity in the rat. Physiology and Behavior 4:699-703.

Sanchez-Montanes MA, Pearce TC (2002) Why do olfactory neurons have unspecific receptive fields? Biosystems 67: 229-238.

Sato T, Hirono J, Tonoike M, Takebayashi M (1994) Tuning specificities to aliphatic odorants in mouse olfactory receptor neurons and their local distributions. J Neurophysiol 72: 2980-2989.

Satou M (1990) Synaptic organization, local neuronal circuitry, and functional segregation of the teleost olfactory bulb. Prog Neurobiol 34:115-142.

Satou M, Mori K, Tazawa Y, Takagi SF (1983) Neuronal pathways for activation of inhibitory interneurons in pyriform cortex of the rabbit. J Neurophysiol 50:74-88.

Schandar M, Laugwitz KL, Boekhoff I, Kroner C, Gudermann T, Schultz G, Breer H (1998) Odorants selectively activate distinct G protein subtypes in olfactory cilia. J Biol Chem 273:16669-16677.

Schneider SP, Scott JW (1983) Orthodromic response properties of rat olfactory bulb mitral and tufted cells correlate with their projection patterns. J Neurophysiol 50:358-378.

Schoenbaum G, Chiba AA, Gallagher M (1999) Neural encoding in orbito-frontal cortex and basolateral amygdala during olfactory discrimination learning. J Neurosci 19: 1876-1884.

Schoenfeld TA, Macrides F (1984) Topographic organization of connections between the main olfactory bulb and pars externa of the anterior olfactory nucleus in the hamster. J Comp Neurol 227:121-135.

Schoenfeld TA, Marchand JE, Macrides F (1985) Topographic organization of tufted cell axonal projections in the hamster main olfactory bulb: an intrabulbar associational system. J Comp Neurol 235:503-518.

Schoppa NE, Kinzie JM, Sahara Y, Segerson TP, Westbrook GL (1998) Dendrodendritic inhibition in the olfactory bulb is driven by NMDA receptors. J Neurosci 18:6790-6802.

Schwob JE, Haberly LB, Price JL (1984) The development of physiological responses of the piriform cortex in rats to stimulation of the lateral olfactory tract. J Comp Neurol 223:223-237.

Scott JW, McBride R, Schneider SP (1980) The organization of projections from the olfactory bulb to the piriform cortex and olfactory tubercle in the rat. J Comp Neurol 194:519-534.

Scott JW, Ranier EC, Pemberton JL, Orona E, Mouradian LE (1985) Pattern of rat olfactory bulb mitral and tufted cell connections to the anterior olfactory nucleus pars externa. J Comp Neurol 242:415-424.

Serizawa S, Ishii T, Nakatani H, Tsuboi A, Nagawa F, Asano M, Sudo K, Sakagami J, Sakano H, Ijiri T, Matsuda Y, Suzuki M, Yamamori T, Iwakura Y (2000) Mutually exclusive expression of odorant receptor transgenes. Nat Neurosci 3:687-693.

Shafa F, Shineh SN, Bidanjiri` A (1981) Development of spontaneous actvity in the olfactory bulb neurons of postnatal rat. Brain Research 223:409-412.

Sharp FR, Kauer JS, Shepherd GM (1975) Local sites of activity-related glucose metabolism in rat olfactory bulb during olfactory stimulation. Brain Res 98:596-600.

Sharp FR, Kauer JS, Shepherd GM (1977) Laminar analysis of 2-deoxyglucose uptake in olfactory bulb and olfactory cortex of rabbit and rat. J Neurophysiol 40:800-813.

Shepherd GM, Chen WR, Greer CA (2004) Olfactory bulb. In: The Synaptic Organization of the Brain, 5th Edition (Shepherd GM, ed), pp 165-216. New York: Oxford University Press.

Shepherd GM, Greer CA (1998) Olfactory bulb. In: The synaptic organization of the brain (Shepherd GM, ed), pp 159-204. New York: Oxford UP.

Sherman SM (1993) dynamic gating of retinal transmission to the visual cortex by lateral geniculate nucleus. In: Thalamic Networks for Relay and Modulation (Minciacchi D, Molinari M, Macchi G, Jones EG, eds), pp 61-79. New York: Pergamon Press.

Shipley MT, Adamek GD (1984) The connections of the mouse olfactory bulb: a study using orthograde and retrograde transport of wheat germ agglutinin conjugated to horseradish peroxidase. Brain Res Bull 12:669-688.

Shipley MT, Ennis M (1996) Functional organization of olfactory system. J Neurobiol 30:123-176.

Shipley MT, Halloran FJ, Torre JDL (1985) Surprisingly rich projection from locus coeruleus to the olfactory bulb in the rat. Brain Res 329:294-299.

Sicard G, Holley A (1984) Receptor cell responses to odorants: similarities and differences among odorants. Brain Res 292:283-296.

Slotnick B, Bisulco S (2003) Detection and discrimination of carvone enantiomers in rats with olfactory bulb lesions. Neuroscience 121:451-457.

Slotnick B, Cockerham R, Pickett E (2004) Olfaction in olfactory bulbectomized rats. J Neurosci 24:9195-9200.

Spors H, Grinvald A (2002) Spatio-temporal dynamics of odor representations in the mammalian olfactory bulb. Neuron 34:301-315.

Stevenson RJ (2001) Associative learning and odor quality perception: how sniffing an odor mixture can alter the smell of its parts. Learn Motiv 32: 154-177.

Stewart WB, Kauer JS, Shepherd GM (1979) Functional organization of rat olfactory bulb analysed by the 2-deoxyglucose method. J Comp Neurol 185:715-734.

Stopfer M, Bhagavan S, Smith BH, Laurent G (1997) Impaired odour discrimination on desynchronization of odour-encoding neural assemblies. Nature 390:70-74.

Sugai T, Miyazawa T, Fukuda M, Yoshimura H, Onoda N (2005) Odor-concentration coding in the guinea-pig piriform cortex. Neuroscience 130:769-781.

Sullivan RM, Wilson DA, Leon M (1989) Norepinephrine and learning-induced plasticity in infant rat olfactory system. J Neurosci 9: 3998-4006.

Sullivan SL, Bohm S, Ressler KJ, Horowitz LF, Buck LB (1995) Target-independent pattern specification in the olfactory epithelium. Neuron 15:779-789.

Toida K, Kosaka K, Heizmann C, Kosaka T (1998) Chemically defined neuron groups and their subpopulations in the glomerular layer of the rat main olfactory bulb: III. Structural features of calbindin D28K-immunoreactive neurons. J Comp Neurol 392:179-198.

Touhara K, Sengoku S, Inaki K, Tsuboi A, Hirono J, Sato T, Sakano H, Haga T (1999) Functional identification and reconstitution of an odorant receptor in single olfactory neurons. Proc Natl Acad Sci USA 96:4040-4045.

Treloar H, Walters E, Margolis F, Key B (1996) Olfactory glomeruli are inervated by more than one distinct subset of of primary sensory neurons in mice. The Journal of Comparative Neurology 367:550-562.

Treloar HB, Feinstein P, Mombaerts P, Greer CA (2002) Specificity of glomerular targeting by olfactory sensory axons. J Neurosci 22:2469-2477.

Tseng GF, Haberly LB (1988) Characterization of synaptically mediated fast and slow inhibitory processes in piriform cortex in an in vitro slice preparation. J Neurophysiol 59:1352-1376.

Tseng GF, Haberly LB (1989) Deep neurons in piriform cortex. I. Morphology and synaptically evoked responses including a unique high-amplitude paired shock facilitation. J Neurophysiol 62:369-385.

Tsuboi A (1999) Olfactory neurons expressing closely linked and homologous odorant receptor genes tend to project their axons to neighboring glomeruli on the olfactory bulb. J Neurosci. 19:8409-8414.

Tsuboi A, Yoshihara S, Yamazaki N, Kasai H, Asai-Tsuboi H, Komatsu M, Serizawa S, Ishii T, Matsuda Y, Nagawa F, Sakano H (1999) Olfactory neurons expressing closely linked and homologous odorant receptor genes tend to project their axons to neighboring glomeruli on the olfactory bulb. J Neurosci 19: 8409-8414.

Turin L, Yoshii F (2003) Structure-Odor Relationships: A Modern Perspective. In: Handbook of Olfaction and Gustation, 2 Edition (Doty RL, ed), pp 175-294. New York: Marcel Dekker, Inc.

Uchida N, Takahashi YK, Tanifuji M, Mori K (2000) Odor maps in the mammalian olfactory bulb: domain organization and odorant structural features. Nat Neurosci 3: 1035-1043.

Van Groen T, Wyss JM (1990) Extrinsic projections from area CA1 of the rat hippocampus: Olfactory, cortical, subcortical, and bilateral hippocampal formation projections. J Comp Neurol 302:515-528.

Vanderwolf CH, Zibrowski EM (2001) Pyriform cortex beta-waves: odor-specific sensitization following repeated olfactory stimulation. Brain Res 892:301-308.

Vassar R, Chao SK, Sitcheran R, Nunez JM, Vosshall LB, Axel R (1994) Topographic organization of sensory projections to the olfactory bulb. Cell 79: 981-991.

Vassar R, Ngal J, Axel R (1993) Spatial segregation of odorant receptor expression in the mammalian olfactory epithelium. Cell 74:309-318.

Wachowiak M, Cohen LB (1999) Presynaptic inhibition of primary olfactory afferents mediated by different mechanisms in lobster and turtle. J Neurosci 19:8808-8817.

Wada E, Shigemoto R, Kinoshita A, Ohishi H, Mizuno N (1998) Metabotropic glutamate receptor subtypes in axon terminals of projection fibers from the main and accessory olfactory bulbs: a light and electron microscopic immunohistochemical study in the rat. J Comp Neurol 393:493-504.

Weinberger NM (1995) Dynamic regulation of receptive fields and maps in the adult sensory cortex. Annu Rev Neurosci 18: 129-158.

Weinberger NM, Javid R, Lepan B (1993) Long-term retention of learning-induced receptive field plasticity in the auditory cortex. Proc Natl Acad Sci USA 90: 2394-2398.

Wellis DP, Kauer JS (1993) GABAA and glutamate receptor involvement in dendrodendritic synaptic interactions from salamander olfactory bulb. J Physiol 469:315-339.

Wellis DP, Scott JW (1990) Intracellular responses of identified rat olfactory bulb interneurons to electrical and odor stimulation. J Neurophysiol 64:932-947.

Wellis DP, Scott JW, Harrison TA (1989) Discrimination among odorants by single neurons of the rat olfactory bulb. J Neurophysiol 61:1161-1177.

Wilson DA (1997) Binaral interactions in rat piriform cortex. J Neurophysiol 78: 160-169.

Wilson DA (1998) Habituation of odor responses in the rat anterior piriform cortex. J Neurophysiol 79:1425-1440.

Wilson DA (2000a) Odor specificity of habituation in the rat anterior piriform cortex. J Neurophysiol 83: 139-145.

Wilson DA (2000b) Comparison of odor receptive field plasticity in the rat olfactory bulb and anterior piriform cortex. J Neurophysiol 84: 3036-3042.

Wilson D (2001a) Scopolamine enhances generalization between odor representations in the rat olfactory cortex. Learning & Memory 8:279-285.

Wilson DA (2001b) Receptive fields in the rat piriform cortex. Chem Senses 26:577-584.

Wilson DA (2003) Rapid, experience-induced enhancement in odorant discrimination by anterior piriform cortex neurons. J Neurophysiol 90:65-72.

Wilson DA, Leon M (1986) Early appearance of inhibition in the neonatal rat olfactory bulb. Brain Res 391:289-292.

Wilson DA, Stevenson RJ (2003) Olfactory perceptual learning: the critical role of memory in odor discrimination. Neurosci Biobehav Rev 27:307-328.

Wilson DA, Stevenson RJ (2003) The fundamental role of memory in olfactory perception. Trends Neurosci 26:243-247.

Wilson DA, Sullivan RM (1990) Olfactory associative conditioning in infant rats with brain stimulation as reward. I. Neurobehavioral consequences. Brain Res Dev Brain Res 53:215-221.

Wilson DA, Sullivan RM (1994) Neurobiology of associative learning in the neonate: early olfactory learning. Behav Neural Biol 61: 1-18.

Wilson DA, Sullivan RM (1995) The D2 antagonist spiperone mimics the effects of olfactory deprivation on mitral-tufted cell odor response patterns. J Neurosci 8: 5574-5581.

Woolf TB, Shepherd GM, Greer CA (1991) Local information processing in dendritic trees: subsets of spines in granule cells of the mammalian olfactory bulb. J Neurosci 11:1837-1854.

Wright GA, Smith BH (2004) Different thresholds for detection and discrimination of odors in the honey bee (Apis mellifera). Chem Senses 29:127-135.

Xiong W, Chen WR (2002) Dynamic gating of spike propagation in the mitral cell lateral dendrites. Neuron 34:115-126.

Xu F, Greer CA, Shepherd GM (2000) Odor maps in the olfactory bulb. J Comp Neurol 422:489-495.

Yokoi M, Mori K, Nakanishi S (1995) Refinement of odor molecule tuning by dendrodendritic synaptic inhibition in the olfactory bulb. Proc Natl Acad Sci USA 92: 3371-3375.

Yuan Q, Harley CW, McLean JH (2003) Mitral-tufted cell beta(1) and 5-HT(2A) receptor colocalization and cAMP coregulation: a new model of norepinephrine-induced learning in the olfactory bulb. Learn Mem 10: 5-15.

Zaborszky L, Carlsen J, Brashear HR, Heimer L (1986) Cholinergic and GABAergic afferents to the olfactory bulb in the rat with special emphasis on the projection neurons in the nucleus of the horizontal limb of the diagonal band. J Comp Neurol 243:488-509.

Zou DJ, Feinstein P, Rivers AL, Mathews GA, Kim A, Greer CA, Mombaerts P, Firestein S (2004) Postnatal refinement of peripheral olfactory projections. Science 304:1976-1979.

Zou Z, Horowitz LF, Montmayeur JP, Snapper S, Buck LB (2001) Genetic tracing reveals a stereotyped sensory map in the olfactory cortex. Nature 414:173-179.